the fraction of counts of each outcome observed in the training set:

$$\text{softmax}(\boldsymbol{z}(\boldsymbol{x};\boldsymbol{\theta}))_i \approx \frac{\sum_{j=1}^{m} \mathbf{1}_{y^{(j)}=i,\boldsymbol{x}^{(j)}=\boldsymbol{x}}}{\sum_{j=1}^{m} \mathbf{1}_{\boldsymbol{x}^{(j)}=\boldsymbol{x}}}. \tag{6.31}$$

Because maximum likelihood is a consistent estimator, this is guaranteed to happen so long as the model family is capable of representing the training distribution. In practice, limited model capacity and imperfect optimization will mean that the model is only able to approximate these fractions.

Many objective functions other than the log-likelihood do not work as well with the softmax function. Specifically, objective functions that do not use a log to undo the exp of the softmax fail to learn when the argument to the exp becomes very negative, causing the gradient to vanish. In particular, squared error is a poor loss function for softmax units, and can fail to train the model to change its output, even when the model makes highly confident incorrect predictions (Bridle, 1990). To understand why these other loss functions can fail, we need to examine the softmax function itself.

Like the sigmoid, the softmax activation can saturate. The sigmoid function has a single output that saturates when its input is extremely negative or extremely positive. In the case of the softmax, there are multiple output values. These output values can saturate when the differences between input values become extreme. When the softmax saturates, many cost functions based on the softmax also saturate, unless they are able to invert the saturating activating function.

To see that the softmax function responds to the difference between its inputs, observe that the softmax output is invariant to adding the same scalar to all of its inputs:

$$\text{softmax}(\boldsymbol{z}) = \text{softmax}(\boldsymbol{z} + c). \tag{6.32}$$

Using this property, we can derive a numerically stable variant of the softmax:

$$\text{softmax}(\boldsymbol{z}) = \text{softmax}(\boldsymbol{z} - \max_i z_i). \tag{6.33}$$

The reformulated version allows us to evaluate softmax with only small numerical errors even when z contains extremely large or extremely negative numbers. Examining the numerically stable variant, we see that the softmax function is driven by the amount that its arguments deviate from $\max_i z_i$.

An output $\text{softmax}(\boldsymbol{z})_i$ saturates to 1 when the corresponding input is maximal ($z_i = \max_i z_i$) and z_i is much greater than all of the other inputs. The output $\text{softmax}(\boldsymbol{z})_i$ can also saturate to 0 when z_i is not maximal and the maximum is much greater. This is a generalization of the way that sigmoid units saturate, and can cause similar difficulties for learning if the loss function is not designed to compensate for it.

The argument $\boldsymbol{z}$ to the softmax function can be produced in two different ways. The most common is simply to have an earlier layer of the neural network output every element of $\boldsymbol{z}$, as described above using the linear layer $\boldsymbol{z} = \boldsymbol{W}^\top \boldsymbol{h} + \boldsymbol{b}$. While straightforward, this approach actually overparametrizes the distribution. The constraint that the n outputs must sum to 1 means that only $n-1$ parameters are necessary; the probability of the n-th value may be obtained by subtracting the first $n-1$ probabilities from 1. We can thus impose a requirement that one element of $\boldsymbol{z}$ be fixed. For example, we can require that $z_n = 0$. Indeed, this is exactly what the sigmoid unit does. Defining $P(y=1 \mid \boldsymbol{x}) = \sigma(z)$ is equivalent to defining $P(y=1 \mid \boldsymbol{x}) = \text{softmax}(\boldsymbol{z})_1$ with a two-dimensional $\boldsymbol{z}$ and $z_1 = 0$. Both the $n-1$ argument and the n argument approaches to the softmax can describe the same set of probability distributions, but have different learning dynamics. In practice, there is rarely much difference between using the overparametrized version or the restricted version, and it is simpler to implement the overparametrized version.

From a neuroscientific point of view, it is interesting to think of the softmax as a way to create a form of competition between the units that participate in it: the softmax outputs always sum to 1 so an increase in the value of one unit necessarily corresponds to a decrease in the value of others. This is analogous to the lateral inhibition that is believed to exist between nearby neurons in the cortex. At the extreme (when the difference between the maximal a_i and the others is large in magnitude) it becomes a form of **winner-take-all** (one of the outputs is nearly 1 and the others are nearly 0).

The name "softmax" can be somewhat confusing. The function is more closely related to the $\arg\max$ function than the max function. The term "soft" derives from the fact that the softmax function is continuous and differentiable. The $\arg\max$ function, with its result represented as a one-hot vector, is not continuous or differentiable. The softmax function thus provides a "softened" version of the $\arg\max$. The corresponding soft version of the maximum function is $\text{softmax}(\boldsymbol{z})^\top \boldsymbol{z}$. It would perhaps be better to call the softmax function "softargmax," but the current name is an entrenched convention.

6.2.2.4 Other Output Types

The linear, sigmoid, and softmax output units described above are the most common. Neural networks can generalize to almost any kind of output layer that we wish. The principle of maximum likelihood provides a guide for how to design a good cost function for nearly any kind of output layer.

In general, if we define a conditional distribution $p(\boldsymbol{y} \mid \boldsymbol{x}; \boldsymbol{\theta})$, the principle of maximum likelihood suggests we use $-\log p(\boldsymbol{y} \mid \boldsymbol{x}; \boldsymbol{\theta})$ as our cost function.

In general, we can think of the neural network as representing a function $f(\boldsymbol{x};\boldsymbol{\theta})$. The outputs of this function are not direct predictions of the value $\boldsymbol{y}$. Instead, $f(\boldsymbol{x};\boldsymbol{\theta}) = \boldsymbol{\omega}$ provides the parameters for a distribution over y. Our loss function can then be interpreted as $-\log p(\mathbf{y}; \boldsymbol{\omega}(\boldsymbol{x}))$.

For example, we may wish to learn the variance of a conditional Gaussian for $\mathbf{y}$, given $\mathbf{x}$. In the simple case, where the variance σ^2 is a constant, there is a closed form expression because the maximum likelihood estimator of variance is simply the empirical mean of the squared difference between observations $\mathbf{y}$ and their expected value. A computationally more expensive approach that does not require writing special-case code is to simply include the variance as one of the properties of the distribution $p(\mathbf{y} \mid \boldsymbol{x})$ that is controlled by $\boldsymbol{\omega} = f(\boldsymbol{x}; \boldsymbol{\theta})$. The negative log-likelihood $-\log p(\boldsymbol{y}; \boldsymbol{\omega}(\boldsymbol{x}))$ will then provide a cost function with the appropriate terms necessary to make our optimization procedure incrementally learn the variance. In the simple case where the standard deviation does not depend on the input, we can make a new parameter in the network that is copied directly into $\boldsymbol{\omega}$. This new parameter might be σ itself or could be a parameter v representing σ^2 or it could be a parameter β representing $\frac{1}{\sigma^2}$, depending on how we choose to parametrize the distribution. We may wish our model to predict a different amount of variance in $\mathbf{y}$ for different values of $\mathbf{x}$. This is called a **heteroscedastic** model. In the heteroscedastic case, we simply make the specification of the variance be one of the values output by $f(\mathbf{x};\boldsymbol{\theta})$. A typical way to do this is to formulate the Gaussian distribution using precision, rather than variance, as described in equation 3.22. In the multivariate case it is most common to use a diagonal precision matrix

$$\mathrm{diag}(\boldsymbol{\beta}). \tag{6.34}$$

This formulation works well with gradient descent because the formula for the log-likelihood of the Gaussian distribution parametrized by $\boldsymbol{\beta}$ involves only multiplication by β_i and addition of $\log \boldsymbol{\beta}_i$. The gradient of multiplication, addition, and logarithm operations is well-behaved. By comparison, if we parametrized the output in terms of variance, we would need to use division. The division function becomes arbitrarily steep near zero. While large gradients can help learning, arbitrarily large gradients usually result in instability. If we parametrized the output in terms of standard deviation, the log-likelihood would still involve division, and would also involve squaring. The gradient through the squaring operation can vanish near zero, making it difficult to learn parameters that are squared.

Regardless of whether we use standard deviation, variance, or precision, we must ensure that the covariance matrix of the Gaussian is positive definite. Because the eigenvalues of the precision matrix are the reciprocals of the eigenvalues of the covariance matrix, this is equivalent to ensuring that the precision matrix is positive definite. If we use a diagonal matrix, or a scalar times the diagonal matrix, then the only condition we need to enforce on the output of the model is positivity. If we suppose that $\boldsymbol{a}$ is the raw activation of the model used to determine the diagonal precision, we can use the softplus function to obtain a positive precision vector: $\boldsymbol{\beta} = \zeta(\boldsymbol{a})$. This same strategy applies equally if using variance or standard deviation rather than precision or if using a scalar times identity rather than diagonal matrix.

It is rare to learn a covariance or precision matrix with richer structure than diagonal. If the covariance is full and conditional, then a parametrization must be chosen that guarantees positive-definiteness of the predicted covariance matrix. This can be achieved by writing $\boldsymbol{\Sigma}(\boldsymbol{x}) = \boldsymbol{B}(\boldsymbol{x})\boldsymbol{B}^{\top}(\boldsymbol{x})$, where $\boldsymbol{B}$ is an unconstrained square matrix. One practical issue if the matrix is full rank is that computing the likelihood is expensive, with a $d \times d$ matrix requiring $O(d^3)$ computation for the determinant and inverse of $\boldsymbol{\Sigma}(\boldsymbol{x})$ (or equivalently, and more commonly done, its eigendecomposition or that of $\boldsymbol{B}(\boldsymbol{x})$).

We often want to perform multimodal regression, that is, to predict real values that come from a conditional distribution $p(\boldsymbol{y} \mid \boldsymbol{x})$ that can have several different peaks in $\boldsymbol{y}$ space for the same value of $\boldsymbol{x}$. In this case, a Gaussian mixture is a natural representation for the output (Jacobs *et al.*, 1991; Bishop, 1994). Neural networks with Gaussian mixtures as their output are often called **mixture density networks**. A Gaussian mixture output with n components is defined by the conditional probability distribution

$$p(\boldsymbol{y} \mid \boldsymbol{x}) = \sum_{i=1}^{n} p(\mathrm{c} = i \mid \boldsymbol{x}) \mathcal{N}(\boldsymbol{y}; \boldsymbol{\mu}^{(i)}(\boldsymbol{x}), \boldsymbol{\Sigma}^{(i)}(\boldsymbol{x})). \tag{6.35}$$

The neural network must have three outputs: a vector defining $p(\mathrm{c} = i \mid \boldsymbol{x})$, a matrix providing $\boldsymbol{\mu}^{(i)}(\boldsymbol{x})$ for all i, and a tensor providing $\boldsymbol{\Sigma}^{(i)}(\boldsymbol{x})$ for all i. These outputs must satisfy different constraints:

1. Mixture components $p(\mathrm{c} = i \mid \boldsymbol{x})$: these form a multinoulli distribution over the n different components associated with latent variable[1] c, and can

[1]We consider c to be latent because we do not observe it in the data: given input $\mathbf{x}$ and target $\mathbf{y}$, it is not possible to know with certainty which Gaussian component was responsible for $\mathbf{y}$, but we can imagine that $\mathbf{y}$ was generated by picking one of them, and make that unobserved choice a random variable.

typically be obtained by a softmax over an n-dimensional vector, to guarantee that these outputs are positive and sum to 1.

2. Means $\boldsymbol{\mu}^{(i)}(\boldsymbol{x})$: these indicate the center or mean associated with the i-th Gaussian component, and are unconstrained (typically with no nonlinearity at all for these output units). If $\mathbf{y}$ is a d-vector, then the network must output an $n \times d$ matrix containing all n of these d-dimensional vectors. Learning these means with maximum likelihood is slightly more complicated than learning the means of a distribution with only one output mode. We only want to update the mean for the component that actually produced the observation. In practice, we do not know which component produced each observation. The expression for the negative log-likelihood naturally weights each example's contribution to the loss for each component by the probability that the component produced the example.

3. Covariances $\boldsymbol{\Sigma}^{(i)}(\boldsymbol{x})$: these specify the covariance matrix for each component i. As when learning a single Gaussian component, we typically use a diagonal matrix to avoid needing to compute determinants. As with learning the means of the mixture, maximum likelihood is complicated by needing to assign partial responsibility for each point to each mixture component. Gradient descent will automatically follow the correct process if given the correct specification of the negative log-likelihood under the mixture model.

It has been reported that gradient-based optimization of conditional Gaussian mixtures (on the output of neural networks) can be unreliable, in part because one gets divisions (by the variance) which can be numerically unstable (when some variance gets to be small for a particular example, yielding very large gradients). One solution is to **clip gradients** (see section 10.11.1) while another is to scale the gradients heuristically (Murray and Larochelle, 2014).

Gaussian mixture outputs are particularly effective in generative models of speech (Schuster, 1999) or movements of physical objects (Graves, 2013). The mixture density strategy gives a way for the network to represent multiple output modes and to control the variance of its output, which is crucial for obtaining a high degree of quality in these real-valued domains. An example of a mixture density network is shown in figure 6.4.

In general, we may wish to continue to model larger vectors $\boldsymbol{y}$ containing more variables, and to impose richer and richer structures on these output variables. For example, we may wish for our neural network to output a sequence of characters that forms a sentence. In these cases, we may continue to use the principle of maximum likelihood applied to our model $p(\boldsymbol{y}; \boldsymbol{\omega}(\boldsymbol{x}))$, but the model we use

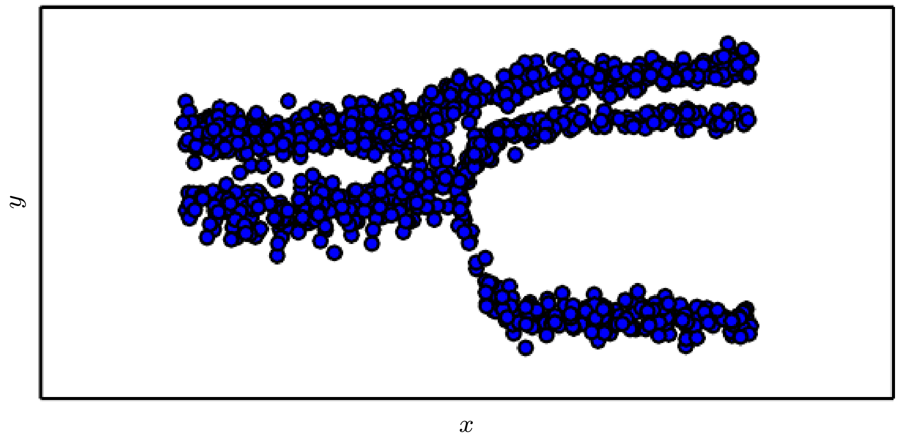

Figure 6.4: Samples drawn from a neural network with a mixture density output layer. The input x is sampled from a uniform distribution and the output y is sampled from $p_{\text{model}}(y \mid x)$. The neural network is able to learn nonlinear mappings from the input to the parameters of the output distribution. These parameters include the probabilities governing which of three mixture components will generate the output as well as the parameters for each mixture component. Each mixture component is Gaussian with predicted mean and variance. All of these aspects of the output distribution are able to vary with respect to the input x, and to do so in nonlinear ways.

to describe $\boldsymbol{y}$ becomes complex enough to be beyond the scope of this chapter. Chapter 10 describes how to use recurrent neural networks to define such models over sequences, and part III describes advanced techniques for modeling arbitrary probability distributions.

6.3 Hidden Units

So far we have focused our discussion on design choices for neural networks that are common to most parametric machine learning models trained with gradient-based optimization. Now we turn to an issue that is unique to feedforward neural networks: how to choose the type of hidden unit to use in the hidden layers of the model.

The design of hidden units is an extremely active area of research and does not yet have many definitive guiding theoretical principles.

Rectified linear units are an excellent default choice of hidden unit. Many other types of hidden units are available. It can be difficult to determine when to use which kind (though rectified linear units are usually an acceptable choice). We describe here some of the basic intuitions motivating each type of hidden units. These intuitions can help decide when to try out each of these units. It is usually impossible to predict in advance which will work best. The design process consists of trial and error, intuiting that a kind of hidden unit may work well, and then training a network with that kind of hidden unit and evaluating its performance on a validation set.

Some of the hidden units included in this list are not actually differentiable at all input points. For example, the rectified linear function $g(z) = \max\{0, z\}$ is not differentiable at $z = 0$. This may seem like it invalidates g for use with a gradient-based learning algorithm. In practice, gradient descent still performs well enough for these models to be used for machine learning tasks. This is in part because neural network training algorithms do not usually arrive at a local minimum of the cost function, but instead merely reduce its value significantly, as shown in figure 4.3. These ideas will be described further in chapter 8. Because we do not expect training to actually reach a point where the gradient is $\mathbf{0}$, it is acceptable for the minima of the cost function to correspond to points with undefined gradient. Hidden units that are not differentiable are usually non-differentiable at only a small number of points. In general, a function $g(z)$ has a left derivative defined by the slope of the function immediately to the left of z and a right derivative defined by the slope of the function immediately to the right of z. A function is differentiable at z only if both the left derivative and the right derivative are defined and equal to each other. The functions used in the context of neural networks usually have defined left derivatives and defined right derivatives. In the case of $g(z) = \max\{0, z\}$, the left derivative at $z = 0$ is 0 and the right derivative is 1. Software implementations of neural network training usually return one of the one-sided derivatives rather than reporting that the derivative is undefined or raising an error. This may be heuristically justified by observing that gradient-based optimization on a digital computer is subject to numerical error anyway. When a function is asked to evaluate $g(0)$, it is very unlikely that the underlying value truly was 0. Instead, it was likely to be some small value ϵ that was rounded to 0. In some contexts, more theoretically pleasing justifications are available, but these usually do not apply to neural network training. The important point is that in practice one can safely disregard the non-differentiability of the hidden unit activation functions described below.

Unless indicated otherwise, most hidden units can be described as accepting a vector of inputs $\boldsymbol{x}$, computing an affine transformation $\boldsymbol{z} = \boldsymbol{W}^\top \boldsymbol{x} + \boldsymbol{b}$, and then applying an element-wise nonlinear function $g(\boldsymbol{z})$. Most hidden units are distinguished from each other only by the choice of the form of the activation function $g(\boldsymbol{z})$.

6.3.1 Rectified Linear Units and Their Generalizations

Rectified linear units use the activation function $g(z) = \max\{0, z\}$.

Rectified linear units are easy to optimize because they are so similar to linear units. The only difference between a linear unit and a rectified linear unit is that a rectified linear unit outputs zero across half its domain. This makes the derivatives through a rectified linear unit remain large whenever the unit is active. The gradients are not only large but also consistent. The second derivative of the rectifying operation is 0 almost everywhere, and the derivative of the rectifying operation is 1 everywhere that the unit is active. This means that the gradient direction is far more useful for learning than it would be with activation functions that introduce second-order effects.

Rectified linear units are typically used on top of an affine transformation:

$$\boldsymbol{h} = g(\boldsymbol{W}^\top \boldsymbol{x} + \boldsymbol{b}). \tag{6.36}$$

When initializing the parameters of the affine transformation, it can be a good practice to set all elements of $\boldsymbol{b}$ to a small, positive value, such as 0.1. This makes it very likely that the rectified linear units will be initially active for most inputs in the training set and allow the derivatives to pass through.

Several generalizations of rectified linear units exist. Most of these generalizations perform comparably to rectified linear units and occasionally perform better.

One drawback to rectified linear units is that they cannot learn via gradient-based methods on examples for which their activation is zero. A variety of generalizations of rectified linear units guarantee that they receive gradient everywhere.

Three generalizations of rectified linear units are based on using a non-zero slope α_i when $z_i < 0$: $h_i = g(\boldsymbol{z}, \boldsymbol{\alpha})_i = \max(0, z_i) + \alpha_i \min(0, z_i)$. **Absolute value rectification** fixes $\alpha_i = -1$ to obtain $g(z) = |z|$. It is used for object recognition from images (Jarrett *et al.*, 2009), where it makes sense to seek features that are invariant under a polarity reversal of the input illumination. Other generalizations of rectified linear units are more broadly applicable. A **leaky ReLU** (Maas *et al.*, 2013) fixes α_i to a small value like 0.01 while a **parametric ReLU** or **PReLU** treats α_i as a learnable parameter (He *et al.*, 2015).

Maxout units (Goodfellow *et al.*, 2013a) generalize rectified linear units further. Instead of applying an element-wise function $g(z)$, maxout units divide $\boldsymbol{z}$ into groups of k values. Each maxout unit then outputs the maximum element of one of these groups:

$$g(\boldsymbol{z})_i = \max_{j \in \mathbb{G}^{(i)}} z_j \tag{6.37}$$

where $\mathbb{G}^{(i)}$ is the set of indices into the inputs for group i, $\{(i-1)k+1, \ldots, ik\}$. This provides a way of learning a piecewise linear function that responds to multiple directions in the input $\boldsymbol{x}$ space.

A maxout unit can learn a piecewise linear, convex function with up to k pieces. Maxout units can thus be seen as *learning the activation function* itself rather than just the relationship between units. With large enough k, a maxout unit can learn to approximate any convex function with arbitrary fidelity. In particular, a maxout layer with two pieces can learn to implement the same function of the input $\boldsymbol{x}$ as a traditional layer using the rectified linear activation function, absolute value rectification function, or the leaky or parametric ReLU, or can learn to implement a totally different function altogether. The maxout layer will of course be parametrized differently from any of these other layer types, so the learning dynamics will be different even in the cases where maxout learns to implement the same function of $\boldsymbol{x}$ as one of the other layer types.

Each maxout unit is now parametrized by k weight vectors instead of just one, so maxout units typically need more regularization than rectified linear units. They can work well without regularization if the training set is large and the number of pieces per unit is kept low (Cai *et al.*, 2013).

Maxout units have a few other benefits. In some cases, one can gain some statistical and computational advantages by requiring fewer parameters. Specifically, if the features captured by n different linear filters can be summarized without losing information by taking the max over each group of k features, then the next layer can get by with k times fewer weights.

Because each unit is driven by multiple filters, maxout units have some redundancy that helps them to resist a phenomenon called **catastrophic forgetting** in which neural networks forget how to perform tasks that they were trained on in the past (Goodfellow *et al.*, 2014a).

Rectified linear units and all of these generalizations of them are based on the principle that models are easier to optimize if their behavior is closer to linear. This same general principle of using linear behavior to obtain easier optimization also applies in other contexts besides deep linear networks. Recurrent networks can learn from sequences and produce a sequence of states and outputs. When training them, one needs to propagate information through several time steps, which is much easier when some linear computations (with some directional derivatives being of magnitude near 1) are involved. One of the best-performing recurrent network architectures, the LSTM, propagates information through time via summation—a particular straightforward kind of such linear activation. This is discussed further in section 10.10.

6.3.2 Logistic Sigmoid and Hyperbolic Tangent

Prior to the introduction of rectified linear units, most neural networks used the logistic sigmoid activation function

$$g(z) = \sigma(z) \tag{6.38}$$

or the hyperbolic tangent activation function

$$g(z) = \tanh(z). \tag{6.39}$$

These activation functions are closely related because $\tanh(z) = 2\sigma(2z) - 1$.

We have already seen sigmoid units as output units, used to predict the probability that a binary variable is 1. Unlike piecewise linear units, sigmoidal units saturate across most of their domain—they saturate to a high value when z is very positive, saturate to a low value when z is very negative, and are only strongly sensitive to their input when z is near 0. The widespread saturation of sigmoidal units can make gradient-based learning very difficult. For this reason, their use as hidden units in feedforward networks is now discouraged. Their use as output units is compatible with the use of gradient-based learning when an appropriate cost function can undo the saturation of the sigmoid in the output layer.

When a sigmoidal activation function must be used, the hyperbolic tangent activation function typically performs better than the logistic sigmoid. It resembles the identity function more closely, in the sense that $\tanh(0) = 0$ while $\sigma(0) = \frac{1}{2}$. Because tanh is similar to the identity function near 0, training a deep neural network $\hat{y} = \boldsymbol{w}^\top \tanh(\boldsymbol{U}^\top \tanh(\boldsymbol{V}^\top \boldsymbol{x}))$ resembles training a linear model $\hat{y} = \boldsymbol{w}^\top \boldsymbol{U}^\top \boldsymbol{V}^\top \boldsymbol{x}$ so long as the activations of the network can be kept small. This makes training the tanh network easier.

Sigmoidal activation functions are more common in settings other than feed-forward networks. Recurrent networks, many probabilistic models, and some autoencoders have additional requirements that rule out the use of piecewise linear activation functions and make sigmoidal units more appealing despite the drawbacks of saturation.

6.3.3 Other Hidden Units

Many other types of hidden units are possible, but are used less frequently.

In general, a wide variety of differentiable functions perform perfectly well. Many unpublished activation functions perform just as well as the popular ones. To provide a concrete example, the authors tested a feedforward network using $\boldsymbol{h} = \cos(\boldsymbol{W}\boldsymbol{x} + \boldsymbol{b})$ on the MNIST dataset and obtained an error rate of less than 1%, which is competitive with results obtained using more conventional activation functions. During research and development of new techniques, it is common to test many different activation functions and find that several variations on standard practice perform comparably. This means that usually new hidden unit types are published only if they are clearly demonstrated to provide a significant improvement. New hidden unit types that perform roughly comparably to known types are so common as to be uninteresting.

It would be impractical to list all of the hidden unit types that have appeared in the literature. We highlight a few especially useful and distinctive ones.

One possibility is to not have an activation $g(z)$ at all. One can also think of this as using the identity function as the activation function. We have already seen that a linear unit can be useful as the output of a neural network. It may also be used as a hidden unit. If every layer of the neural network consists of only linear transformations, then the network as a whole will be linear. However, it is acceptable for some layers of the neural network to be purely linear. Consider a neural network layer with n inputs and p outputs, $\boldsymbol{h} = g(\boldsymbol{W}^\top \boldsymbol{x} + \boldsymbol{b})$. We may replace this with two layers, with one layer using weight matrix $\boldsymbol{U}$ and the other using weight matrix $\boldsymbol{V}$. If the first layer has no activation function, then we have essentially factored the weight matrix of the original layer based on $\boldsymbol{W}$. The factored approach is to compute $\boldsymbol{h} = g(\boldsymbol{V}^\top \boldsymbol{U}^\top \boldsymbol{x} + \boldsymbol{b})$. If $\boldsymbol{U}$ produces q outputs, then $\boldsymbol{U}$ and $\boldsymbol{V}$ together contain only $(n + p)q$ parameters, while $\boldsymbol{W}$ contains np parameters. For small q, this can be a considerable saving in parameters. It comes at the cost of constraining the linear transformation to be low-rank, but these low-rank relationships are often sufficient. Linear hidden units thus offer an effective way of reducing the number of parameters in a network.

Softmax units are another kind of unit that is usually used as an output (as described in section 6.2.2.3) but may sometimes be used as a hidden unit. Softmax units naturally represent a probability distribution over a discrete variable with k possible values, so they may be used as a kind of switch. These kinds of hidden units are usually only used in more advanced architectures that explicitly learn to manipulate memory, described in section 10.12.

A few other reasonably common hidden unit types include:

- **Radial basis function** or RBF unit: $h_i = \exp\left(-\frac{1}{\sigma_i^2}||\boldsymbol{W}_{:,i} - \boldsymbol{x}||^2\right)$. This function becomes more active as $\boldsymbol{x}$ approaches a template $\boldsymbol{W}_{:,i}$. Because it saturates to 0 for most $\boldsymbol{x}$, it can be difficult to optimize.

- **Softplus**: $g(a) = \zeta(a) = \log(1+e^a)$. This is a smooth version of the rectifier, introduced by Dugas *et al.* (2001) for function approximation and by Nair and Hinton (2010) for the conditional distributions of undirected probabilistic models. Glorot *et al.* (2011a) compared the softplus and rectifier and found better results with the latter. The use of the softplus is generally discouraged. The softplus demonstrates that the performance of hidden unit types can be very counterintuitive—one might expect it to have an advantage over the rectifier due to being differentiable everywhere or due to saturating less completely, but empirically it does not.

- **Hard** tanh: this is shaped similarly to the tanh and the rectifier but unlike the latter, it is bounded, $g(a) = \max(-1, \min(1, a))$. It was introduced by Collobert (2004).

Hidden unit design remains an active area of research and many useful hidden unit types remain to be discovered.

6.4 Architecture Design

Another key design consideration for neural networks is determining the architecture. The word **architecture** refers to the overall structure of the network: how many units it should have and how these units should be connected to each other.

Most neural networks are organized into groups of units called layers. Most neural network architectures arrange these layers in a chain structure, with each layer being a function of the layer that preceded it. In this structure, the first layer is given by

$$\boldsymbol{h}^{(1)} = g^{(1)}\left(\boldsymbol{W}^{(1)\top}\boldsymbol{x} + \boldsymbol{b}^{(1)}\right), \tag{6.40}$$

the second layer is given by

$$\boldsymbol{h}^{(2)} = g^{(2)}\left(\boldsymbol{W}^{(2)\top}\boldsymbol{h}^{(1)} + \boldsymbol{b}^{(2)}\right), \tag{6.41}$$

and so on.

In these chain-based architectures, the main architectural considerations are to choose the depth of the network and the width of each layer. As we will see, a network with even one hidden layer is sufficient to fit the training set. Deeper networks often are able to use far fewer units per layer and far fewer parameters and often generalize to the test set, but are also often harder to optimize. The ideal network architecture for a task must be found via experimentation guided by monitoring the validation set error.

6.4.1 Universal Approximation Properties and Depth

A linear model, mapping from features to outputs via matrix multiplication, can by definition represent only linear functions. It has the advantage of being easy to train because many loss functions result in convex optimization problems when applied to linear models. Unfortunately, we often want to learn nonlinear functions.

At first glance, we might presume that learning a nonlinear function requires designing a specialized model family for the kind of nonlinearity we want to learn. Fortunately, feedforward networks with hidden layers provide a universal approximation framework. Specifically, the **universal approximation theorem** (Hornik *et al.*, 1989; Cybenko, 1989) states that a feedforward network with a linear output layer and at least one hidden layer with any "squashing" activation function (such as the logistic sigmoid activation function) can approximate any Borel measurable function from one finite-dimensional space to another with any desired non-zero amount of error, provided that the network is given enough hidden units. The derivatives of the feedforward network can also approximate the derivatives of the function arbitrarily well (Hornik *et al.*, 1990). The concept of Borel measurability is beyond the scope of this book; for our purposes it suffices to say that any continuous function on a closed and bounded subset of $\mathbb{R}^n$ is Borel measurable and therefore may be approximated by a neural network. A neural network may also approximate any function mapping from any finite dimensional discrete space to another. While the original theorems were first stated in terms of units with activation functions that saturate both for very negative and for very positive arguments, universal approximation theorems have also been proved for a wider class of activation functions, which includes the now commonly used rectified linear unit (Leshno *et al.*, 1993).

The universal approximation theorem means that regardless of what function we are trying to learn, we know that a large MLP will be able to *represent* this function. However, we are not guaranteed that the training algorithm will be able to *learn* that function. Even if the MLP is able to represent the function, learning can fail for two different reasons. First, the optimization algorithm used for training may not be able to find the value of the parameters that corresponds to the desired function. Second, the training algorithm might choose the wrong function due to overfitting. Recall from section 5.2.1 that the "no free lunch" theorem shows that there is no universally superior machine learning algorithm. Feedforward networks provide a universal system for representing functions, in the sense that, given a function, there exists a feedforward network that approximates the function. There is no universal procedure for examining a training set of specific examples and choosing a function that will generalize to points not in the training set.

The universal approximation theorem says that there exists a network large enough to achieve any degree of accuracy we desire, but the theorem does not say how large this network will be. Barron (1993) provides some bounds on the size of a single-layer network needed to approximate a broad class of functions. Unfortunately, in the worse case, an exponential number of hidden units (possibly with one hidden unit corresponding to each input configuration that needs to be distinguished) may be required. This is easiest to see in the binary case: the number of possible binary functions on vectors $\boldsymbol{v} \in \{0, 1\}^n$ is 2^{2^n} and selecting one such function requires 2^n bits, which will in general require $O(2^n)$ degrees of freedom.

In summary, a feedforward network with a single layer is sufficient to represent any function, but the layer may be infeasibly large and may fail to learn and generalize correctly. In many circumstances, using deeper models can reduce the number of units required to represent the desired function and can reduce the amount of generalization error.

There exist families of functions which can be approximated efficiently by an architecture with depth greater than some value d, but which require a much larger model if depth is restricted to be less than or equal to d. In many cases, the number of hidden units required by the shallow model is exponential in n. Such results were first proved for models that do not resemble the continuous, differentiable neural networks used for machine learning, but have since been extended to these models. The first results were for circuits of logic gates (Håstad, 1986). Later work extended these results to linear threshold units with non-negative weights (Håstad and Goldmann, 1991; Hajnal *et al.*, 1993), and then to networks with continuous-valued activations (Maass, 1992; Maass *et al.*, 1994). Many modern neural networks use rectified linear units. Leshno *et al.* (1993) demonstrated that shallow networks with a broad family of non-polynomial activation functions, including rectified linear units, have universal approximation properties, but these results do not address the questions of depth or efficiency—they specify only that a sufficiently wide rectifier network could represent any function. Montufar *et al.*

(2014) showed that functions representable with a deep rectifier net can require an exponential number of hidden units with a shallow (one hidden layer) network. More precisely, they showed that piecewise linear networks (which can be obtained from rectifier nonlinearities or maxout units) can represent functions with a number of regions that is exponential in the depth of the network. Figure 6.5 illustrates how a network with absolute value rectification creates mirror images of the function computed on top of some hidden unit, with respect to the input of that hidden unit. Each hidden unit specifies where to fold the input space in order to create mirror responses (on both sides of the absolute value nonlinearity). By composing these folding operations, we obtain an exponentially large number of piecewise linear regions which can capture all kinds of regular (e.g., repeating) patterns.

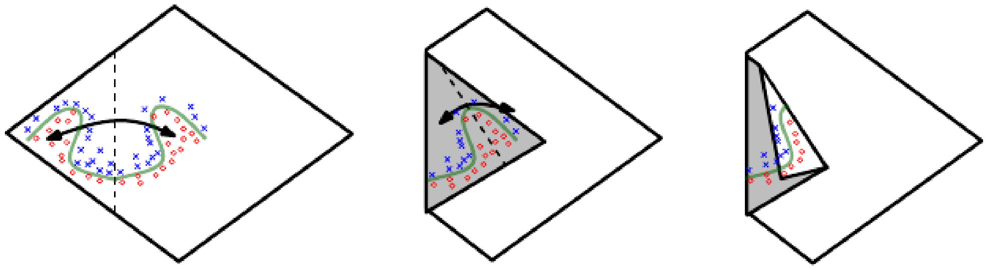

Figure 6.5: An intuitive, geometric explanation of the exponential advantage of deeper rectifier networks formally by Montufar *et al.* (2014). *(Left)*An absolute value rectification unit has the same output for every pair of mirror points in its input. The mirror axis of symmetry is given by the hyperplane defined by the weights and bias of the unit. A function computed on top of that unit (the green decision surface) will be a mirror image of a simpler pattern across that axis of symmetry. *(Center)*The function can be obtained by folding the space around the axis of symmetry. *(Right)*Another repeating pattern can be folded on top of the first (by another downstream unit) to obtain another symmetry (which is now repeated four times, with two hidden layers). Figure reproduced with permission from Montufar *et al.* (2014).

More precisely, the main theorem in Montufar *et al.* (2014) states that the number of linear regions carved out by a deep rectifier network with d inputs, depth l, and n units per hidden layer, is

$$O\left(\binom{n}{d}^{d(l-1)} n^d\right), \tag{6.42}$$

i.e., exponential in the depth l. In the case of maxout networks with k filters per unit, the number of linear regions is

$$O\left(k^{(l-1)+d}\right). \tag{6.43}$$

Of course, there is no guarantee that the kinds of functions we want to learn in applications of machine learning (and in particular for AI) share such a property.

We may also want to choose a deep model for statistical reasons. Any time we choose a specific machine learning algorithm, we are implicitly stating some set of prior beliefs we have about what kind of function the algorithm should learn. Choosing a deep model encodes a very general belief that the function we want to learn should involve composition of several simpler functions. This can be interpreted from a representation learning point of view as saying that we believe the learning problem consists of discovering a set of underlying factors of variation that can in turn be described in terms of other, simpler underlying factors of variation. Alternately, we can interpret the use of a deep architecture as expressing a belief that the function we want to learn is a computer program consisting of multiple steps, where each step makes use of the previous step's output. These intermediate outputs are not necessarily factors of variation, but can instead be analogous to counters or pointers that the network uses to organize its internal processing. Empirically, greater depth does seem to result in better generalization for a wide variety of tasks (Bengio *et al.*, 2007; Erhan *et al.*, 2009; Bengio, 2009; Mesnil *et al.*, 2011; Ciresan *et al.*, 2012; Krizhevsky *et al.*, 2012; Sermanet *et al.*, 2013; Farabet *et al.*, 2013; Couprie *et al.*, 2013; Kahou *et al.*, 2013; Goodfellow *et al.*, 2014d; Szegedy *et al.*, 2014a). See figure 6.6 and figure 6.7 for examples of some of these empirical results. This suggests that using deep architectures does indeed express a useful prior over the space of functions the model learns.

6.4.2 Other Architectural Considerations

So far we have described neural networks as being simple chains of layers, with the main considerations being the depth of the network and the width of each layer. In practice, neural networks show considerably more diversity.

Many neural network architectures have been developed for specific tasks. Specialized architectures for computer vision called convolutional networks are described in chapter 9. Feedforward networks may also be generalized to the recurrent neural networks for sequence processing, described in chapter 10, which have their own architectural considerations.

In general, the layers need not be connected in a chain, even though this is the most common practice. Many architectures build a main chain but then add extra architectural features to it, such as skip connections going from layer i to layer $i+2$ or higher. These skip connections make it easier for the gradient to flow from output layers to layers nearer the input.

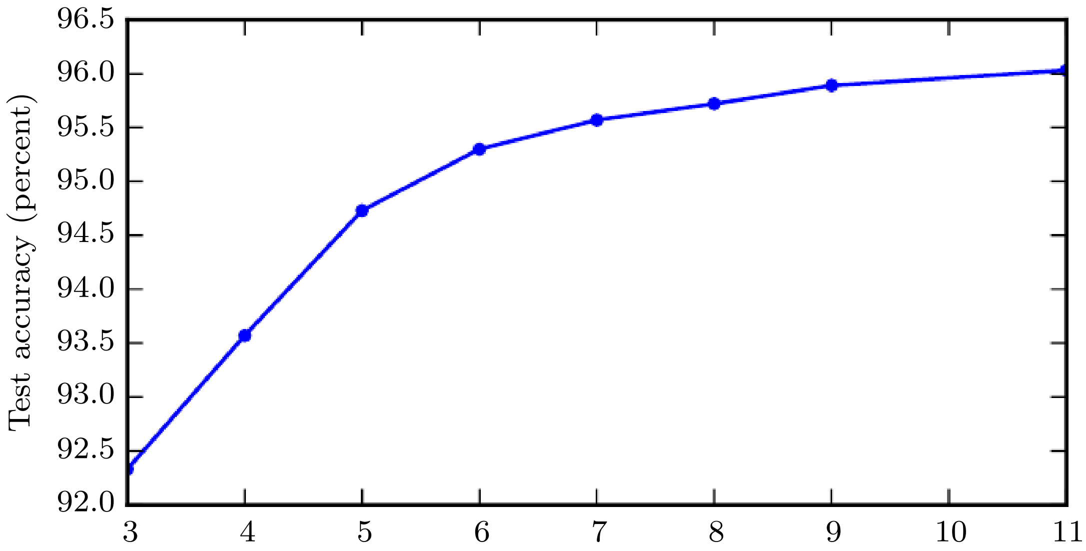

Figure 6.6: Empirical results showing that deeper networks generalize better when used to transcribe multi-digit numbers from photographs of addresses. Data from Goodfellow *et al.* (2014d). The test set accuracy consistently increases with increasing depth. See figure 6.7 for a control experiment demonstrating that other increases to the model size do not yield the same effect.

Another key consideration of architecture design is exactly how to connect a pair of layers to each other. In the default neural network layer described by a linear transformation via a matrix $\boldsymbol{W}$, every input unit is connected to every output unit. Many specialized networks in the chapters ahead have fewer connections, so that each unit in the input layer is connected to only a small subset of units in the output layer. These strategies for reducing the number of connections reduce the number of parameters and the amount of computation required to evaluate the network, but are often highly problem-dependent. For example, convolutional networks, described in chapter 9, use specialized patterns of sparse connections that are very effective for computer vision problems. In this chapter, it is difficult to give much more specific advice concerning the architecture of a generic neural network. Subsequent chapters develop the particular architectural strategies that have been found to work well for different application domains.

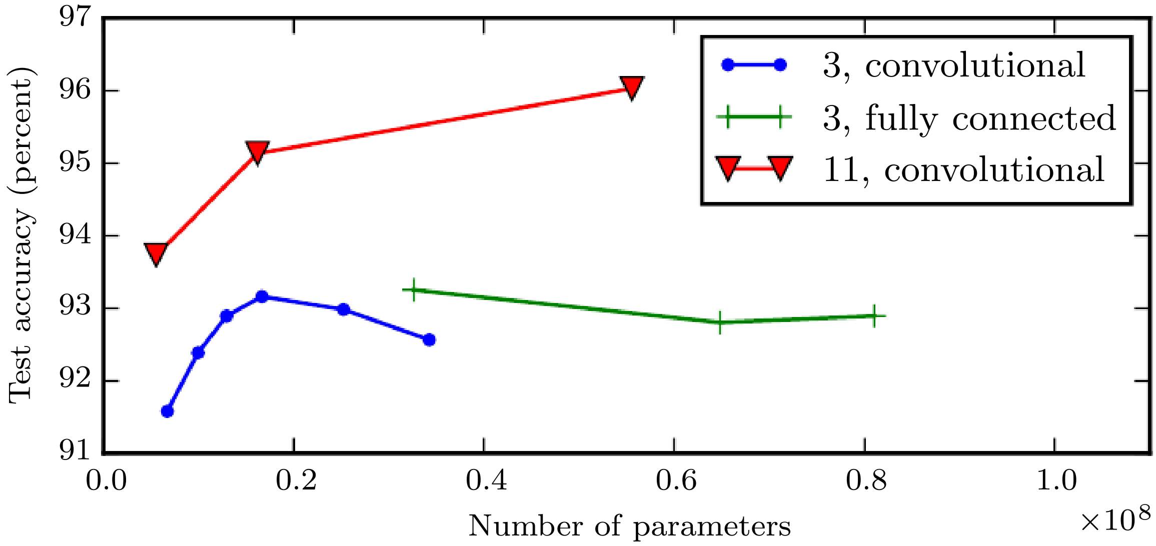

Figure 6.7: Deeper models tend to perform better. This is not merely because the model is larger. This experiment from Goodfellow *et al.* (2014d) shows that increasing the number of parameters in layers of convolutional networks without increasing their depth is not nearly as effective at increasing test set performance. The legend indicates the depth of network used to make each curve and whether the curve represents variation in the size of the convolutional or the fully connected layers. We observe that shallow models in this context overfit at around 20 million parameters while deep ones can benefit from having over 60 million. This suggests that using a deep model expresses a useful preference over the space of functions the model can learn. Specifically, it expresses a belief that the function should consist of many simpler functions composed together. This could result either in learning a representation that is composed in turn of simpler representations (e.g., corners defined in terms of edges) or in learning a program with sequentially dependent steps (e.g., first locate a set of objects, then segment them from each other, then recognize them).

6.5 Back-Propagation and Other Differentiation Algorithms

When we use a feedforward neural network to accept an input $\boldsymbol{x}$ and produce an output $\hat{\boldsymbol{y}}$, information flows forward through the network. The inputs $\boldsymbol{x}$ provide the initial information that then propagates up to the hidden units at each layer and finally produces $\hat{\boldsymbol{y}}$. This is called **forward propagation**. During training, forward propagation can continue onward until it produces a scalar cost $J(\boldsymbol{\theta})$. The **back-propagation** algorithm (Rumelhart *et al.*, 1986a), often simply called **backprop**, allows the information from the cost to then flow backwards through the network, in order to compute the gradient.

Computing an analytical expression for the gradient is straightforward, but numerically evaluating such an expression can be computationally expensive. The back-propagation algorithm does so using a simple and inexpensive procedure.

The term back-propagation is often misunderstood as meaning the whole learning algorithm for multi-layer neural networks. Actually, back-propagation refers only to the method for computing the gradient, while another algorithm, such as stochastic gradient descent, is used to perform learning using this gradient. Furthermore, back-propagation is often misunderstood as being specific to multi-layer neural networks, but in principle it can compute derivatives of any function (for some functions, the correct response is to report that the derivative of the function is undefined). Specifically, we will describe how to compute the gradient $\nabla_{\boldsymbol{x}} f(\boldsymbol{x}, \boldsymbol{y})$ for an arbitrary function f, where $\boldsymbol{x}$ is a set of variables whose derivatives are desired, and $\boldsymbol{y}$ is an additional set of variables that are inputs to the function but whose derivatives are not required. In learning algorithms, the gradient we most often require is the gradient of the cost function with respect to the parameters, $\nabla_{\boldsymbol{\theta}} J(\boldsymbol{\theta})$. Many machine learning tasks involve computing other derivatives, either as part of the learning process, or to analyze the learned model. The back-propagation algorithm can be applied to these tasks as well, and is not restricted to computing the gradient of the cost function with respect to the parameters. The idea of computing derivatives by propagating information through a network is very general, and can be used to compute values such as the Jacobian of a function f with multiple outputs. We restrict our description here to the most commonly used case where f has a single output.

6.5.1 Computational Graphs

So far we have discussed neural networks with a relatively informal graph language. To describe the back-propagation algorithm more precisely, it is helpful to have a more precise **computational graph** language.

Many ways of formalizing computation as graphs are possible.

Here, we use each node in the graph to indicate a variable. The variable may be a scalar, vector, matrix, tensor, or even a variable of another type.

To formalize our graphs, we also need to introduce the idea of an **operation**. An operation is a simple function of one or more variables. Our graph language is accompanied by a set of allowable operations. Functions more complicated than the operations in this set may be described by composing many operations together.

Without loss of generality, we define an operation to return only a single output variable. This does not lose generality because the output variable can have multiple entries, such as a vector. Software implementations of back-propagation usually support operations with multiple outputs, but we avoid this case in our description because it introduces many extra details that are not important to conceptual understanding.

If a variable y is computed by applying an operation to a variable x, then we draw a directed edge from x to y. We sometimes annotate the output node with the name of the operation applied, and other times omit this label when the operation is clear from context.

Examples of computational graphs are shown in figure 6.8.

6.5.2 Chain Rule of Calculus

The chain rule of calculus (not to be confused with the chain rule of probability) is used to compute the derivatives of functions formed by composing other functions whose derivatives are known. Back-propagation is an algorithm that computes the chain rule, with a specific order of operations that is highly efficient.

Let x be a real number, and let f and g both be functions mapping from a real number to a real number. Suppose that $y = g(x)$ and $z = f(g(x)) = f(y)$. Then the chain rule states that

$$\frac{dz}{dx} = \frac{dz}{dy}\frac{dy}{dx}. \tag{6.44}$$

We can generalize this beyond the scalar case. Suppose that $\boldsymbol{x} \in \mathbb{R}^m$, $\boldsymbol{y} \in \mathbb{R}^n$,

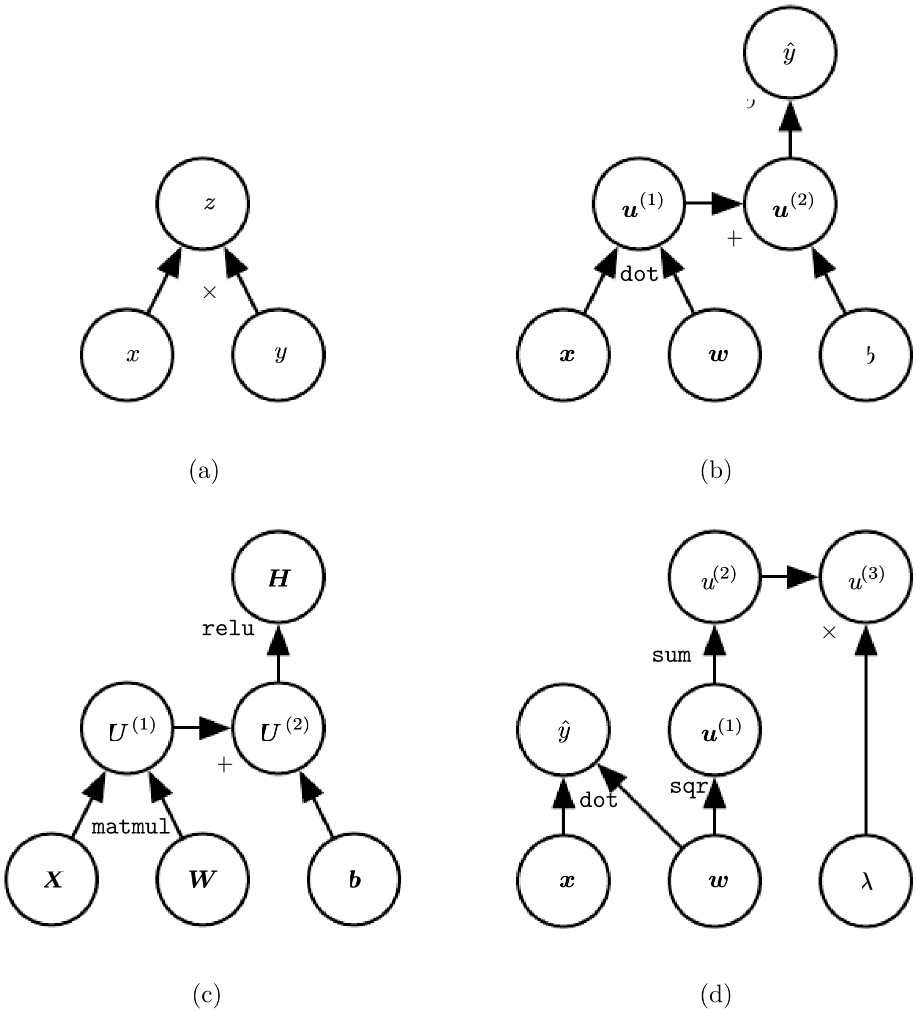

Figure 6.8: Examples of computational graphs. *(a)*The graph using the $\times$ operation to compute $z = xy$. *(b)*The graph for the logistic regression prediction $\hat{y} = \sigma\left(\boldsymbol{x}^\top \boldsymbol{w} + b\right)$. Some of the intermediate expressions do not have names in the algebraic expression but need names in the graph. We simply name the i-th such variable $\boldsymbol{u}^{(i)}$. *(c)*The computational graph for the expression $\boldsymbol{H} = \max\{0, \boldsymbol{X}\boldsymbol{W} + \boldsymbol{b}\}$, which computes a design matrix of rectified linear unit activations $\boldsymbol{H}$ given a design matrix containing a minibatch of inputs $\boldsymbol{X}$. *(d)*Examples a–c applied at most one operation to each variable, but it is possible to apply more than one operation. Here we show a computation graph that applies more than one operation to the weights $\boldsymbol{w}$ of a linear regression model. The weights are used to make both the prediction $\hat{y}$ and the weight decay penalty $\lambda \sum_i w_i^2$.

g maps from $\mathbb{R}^m$ to $\mathbb{R}^n$, and f maps from $\mathbb{R}^n$ to $\mathbb{R}$. If $\boldsymbol{y} = g(\boldsymbol{x})$ and $z = f(\boldsymbol{y})$, then

$$\frac{\partial z}{\partial x_i} = \sum_j \frac{\partial z}{\partial y_j} \frac{\partial y_j}{\partial x_i}. \tag{6.45}$$

In vector notation, this may be equivalently written as

$$\nabla_{\boldsymbol{x}} z = \left(\frac{\partial \boldsymbol{y}}{\partial \boldsymbol{x}} \right)^\top \nabla_{\boldsymbol{y}} z, \tag{6.46}$$

where $\frac{\partial \boldsymbol{y}}{\partial \boldsymbol{x}}$ is the $n \times m$ Jacobian matrix of g.

From this we see that the gradient of a variable $\boldsymbol{x}$ can be obtained by multiplying a Jacobian matrix $\frac{\partial \boldsymbol{y}}{\partial \boldsymbol{x}}$ by a gradient $\nabla_{\boldsymbol{y}} z$. The back-propagation algorithm consists of performing such a Jacobian-gradient product for each operation in the graph.

Usually we do not apply the back-propagation algorithm merely to vectors, but rather to tensors of arbitrary dimensionality. Conceptually, this is exactly the same as back-propagation with vectors. The only difference is how the numbers are arranged in a grid to form a tensor. We could imagine flattening each tensor into a vector before we run back-propagation, computing a vector-valued gradient, and then reshaping the gradient back into a tensor. In this rearranged view, back-propagation is still just multiplying Jacobians by gradients.

To denote the gradient of a value z with respect to a tensor X, we write $\nabla_{\mathsf{X}} z$, just as if X were a vector. The indices into X now have multiple coordinates—for example, a 3-D tensor is indexed by three coordinates. We can abstract this away by using a single variable i to represent the complete tuple of indices. For all possible index tuples i, $(\nabla_{\mathsf{X}} z)_i$ gives $\frac{\partial z}{\partial \mathsf{X}_i}$. This is exactly the same as how for all possible integer indices i into a vector, $(\nabla_{\boldsymbol{x}} z)_i$ gives $\frac{\partial z}{\partial x_i}$. Using this notation, we can write the chain rule as it applies to tensors. If $\mathsf{Y} = g(\mathsf{X})$ and $z = f(\mathsf{Y})$, then

$$\nabla_{\mathsf{X}} z = \sum_j (\nabla_{\mathsf{X}} \mathsf{Y}_j) \frac{\partial z}{\partial \mathsf{Y}_j}. \tag{6.47}$$

6.5.3 Recursively Applying the Chain Rule to Obtain Backprop

Using the chain rule, it is straightforward to write down an algebraic expression for the gradient of a scalar with respect to any node in the computational graph that produced that scalar. However, actually evaluating that expression in a computer introduces some extra considerations.

Specifically, many subexpressions may be repeated several times within the overall expression for the gradient. Any procedure that computes the gradient will need to choose whether to store these subexpressions or to recompute them several times. An example of how these repeated subexpressions arise is given in figure 6.9. In some cases, computing the same subexpression twice would simply be wasteful. For complicated graphs, there can be exponentially many of these wasted computations, making a naive implementation of the chain rule infeasible. In other cases, computing the same subexpression twice could be a valid way to reduce memory consumption at the cost of higher runtime.

We first begin by a version of the back-propagation algorithm that specifies the actual gradient computation directly (algorithm 6.2 along with algorithm 6.1 for the associated forward computation), in the order it will actually be done and according to the recursive application of chain rule. One could either directly perform these computations or view the description of the algorithm as a symbolic specification of the computational graph for computing the back-propagation. However, this formulation does not make explicit the manipulation and the construction of the symbolic graph that performs the gradient computation. Such a formulation is presented below in section 6.5.6, with algorithm 6.5, where we also generalize to nodes that contain arbitrary tensors.

First consider a computational graph describing how to compute a single scalar $u^{(n)}$ (say the loss on a training example). This scalar is the quantity whose gradient we want to obtain, with respect to the n_i input nodes $u^{(1)}$ to $u^{(n_i)}$. In other words we wish to compute $\frac{\partial u^{(n)}}{\partial u^{(i)}}$ for all $i \in \{1, 2, \ldots, n_i\}$. In the application of back-propagation to computing gradients for gradient descent over parameters, $u^{(n)}$ will be the cost associated with an example or a minibatch, while $u^{(1)}$ to $u^{(n_i)}$ correspond to the parameters of the model.

We will assume that the nodes of the graph have been ordered in such a way that we can compute their output one after the other, starting at $u^{(n_i+1)}$ and going up to $u^{(n)}$. As defined in algorithm 6.1, each node $u^{(i)}$ is associated with an operation $f^{(i)}$ and is computed by evaluating the function

$$u^{(i)} = f(\mathbb{A}^{(i)}) \tag{6.48}$$

where $\mathbb{A}^{(i)}$ is the set of all nodes that are parents of $u^{(i)}$.

That algorithm specifies the forward propagation computation, which we could put in a graph $\mathcal{G}$. In order to perform back-propagation, we can construct a computational graph that depends on $\mathcal{G}$ and adds to it an extra set of nodes. These form a subgraph $\mathcal{B}$ with one node per node of $\mathcal{G}$. Computation in $\mathcal{B}$ proceeds in exactly the reverse of the order of computation in $\mathcal{G}$, and each node of $\mathcal{B}$ computes the derivative $\frac{\partial u^{(n)}}{\partial u^{(i)}}$ associated with the forward graph node $u^{(i)}$. This is done

Algorithm 6.1 A procedure that performs the computations mapping n_i inputs $u^{(1)}$ to $u^{(n_i)}$ to an output $u^{(n)}$. This defines a computational graph where each node computes numerical value $u^{(i)}$ by applying a function $f^{(i)}$ to the set of arguments $\mathbb{A}^{(i)}$ that comprises the values of previous nodes $u^{(j)}$, $j < i$, with $j \in Pa(u^{(i)})$. The input to the computational graph is the vector $\boldsymbol{x}$, and is set into the first n_i nodes $u^{(1)}$ to $u^{(n_i)}$. The output of the computational graph is read off the last (output) node $u^{(n)}$.

for $i = 1, \ldots, n_i$ **do**
  $u^{(i)} \leftarrow x_i$
end for
for $i = n_i + 1, \ldots, n$ **do**
  $\mathbb{A}^{(i)} \leftarrow \{u^{(j)} \mid j \in Pa(u^{(i)})\}$
  $u^{(i)} \leftarrow f^{(i)}(\mathbb{A}^{(i)})$
end for
return $u^{(n)}$

using the chain rule with respect to scalar output $u^{(n)}$:

$$\frac{\partial u^{(n)}}{\partial u^{(j)}} = \sum_{i:j \in Pa(u^{(i)})} \frac{\partial u^{(n)}}{\partial u^{(i)}} \frac{\partial u^{(i)}}{\partial u^{(j)}} \tag{6.49}$$

as specified by algorithm 6.2. The subgraph $\mathcal{B}$ contains exactly one edge for each edge from node $u^{(j)}$ to node $u^{(i)}$ of $\mathcal{G}$. The edge from $u^{(j)}$ to $u^{(i)}$ is associated with the computation of $\frac{\partial u^{(i)}}{\partial u^{(j)}}$. In addition, a dot product is performed for each node, between the gradient already computed with respect to nodes $u^{(i)}$ that are children of $u^{(j)}$ and the vector containing the partial derivatives $\frac{\partial u^{(i)}}{\partial u^{(j)}}$ for the same children nodes $u^{(i)}$. To summarize, the amount of computation required for performing the back-propagation scales linearly with the number of edges in $\mathcal{G}$, where the computation for each edge corresponds to computing a partial derivative (of one node with respect to one of its parents) as well as performing one multiplication and one addition. Below, we generalize this analysis to tensor-valued nodes, which is just a way to group multiple scalar values in the same node and enable more efficient implementations.

The back-propagation algorithm is designed to reduce the number of common subexpressions without regard to memory. Specifically, it performs on the order of one Jacobian product per node in the graph. This can be seen from the fact that backprop (algorithm 6.2) visits each edge from node $u^{(j)}$ to node $u^{(i)}$ of the graph exactly once in order to obtain the associated partial derivative $\frac{\partial u^{(i)}}{\partial u^{(j)}}$.

Algorithm 6.2 Simplified version of the back-propagation algorithm for computing the derivatives of $u^{(n)}$ with respect to the variables in the graph. This example is intended to further understanding by showing a simplified case where all variables are scalars, and we wish to compute the derivatives with respect to $u^{(1)}, \ldots, u^{(n_i)}$. This simplified version computes the derivatives of all nodes in the graph. The computational cost of this algorithm is proportional to the number of edges in the graph, assuming that the partial derivative associated with each edge requires a constant time. This is of the same order as the number of computations for the forward propagation. Each $\frac{\partial u^{(i)}}{\partial u^{(j)}}$ is a function of the parents $u^{(j)}$ of $u^{(i)}$, thus linking the nodes of the forward graph to those added for the back-propagation graph.

Run forward propagation (algorithm 6.1 for this example) to obtain the activations of the network

Initialize `grad_table`, a data structure that will store the derivatives that have been computed. The entry $\texttt{grad\_table}[u^{(i)}]$ will store the computed value of $\frac{\partial u^{(n)}}{\partial u^{(i)}}$.

$\texttt{grad\_table}[u^{(n)}] \leftarrow 1$

for $j = n - 1$ down to 1 **do**

  The next line computes $\frac{\partial u^{(n)}}{\partial u^{(j)}} = \sum_{i:j \in Pa(u^{(i)})} \frac{\partial u^{(n)}}{\partial u^{(i)}} \frac{\partial u^{(i)}}{\partial u^{(j)}}$ using stored values:

  $\texttt{grad\_table}[u^{(j)}] \leftarrow \sum_{i:j \in Pa(u^{(i)})} \texttt{grad\_table}[u^{(i)}] \frac{\partial u^{(i)}}{\partial u^{(j)}}$

end for

return $\{\texttt{grad\_table}[u^{(i)}] \mid i = 1, \ldots, n_i\}$

Back-propagation thus avoids the exponential explosion in repeated subexpressions. However, other algorithms may be able to avoid more subexpressions by performing simplifications on the computational graph, or may be able to conserve memory by recomputing rather than storing some subexpressions. We will revisit these ideas after describing the back-propagation algorithm itself.

6.5.4 Back-Propagation Computation in Fully-Connected MLP

To clarify the above definition of the back-propagation computation, let us consider the specific graph associated with a fully-connected multi-layer MLP.

Algorithm 6.3 first shows the forward propagation, which maps parameters to the supervised loss $L(\hat{\boldsymbol{y}}, \boldsymbol{y})$ associated with a single (input,target) training example $(\boldsymbol{x}, \boldsymbol{y})$, with $\hat{\boldsymbol{y}}$ the output of the neural network when $\boldsymbol{x}$ is provided in input.

Algorithm 6.4 then shows the corresponding computation to be done for

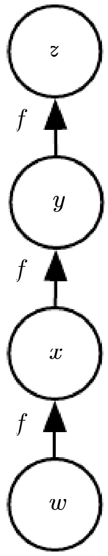

Figure 6.9: A computational graph that results in repeated subexpressions when computing the gradient. Let $w \in \mathbb{R}$ be the input to the graph. We use the same function $f : \mathbb{R} \rightarrow \mathbb{R}$ as the operation that we apply at every step of a chain: $x = f(w)$, $y = f(x)$, $z = f(y)$. To compute $\frac{\partial z}{\partial w}$, we apply equation 6.44 and obtain:

$$\frac{\partial z}{\partial w} \tag{6.50}$$

$$= \frac{\partial z}{\partial y}\frac{\partial y}{\partial x}\frac{\partial x}{\partial w} \tag{6.51}$$

$$= f'(y)f'(x)f'(w) \tag{6.52}$$

$$= f'(f(f(w)))f'(f(w))f'(w) \tag{6.53}$$

Equation 6.52 suggests an implementation in which we compute the value of $f(w)$ only once and store it in the variable x. This is the approach taken by the back-propagation algorithm. An alternative approach is suggested by equation 6.53, where the subexpression $f(w)$ appears more than once. In the alternative approach, $f(w)$ is recomputed each time it is needed. When the memory required to store the value of these expressions is low, the back-propagation approach of equation 6.52 is clearly preferable because of its reduced runtime. However, equation 6.53 is also a valid implementation of the chain rule, and is useful when memory is limited.

applying the back-propagation algorithm to this graph.

Algorithms 6.3 and 6.4 are demonstrations that are chosen to be simple and straightforward to understand. However, they are specialized to one specific problem.

Modern software implementations are based on the generalized form of back-propagation described in section 6.5.6 below, which can accommodate any computational graph by explicitly manipulating a data structure for representing symbolic computation.

Algorithm 6.3 Forward propagation through a typical deep neural network and the computation of the cost function. The loss $L(\hat{\boldsymbol{y}}, \boldsymbol{y})$ depends on the output $\hat{\boldsymbol{y}}$ and on the target $\boldsymbol{y}$ (see section 6.2.1.1 for examples of loss functions). To obtain the total cost J, the loss may be added to a regularizer $\Omega(\theta)$, where θ contains all the parameters (weights and biases). Algorithm 6.4 shows how to compute gradients of J with respect to parameters $\boldsymbol{W}$ and $\boldsymbol{b}$. For simplicity, this demonstration uses only a single input example $\boldsymbol{x}$. Practical applications should use a minibatch. See section 6.5.7 for a more realistic demonstration.

Require: Network depth, l
Require: $\boldsymbol{W}^{(i)}, i \in \{1, \ldots, l\}$, the weight matrices of the model
Require: $\boldsymbol{b}^{(i)}, i \in \{1, \ldots, l\}$, the bias parameters of the model
Require: $\boldsymbol{x}$, the input to process
Require: $\boldsymbol{y}$, the target output
  $\boldsymbol{h}^{(0)} = \boldsymbol{x}$
  for $k = 1, \ldots, l$ **do**
    $\boldsymbol{a}^{(k)} = \boldsymbol{b}^{(k)} + \boldsymbol{W}^{(k)} \boldsymbol{h}^{(k-1)}$
    $\boldsymbol{h}^{(k)} = f(\boldsymbol{a}^{(k)})$
  end for
  $\hat{\boldsymbol{y}} = \boldsymbol{h}^{(l)}$
  $J = L(\hat{\boldsymbol{y}}, \boldsymbol{y}) + \lambda\Omega(\theta)$

6.5.5 Symbol-to-Symbol Derivatives

Algebraic expressions and computational graphs both operate on **symbols**, or variables that do not have specific values. These algebraic and graph-based representations are called **symbolic** representations. When we actually use or train a neural network, we must assign specific values to these symbols. We replace a symbolic input to the network $\boldsymbol{x}$ with a specific **numeric** value, such as $[1.2, 3.765, -1.8]^\top$.

Algorithm 6.4 Backward computation for the deep neural network of algorithm 6.3, which uses in addition to the input $\boldsymbol{x}$ a target $\boldsymbol{y}$. This computation yields the gradients on the activations $\boldsymbol{a}^{(k)}$ for each layer k, starting from the output layer and going backwards to the first hidden layer. From these gradients, which can be interpreted as an indication of how each layer's output should change to reduce error, one can obtain the gradient on the parameters of each layer. The gradients on weights and biases can be immediately used as part of a stochastic gradient update (performing the update right after the gradients have been computed) or used with other gradient-based optimization methods.

After the forward computation, compute the gradient on the output layer:
$\boldsymbol{g} \leftarrow \nabla_{\hat{\boldsymbol{y}}} J = \nabla_{\hat{\boldsymbol{y}}} L(\hat{\boldsymbol{y}}, \boldsymbol{y})$
for $k = l, l-1, \ldots, 1$ **do**
  Convert the gradient on the layer's output into a gradient into the pre-nonlinearity activation (element-wise multiplication if f is element-wise):
  $\boldsymbol{g} \leftarrow \nabla_{\boldsymbol{a}^{(k)}} J = \boldsymbol{g} \odot f'(\boldsymbol{a}^{(k)})$
  Compute gradients on weights and biases (including the regularization term, where needed):
  $\nabla_{\boldsymbol{b}^{(k)}} J = \boldsymbol{g} + \lambda \nabla_{\boldsymbol{b}^{(k)}} \Omega(\theta)$
  $\nabla_{\boldsymbol{W}^{(k)}} J = \boldsymbol{g}\, \boldsymbol{h}^{(k-1)\top} + \lambda \nabla_{\boldsymbol{W}^{(k)}} \Omega(\theta)$
  Propagate the gradients w.r.t. the next lower-level hidden layer's activations:
  $\boldsymbol{g} \leftarrow \nabla_{\boldsymbol{h}^{(k-1)}} J = \boldsymbol{W}^{(k)\top}\, \boldsymbol{g}$
end for

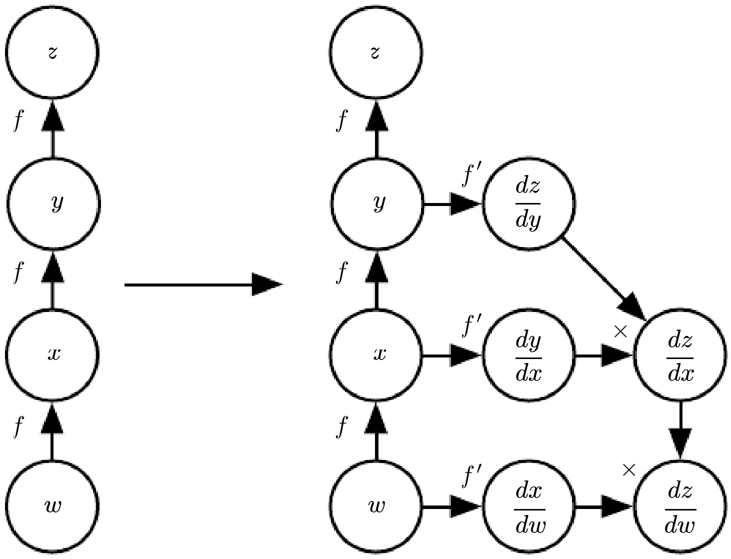

Figure 6.10: An example of the symbol-to-symbol approach to computing derivatives. In this approach, the back-propagation algorithm does not need to ever access any actual specific numeric values. Instead, it adds nodes to a computational graph describing how to compute these derivatives. A generic graph evaluation engine can later compute the derivatives for any specific numeric values. *(Left)*In this example, we begin with a graph representing $z = f(f(f(w)))$. *(Right)*We run the back-propagation algorithm, instructing it to construct the graph for the expression corresponding to $\frac{dz}{dw}$. In this example, we do not explain how the back-propagation algorithm works. The purpose is only to illustrate what the desired result is: a computational graph with a symbolic description of the derivative.

Some approaches to back-propagation take a computational graph and a set of numerical values for the inputs to the graph, then return a set of numerical values describing the gradient at those input values. We call this approach "symbol-to-number" differentiation. This is the approach used by libraries such as Torch (Collobert *et al.*, 2011b) and Caffe (Jia, 2013).

Another approach is to take a computational graph and add additional nodes to the graph that provide a symbolic description of the desired derivatives. This is the approach taken by Theano (Bergstra *et al.*, 2010; Bastien *et al.*, 2012) and TensorFlow (Abadi *et al.*, 2015). An example of how this approach works is illustrated in figure 6.10. The primary advantage of this approach is that the derivatives are described in the same language as the original expression. Because the derivatives are just another computational graph, it is possible to run back-propagation again, differentiating the derivatives in order to obtain higher derivatives. Computation of higher-order derivatives is described in section 6.5.10.

We will use the latter approach and describe the back-propagation algorithm in terms of constructing a computational graph for the derivatives. Any subset of the graph may then be evaluated using specific numerical values at a later time. This allows us to avoid specifying exactly when each operation should be computed. Instead, a generic graph evaluation engine can evaluate every node as soon as its parents' values are available.

The description of the symbol-to-symbol based approach subsumes the symbol-to-number approach. The symbol-to-number approach can be understood as performing exactly the same computations as are done in the graph built by the symbol-to-symbol approach. The key difference is that the symbol-to-number approach does not expose the graph.

6.5.6 General Back-Propagation

The back-propagation algorithm is very simple. To compute the gradient of some scalar z with respect to one of its ancestors $\boldsymbol{x}$ in the graph, we begin by observing that the gradient with respect to z is given by $\frac{dz}{dz} = 1$. We can then compute the gradient with respect to each parent of z in the graph by multiplying the current gradient by the Jacobian of the operation that produced z. We continue multiplying by Jacobians traveling backwards through the graph in this way until we reach $\boldsymbol{x}$. For any node that may be reached by going backwards from z through two or more paths, we simply sum the gradients arriving from different paths at that node.

More formally, each node in the graph $\mathcal{G}$ corresponds to a variable. To achieve maximum generality, we describe this variable as being a tensor V. Tensor can in general have any number of dimensions. They subsume scalars, vectors, and matrices.

We assume that each variable V is associated with the following subroutines:

- `get_operation`(V): This returns the operation that computes V, represented by the edges coming into V in the computational graph. For example, there may be a Python or C++ class representing the matrix multiplication operation, and the `get_operation` function. Suppose we have a variable that is created by matrix multiplication, $\boldsymbol{C} = \boldsymbol{AB}$. Then `get_operation`($\mathsf{V}$) returns a pointer to an instance of the corresponding C++ class.

- `get_consumers`($\mathsf{V}, \mathcal{G}$): This returns the list of variables that are children of V in the computational graph $\mathcal{G}$.

- `get_inputs`($\mathsf{V}, \mathcal{G}$): This returns the list of variables that are parents of V in the computational graph $\mathcal{G}$.

Each operation `op` is also associated with a `bprop` operation. This `bprop` operation can compute a Jacobian-vector product as described by equation 6.47. This is how the back-propagation algorithm is able to achieve great generality. Each operation is responsible for knowing how to back-propagate through the edges in the graph that it participates in. For example, we might use a matrix multiplication operation to create a variable $\boldsymbol{C} = \boldsymbol{AB}$. Suppose that the gradient of a scalar z with respect to $\boldsymbol{C}$ is given by $\boldsymbol{G}$. The matrix multiplication operation is responsible for defining two back-propagation rules, one for each of its input arguments. If we call the `bprop` method to request the gradient with respect to $\boldsymbol{A}$ given that the gradient on the output is $\boldsymbol{G}$, then the `bprop` method of the matrix multiplication operation must state that the gradient with respect to $\boldsymbol{A}$ is given by $\boldsymbol{G}\boldsymbol{B}^\top$. Likewise, if we call the `bprop` method to request the gradient with respect to $\boldsymbol{B}$, then the matrix operation is responsible for implementing the `bprop` method and specifying that the desired gradient is given by $\boldsymbol{A}^\top\boldsymbol{G}$. The back-propagation algorithm itself does not need to know any differentiation rules. It only needs to call each operation's `bprop` rules with the right arguments. Formally, $\texttt{op.bprop}(\texttt{inputs}, \mathsf{X}, \mathsf{G})$ must return

$$\sum_i (\nabla_{\mathsf{X}} \texttt{op.f}(\texttt{inputs})_i)\, \mathsf{G}_i, \tag{6.54}$$

which is just an implementation of the chain rule as expressed in equation 6.47. Here, `inputs` is a list of inputs that are supplied to the operation, `op.f` is the mathematical function that the operation implements, X is the input whose gradient we wish to compute, and G is the gradient on the output of the operation.

The `op.bprop` method should always pretend that all of its inputs are distinct from each other, even if they are not. For example, if the `mul` operator is passed two copies of x to compute x^2, the `op.bprop` method should still return x as the derivative with respect to both inputs. The back-propagation algorithm will later add both of these arguments together to obtain $2x$, which is the correct total derivative on x.

Software implementations of back-propagation usually provide both the operations and their `bprop` methods, so that users of deep learning software libraries are able to back-propagate through graphs built using common operations like matrix multiplication, exponents, logarithms, and so on. Software engineers who build a new implementation of back-propagation or advanced users who need to add their own operation to an existing library must usually derive the `op.bprop` method for any new operations manually.

The back-propagation algorithm is formally described in algorithm 6.5.

Algorithm 6.5 The outermost skeleton of the back-propagation algorithm. This portion does simple setup and cleanup work. Most of the important work happens in the `build_grad` subroutine of algorithm 6.6
.

Require: $\mathbb{T}$, the target set of variables whose gradients must be computed.
Require: $\mathcal{G}$, the computational graph
Require: z, the variable to be differentiated
  Let $\mathcal{G}'$ be $\mathcal{G}$ pruned to contain only nodes that are ancestors of z and descendents of nodes in $\mathbb{T}$.
  Initialize `grad_table`, a data structure associating tensors to their gradients
  `grad_table`$[z] \leftarrow 1$
  for V in $\mathbb{T}$ **do**
    `build_grad`$(\mathsf{V}, \mathcal{G}, \mathcal{G}',$ `grad_table`$)$
  end for
  Return `grad_table` restricted to $\mathbb{T}$

In section 6.5.2, we explained that back-propagation was developed in order to avoid computing the same subexpression in the chain rule multiple times. The naive algorithm could have exponential runtime due to these repeated subexpressions. Now that we have specified the back-propagation algorithm, we can understand its computational cost. If we assume that each operation evaluation has roughly the same cost, then we may analyze the computational cost in terms of the number of operations executed. Keep in mind here that we refer to an operation as the fundamental unit of our computational graph, which might actually consist of very many arithmetic operations (for example, we might have a graph that treats matrix multiplication as a single operation). Computing a gradient in a graph with n nodes will never execute more than $O(n^2)$ operations or store the output of more than $O(n^2)$ operations. Here we are counting operations in the computational graph, not individual operations executed by the underlying hardware, so it is important to remember that the runtime of each operation may be highly variable. For example, multiplying two matrices that each contain millions of entries might correspond to a single operation in the graph. We can see that computing the gradient requires as most $O(n^2)$ operations because the forward propagation stage will at worst execute all n nodes in the original graph (depending on which values we want to compute, we may not need to execute the entire graph). The back-propagation algorithm adds one Jacobian-vector product, which should be expressed with $O(1)$ nodes, per edge in the original graph. Because the computational graph is a directed acyclic graph it has at most $O(n^2)$ edges. For the kinds of graphs that are commonly used in practice, the situation is even better. Most neural network cost functions are

Algorithm 6.6 The inner loop subroutine `build_grad`($\mathsf{V}, \mathcal{G}, \mathcal{G}'$, `grad_table`) of the back-propagation algorithm, called by the back-propagation algorithm defined in algorithm 6.5.

Require: V, the variable whose gradient should be added to $\mathcal{G}$ and `grad_table`.
Require: $\mathcal{G}$, the graph to modify.
Require: $\mathcal{G}'$, the restriction of $\mathcal{G}$ to nodes that participate in the gradient.
Require: `grad_table`, a data structure mapping nodes to their gradients

```
if V is in grad_table then
  Return grad_table[V]
end if
i ← 1
for C in get_consumers(V, G') do
  op ← get_operation(C)
  D ← build_grad(C, G, G', grad_table)
  G^(i) ← op.bprop(get_inputs(C, G'), V, D)
  i ← i + 1
end for
G ← Σ_i G^(i)
grad_table[V] = G
Insert G and the operations creating it into G
Return G
```

roughly chain-structured, causing back-propagation to have $O(n)$ cost. This is far better than the naive approach, which might need to execute exponentially many nodes. This potentially exponential cost can be seen by expanding and rewriting the recursive chain rule (equation 6.49) non-recursively:

$$\frac{\partial u^{(n)}}{\partial u^{(j)}} = \sum_{\substack{\text{path}\,(u^{(\pi_1)}, u^{(\pi_2)}, \ldots, u^{(\pi_t)}),\\ \text{from}\,\pi_1 = j\,\text{to}\,\pi_t = n}} \prod_{k=2}^{t} \frac{\partial u^{(\pi_k)}}{\partial u^{(\pi_{k-1})}}. \tag{6.55}$$

Since the number of paths from node j to node n can grow exponentially in the length of these paths, the number of terms in the above sum, which is the number of such paths, can grow exponentially with the depth of the forward propagation graph. This large cost would be incurred because the same computation for $\frac{\partial u^{(i)}}{\partial u^{(j)}}$ would be redone many times. To avoid such recomputation, we can think of back-propagation as a table-filling algorithm that takes advantage of storing intermediate results $\frac{\partial u^{(n)}}{\partial u^{(i)}}$. Each node in the graph has a corresponding slot in a table to store the gradient for that node. By filling in these table entries in order, back-propagation avoids repeating many common subexpressions. This table-filling strategy is sometimes called **dynamic programming**.

6.5.7 Example: Back-Propagation for MLP Training

As an example, we walk through the back-propagation algorithm as it is used to train a multilayer perceptron.

Here we develop a very simple multilayer perception with a single hidden layer. To train this model, we will use minibatch stochastic gradient descent. The back-propagation algorithm is used to compute the gradient of the cost on a single minibatch. Specifically, we use a minibatch of examples from the training set formatted as a design matrix $\boldsymbol{X}$ and a vector of associated class labels $\boldsymbol{y}$. The network computes a layer of hidden features $\boldsymbol{H} = \max\{0, \boldsymbol{X}\boldsymbol{W}^{(1)}\}$. To simplify the presentation we do not use biases in this model. We assume that our graph language includes a `relu` operation that can compute $\max\{0, \boldsymbol{Z}\}$ element-wise. The predictions of the unnormalized log probabilities over classes are then given by $\boldsymbol{H}\boldsymbol{W}^{(2)}$. We assume that our graph language includes a `cross_entropy` operation that computes the cross-entropy between the targets $\boldsymbol{y}$ and the probability distribution defined by these unnormalized log probabilities. The resulting cross-entropy defines the cost J_{MLE}. Minimizing this cross-entropy performs maximum likelihood estimation of the classifier. However, to make this example more realistic, we also include a regularization term. The total cost

$$J = J_{\text{MLE}} + \lambda \left(\sum_{i,j} \left(W_{i,j}^{(1)} \right)^2 + \sum_{i,j} \left(W_{i,j}^{(2)} \right)^2 \right) \tag{6.56}$$

consists of the cross-entropy and a weight decay term with coefficient λ. The computational graph is illustrated in figure 6.11.

The computational graph for the gradient of this example is large enough that it would be tedious to draw or to read. This demonstrates one of the benefits of the back-propagation algorithm, which is that it can automatically generate gradients that would be straightforward but tedious for a software engineer to derive manually.

We can roughly trace out the behavior of the back-propagation algorithm by looking at the forward propagation graph in figure 6.11. To train, we wish to compute both $\nabla_{\boldsymbol{W}^{(1)}} J$ and $\nabla_{\boldsymbol{W}^{(2)}} J$. There are two different paths leading backward from J to the weights: one through the cross-entropy cost, and one through the weight decay cost. The weight decay cost is relatively simple; it will always contribute $2\lambda \boldsymbol{W}^{(i)}$ to the gradient on $\boldsymbol{W}^{(i)}$.

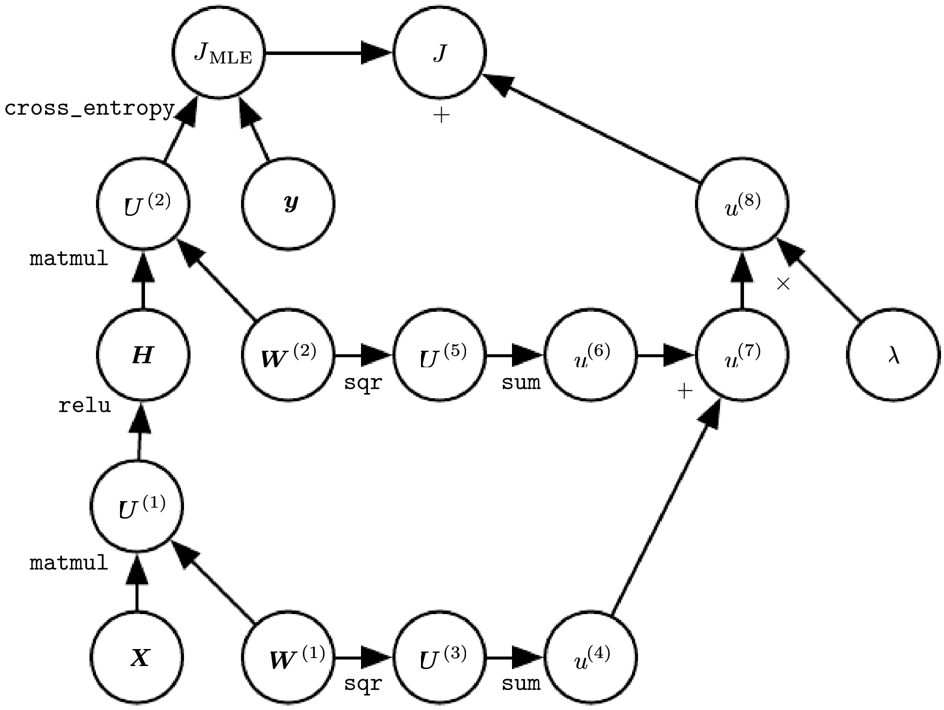

Figure 6.11: The computational graph used to compute the cost used to train our example of a single-layer MLP using the cross-entropy loss and weight decay.

The other path through the cross-entropy cost is slightly more complicated. Let $\boldsymbol{G}$ be the gradient on the unnormalized log probabilities $\boldsymbol{U}^{(2)}$ provided by the `cross_entropy` operation. The back-propagation algorithm now needs to explore two different branches. On the shorter branch, it adds $\boldsymbol{H}^\top\boldsymbol{G}$ to the gradient on $\boldsymbol{W}^{(2)}$, using the back-propagation rule for the second argument to the matrix multiplication operation. The other branch corresponds to the longer chain descending further along the network. First, the back-propagation algorithm computes $\nabla_{\boldsymbol{H}}J = \boldsymbol{G}\boldsymbol{W}^{(2)\top}$ using the back-propagation rule for the first argument to the matrix multiplication operation. Next, the `relu` operation uses its back-propagation rule to zero out components of the gradient corresponding to entries of $\boldsymbol{U}^{(1)}$ that were less than 0. Let the result be called $\boldsymbol{G}'$. The last step of the back-propagation algorithm is to use the back-propagation rule for the second argument of the `matmul` operation to add $\boldsymbol{X}^\top\boldsymbol{G}'$ to the gradient on $\boldsymbol{W}^{(1)}$.

After these gradients have been computed, it is the responsibility of the gradient descent algorithm, or another optimization algorithm, to use these gradients to update the parameters.

For the MLP, the computational cost is dominated by the cost of matrix multiplication. During the forward propagation stage, we multiply by each weight matrix, resulting in $O(w)$ multiply-adds, where w is the number of weights. During the backward propagation stage, we multiply by the transpose of each weight matrix, which has the same computational cost. The main memory cost of the algorithm is that we need to store the input to the nonlinearity of the hidden layer. This value is stored from the time it is computed until the backward pass has returned to the same point. The memory cost is thus $O(mn_h)$, where m is the number of examples in the minibatch and n_h is the number of hidden units.

6.5.8 Complications

Our description of the back-propagation algorithm here is simpler than the implementations actually used in practice.

As noted above, we have restricted the definition of an operation to be a function that returns a single tensor. Most software implementations need to support operations that can return more than one tensor. For example, if we wish to compute both the maximum value in a tensor and the index of that value, it is best to compute both in a single pass through memory, so it is most efficient to implement this procedure as a single operation with two outputs.

We have not described how to control the memory consumption of back-propagation. Back-propagation often involves summation of many tensors together. In the naive approach, each of these tensors would be computed separately, then all of them would be added in a second step. The naive approach has an overly high memory bottleneck that can be avoided by maintaining a single buffer and adding each value to that buffer as it is computed.

Real-world implementations of back-propagation also need to handle various data types, such as 32-bit floating point, 64-bit floating point, and integer values. The policy for handling each of these types takes special care to design.

Some operations have undefined gradients, and it is important to track these cases and determine whether the gradient requested by the user is undefined.

Various other technicalities make real-world differentiation more complicated. These technicalities are not insurmountable, and this chapter has described the key intellectual tools needed to compute derivatives, but it is important to be aware that many more subtleties exist.

6.5.9 Differentiation outside the Deep Learning Community

The deep learning community has been somewhat isolated from the broader computer science community and has largely developed its own cultural attitudes concerning how to perform differentiation. More generally, the field of **automatic differentiation** is concerned with how to compute derivatives algorithmically. The back-propagation algorithm described here is only one approach to automatic differentiation. It is a special case of a broader class of techniques called **reverse mode accumulation**. Other approaches evaluate the subexpressions of the chain rule in different orders. In general, determining the order of evaluation that results in the lowest computational cost is a difficult problem. Finding the optimal sequence of operations to compute the gradient is NP-complete (Naumann, 2008), in the sense that it may require simplifying algebraic expressions into their least expensive form.

For example, suppose we have variables $p_1, p_2, \ldots, p_n$ representing probabilities and variables $z_1, z_2, \ldots, z_n$ representing unnormalized log probabilities. Suppose we define

$$q_i = \frac{\exp(z_i)}{\sum_i \exp(z_i)}, \tag{6.57}$$

where we build the softmax function out of exponentiation, summation and division operations, and construct a cross-entropy loss $J = -\sum_i p_i \log q_i$. A human mathematician can observe that the derivative of J with respect to z_i takes a very simple form: $q_i - p_i$. The back-propagation algorithm is not capable of simplifying the gradient this way, and will instead explicitly propagate gradients through all of the logarithm and exponentiation operations in the original graph. Some software libraries such as Theano (Bergstra *et al.*, 2010; Bastien *et al.*, 2012) are able to perform some kinds of algebraic substitution to improve over the graph proposed by the pure back-propagation algorithm.

When the forward graph $\mathcal{G}$ has a single output node and each partial derivative $\frac{\partial u^{(i)}}{\partial u^{(j)}}$ can be computed with a constant amount of computation, back-propagation guarantees that the number of computations for the gradient computation is of the same order as the number of computations for the forward computation: this can be seen in algorithm 6.2 because each local partial derivative $\frac{\partial u^{(i)}}{\partial u^{(j)}}$ needs to be computed only once along with an associated multiplication and addition for the recursive chain-rule formulation (equation 6.49). The overall computation is therefore $O(\#\text{ edges})$. However, it can potentially be reduced by simplifying the computational graph constructed by back-propagation, and this is an NP-complete task. Implementations such as Theano and TensorFlow use heuristics based on matching known simplification patterns in order to iteratively attempt to simplify the graph. We defined back-propagation only for the computation of a gradient of a scalar output but back-propagation can be extended to compute a Jacobian (either of k different scalar nodes in the graph, or of a tensor-valued node containing k values). A naive implementation may then need k times more computation: for each scalar internal node in the original forward graph, the naive implementation computes k gradients instead of a single gradient. When the number of outputs of the graph is larger than the number of inputs, it is sometimes preferable to use another form of automatic differentiation called **forward mode accumulation**. Forward mode computation has been proposed for obtaining real-time computation of gradients in recurrent networks, for example (Williams and Zipser, 1989). This also avoids the need to store the values and gradients for the whole graph, trading off computational efficiency for memory. The relationship between forward mode and backward mode is analogous to the relationship between left-multiplying versus right-multiplying a sequence of matrices, such as

$$\boldsymbol{ABCD}, \tag{6.58}$$

where the matrices can be thought of as Jacobian matrices. For example, if $\boldsymbol{D}$ is a column vector while $\boldsymbol{A}$ has many rows, this corresponds to a graph with a single output and many inputs, and starting the multiplications from the end and going backwards only requires matrix-vector products. This corresponds to the backward mode. Instead, starting to multiply from the left would involve a series of matrix-matrix products, which makes the whole computation much more expensive. However, if $\boldsymbol{A}$ has fewer rows than $\boldsymbol{D}$ has columns, it is cheaper to run the multiplications left-to-right, corresponding to the forward mode.

In many communities outside of machine learning, it is more common to implement differentiation software that acts directly on traditional programming language code, such as Python or C code, and automatically generates programs that differentiate functions written in these languages. In the deep learning community, computational graphs are usually represented by explicit data structures created by specialized libraries. The specialized approach has the drawback of requiring the library developer to define the `bprop` methods for every operation and limiting the user of the library to only those operations that have been defined. However, the specialized approach also has the benefit of allowing customized back-propagation rules to be developed for each operation, allowing the developer to improve speed or stability in non-obvious ways that an automatic procedure would presumably be unable to replicate.

Back-propagation is therefore not the only way or the optimal way of computing the gradient, but it is a very practical method that continues to serve the deep learning community very well. In the future, differentiation technology for deep networks may improve as deep learning practitioners become more aware of advances in the broader field of automatic differentiation.

6.5.10 Higher-Order Derivatives

Some software frameworks support the use of higher-order derivatives. Among the deep learning software frameworks, this includes at least Theano and TensorFlow. These libraries use the same kind of data structure to describe the expressions for derivatives as they use to describe the original function being differentiated. This means that the symbolic differentiation machinery can be applied to derivatives.

In the context of deep learning, it is rare to compute a single second derivative of a scalar function. Instead, we are usually interested in properties of the Hessian matrix. If we have a function $f : \mathbb{R}^n \rightarrow \mathbb{R}$, then the Hessian matrix is of size $n \times n$. In typical deep learning applications, n will be the number of parameters in the model, which could easily number in the billions. The entire Hessian matrix is thus infeasible to even represent.

Instead of explicitly computing the Hessian, the typical deep learning approach is to use **Krylov methods**. Krylov methods are a set of iterative techniques for performing various operations like approximately inverting a matrix or finding approximations to its eigenvectors or eigenvalues, without using any operation other than matrix-vector products.

In order to use Krylov methods on the Hessian, we only need to be able to compute the product between the Hessian matrix $\boldsymbol{H}$ and an arbitrary vector $\boldsymbol{v}$. A straightforward technique (Christianson, 1992) for doing so is to compute

$$\boldsymbol{H}\boldsymbol{v} = \nabla_{\boldsymbol{x}} \left[\left(\nabla_{\boldsymbol{x}} f(x) \right)^\top \boldsymbol{v} \right]. \tag{6.59}$$

Both of the gradient computations in this expression may be computed automatically by the appropriate software library. Note that the outer gradient expression takes the gradient of a function of the inner gradient expression.

If $\boldsymbol{v}$ is itself a vector produced by a computational graph, it is important to specify that the automatic differentiation software should not differentiate through the graph that produced $\boldsymbol{v}$.

While computing the Hessian is usually not advisable, it is possible to do with Hessian vector products. One simply computes $\boldsymbol{H}\boldsymbol{e}^{(i)}$ for all $i = 1, \ldots, n$, where $\boldsymbol{e}^{(i)}$ is the one-hot vector with $e_i^{(i)} = 1$ and all other entries equal to 0.

6.6 Historical Notes

Feedforward networks can be seen as efficient nonlinear function approximators based on using gradient descent to minimize the error in a function approximation.

From this point of view, the modern feedforward network is the culmination of centuries of progress on the general function approximation task.

The chain rule that underlies the back-propagation algorithm was invented in the 17th century (Leibniz, 1676; L'Hôpital, 1696). Calculus and algebra have long been used to solve optimization problems in closed form, but gradient descent was not introduced as a technique for iteratively approximating the solution to optimization problems until the 19th century (Cauchy, 1847).

Beginning in the 1940s, these function approximation techniques were used to motivate machine learning models such as the perceptron. However, the earliest models were based on linear models. Critics including Marvin Minsky pointed out several of the flaws of the linear model family, such as its inability to learn the XOR function, which led to a backlash against the entire neural network approach.

Learning nonlinear functions required the development of a multilayer perceptron and a means of computing the gradient through such a model. Efficient applications of the chain rule based on dynamic programming began to appear in the 1960s and 1970s, mostly for control applications (Kelley, 1960; Bryson and Denham, 1961; Dreyfus, 1962; Bryson and Ho, 1969; Dreyfus, 1973) but also for sensitivity analysis (Linnainmaa, 1976). Werbos (1981) proposed applying these techniques to training artificial neural networks. The idea was finally developed in practice after being independently rediscovered in different ways (LeCun, 1985; Parker, 1985; Rumelhart *et al.*, 1986a). The book **Parallel Distributed Processing** presented the results of some of the first successful experiments with back-propagation in a chapter (Rumelhart *et al.*, 1986b) that contributed greatly to the popularization of back-propagation and initiated a very active period of research in multi-layer neural networks. However, the ideas put forward by the authors of that book and in particular by Rumelhart and Hinton go much beyond back-propagation. They include crucial ideas about the possible computational implementation of several central aspects of cognition and learning, which came under the name of "connectionism" because of the importance this school of thought places on the connections between neurons as the locus of learning and memory. In particular, these ideas include the notion of distributed representation (Hinton *et al.*, 1986).

Following the success of back-propagation, neural network research gained popularity and reached a peak in the early 1990s. Afterwards, other machine learning techniques became more popular until the modern deep learning renaissance that began in 2006.

The core ideas behind modern feedforward networks have not changed substantially since the 1980s. The same back-propagation algorithm and the same approaches to gradient descent are still in use. Most of the improvement in neural network performance from 1986 to 2015 can be attributed to two factors. First, larger datasets have reduced the degree to which statistical generalization is a challenge for neural networks. Second, neural networks have become much larger, due to more powerful computers, and better software infrastructure. However, a small number of algorithmic changes have improved the performance of neural networks noticeably.

One of these algorithmic changes was the replacement of mean squared error with the cross-entropy family of loss functions. Mean squared error was popular in the 1980s and 1990s, but was gradually replaced by cross-entropy losses and the principle of maximum likelihood as ideas spread between the statistics community and the machine learning community. The use of cross-entropy losses greatly improved the performance of models with sigmoid and softmax outputs, which had previously suffered from saturation and slow learning when using the mean squared error loss.

The other major algorithmic change that has greatly improved the performance of feedforward networks was the replacement of sigmoid hidden units with piecewise linear hidden units, such as rectified linear units. Rectification using the $\max\{0, z\}$ function was introduced in early neural network models and dates back at least as far as the Cognitron and Neocognitron (Fukushima, 1975, 1980). These early models did not use rectified linear units, but instead applied rectification to nonlinear functions. Despite the early popularity of rectification, rectification was largely replaced by sigmoids in the 1980s, perhaps because sigmoids perform better when neural networks are very small. As of the early 2000s, rectified linear units were avoided due to a somewhat superstitious belief that activation functions with non-differentiable points must be avoided. This began to change in about 2009. Jarrett *et al.* (2009) observed that "using a rectifying nonlinearity is the single most important factor in improving the performance of a recognition system" among several different factors of neural network architecture design.

For small datasets, Jarrett *et al.* (2009) observed that using rectifying nonlinearities is even more important than learning the weights of the hidden layers. Random weights are sufficient to propagate useful information through a rectified linear network, allowing the classifier layer at the top to learn how to map different feature vectors to class identities.

When more data is available, learning begins to extract enough useful knowledge to exceed the performance of randomly chosen parameters. Glorot *et al.* (2011a) showed that learning is far easier in deep rectified linear networks than in deep networks that have curvature or two-sided saturation in their activation functions.

Rectified linear units are also of historical interest because they show that neuroscience has continued to have an influence on the development of deep learning algorithms. Glorot *et al.* (2011a) motivate rectified linear units from biological considerations. The half-rectifying nonlinearity was intended to capture these properties of biological neurons: 1) For some inputs, biological neurons are completely inactive. 2) For some inputs, a biological neuron's output is proportional to its input. 3) Most of the time, biological neurons operate in the regime where they are inactive (i.e., they should have **sparse activations**).

When the modern resurgence of deep learning began in 2006, feedforward networks continued to have a bad reputation. From about 2006-2012, it was widely believed that feedforward networks would not perform well unless they were assisted by other models, such as probabilistic models. Today, it is now known that with the right resources and engineering practices, feedforward networks perform very well. Today, gradient-based learning in feedforward networks is used as a tool to develop probabilistic models, such as the variational autoencoder and generative adversarial networks, described in chapter 20. Rather than being viewed as an unreliable technology that must be supported by other techniques, gradient-based learning in feedforward networks has been viewed since 2012 as a powerful technology that may be applied to many other machine learning tasks. In 2006, the community used unsupervised learning to support supervised learning, and now, ironically, it is more common to use supervised learning to support unsupervised learning.

Feedforward networks continue to have unfulfilled potential. In the future, we expect they will be applied to many more tasks, and that advances in optimization algorithms and model design will improve their performance even further. This chapter has primarily described the neural network family of models. In the subsequent chapters, we turn to how to use these models—how to regularize and train them.

Chapter 7

Regularization for Deep Learning

A central problem in machine learning is how to make an algorithm that will perform well not just on the training data, but also on new inputs. Many strategies used in machine learning are explicitly designed to reduce the test error, possibly at the expense of increased training error. These strategies are known collectively as regularization. As we will see there are a great many forms of regularization available to the deep learning practitioner. In fact, developing more effective regularization strategies has been one of the major research efforts in the field.

Chapter 5 introduced the basic concepts of generalization, underfitting, overfitting, bias, variance and regularization. If you are not already familiar with these notions, please refer to that chapter before continuing with this one.

In this chapter, we describe regularization in more detail, focusing on regularization strategies for deep models or models that may be used as building blocks to form deep models.

Some sections of this chapter deal with standard concepts in machine learning. If you are already familiar with these concepts, feel free to skip the relevant sections. However, most of this chapter is concerned with the extension of these basic concepts to the particular case of neural networks.

In section 5.2.2, we defined regularization as "any modification we make to a learning algorithm that is intended to reduce its generalization error but not its training error." There are many regularization strategies. Some put extra constraints on a machine learning model, such as adding restrictions on the parameter values. Some add extra terms in the objective function that can be thought of as corresponding to a soft constraint on the parameter values. If chosen carefully, these extra constraints and penalties can lead to improved performance on the test set. Sometimes these constraints and penalties are designed to encode specific kinds of prior knowledge. Other times, these constraints and penalties are designed to express a generic preference for a simpler model class in order to promote generalization. Sometimes penalties and constraints are necessary to make an underdetermined problem determined. Other forms of regularization, known as ensemble methods, combine multiple hypotheses that explain the training data.

In the context of deep learning, most regularization strategies are based on regularizing estimators. Regularization of an estimator works by trading increased bias for reduced variance. An effective regularizer is one that makes a profitable trade, reducing variance significantly while not overly increasing the bias. When we discussed generalization and overfitting in chapter 5, we focused on three situations, where the model family being trained either (1) excluded the true data generating process—corresponding to underfitting and inducing bias, or (2) matched the true data generating process, or (3) included the generating process but also many other possible generating processes—the overfitting regime where variance rather than bias dominates the estimation error. The goal of regularization is to take a model from the third regime into the second regime.

In practice, an overly complex model family does not necessarily include the target function or the true data generating process, or even a close approximation of either. We almost never have access to the true data generating process so we can never know for sure if the model family being estimated includes the generating process or not. However, most applications of deep learning algorithms are to domains where the true data generating process is almost certainly outside the model family. Deep learning algorithms are typically applied to extremely complicated domains such as images, audio sequences and text, for which the true generation process essentially involves simulating the entire universe. To some extent, we are always trying to fit a square peg (the data generating process) into a round hole (our model family).

What this means is that controlling the complexity of the model is not a simple matter of finding the model of the right size, with the right number of parameters. Instead, we might find—and indeed in practical deep learning scenarios, we almost always do find—that the best fitting model (in the sense of minimizing generalization error) is a large model that has been regularized appropriately.

We now review several strategies for how to create such a large, deep, regularized model.

7.1 Parameter Norm Penalties

Regularization has been used for decades prior to the advent of deep learning. Linear models such as linear regression and logistic regression allow simple, straightforward, and effective regularization strategies.

Many regularization approaches are based on limiting the capacity of models, such as neural networks, linear regression, or logistic regression, by adding a parameter norm penalty $\Omega(\boldsymbol{\theta})$ to the objective function J. We denote the regularized objective function by $\tilde{J}$:

$$\tilde{J}(\boldsymbol{\theta}; \boldsymbol{X}, \boldsymbol{y}) = J(\boldsymbol{\theta}; \boldsymbol{X}, \boldsymbol{y}) + \alpha\Omega(\boldsymbol{\theta}) \tag{7.1}$$

where $\alpha \in [0, \infty)$ is a hyperparameter that weights the relative contribution of the norm penalty term, Ω, relative to the standard objective function J. Setting α to 0 results in no regularization. Larger values of α correspond to more regularization.

When our training algorithm minimizes the regularized objective function $\tilde{J}$ it will decrease both the original objective J on the training data and some measure of the size of the parameters $\boldsymbol{\theta}$ (or some subset of the parameters). Different choices for the parameter norm Ω can result in different solutions being preferred. In this section, we discuss the effects of the various norms when used as penalties on the model parameters.

Before delving into the regularization behavior of different norms, we note that for neural networks, we typically choose to use a parameter norm penalty Ω that penalizes *only the weights* of the affine transformation at each layer and leaves the biases unregularized. The biases typically require less data to fit accurately than the weights. Each weight specifies how two variables interact. Fitting the weight well requires observing both variables in a variety of conditions. Each bias controls only a single variable. This means that we do not induce too much variance by leaving the biases unregularized. Also, regularizing the bias parameters can introduce a significant amount of underfitting. We therefore use the vector $\boldsymbol{w}$ to indicate all of the weights that should be affected by a norm penalty, while the vector $\boldsymbol{\theta}$ denotes all of the parameters, including both $\boldsymbol{w}$ and the unregularized parameters.

In the context of neural networks, it is sometimes desirable to use a separate penalty with a different α coefficient for each layer of the network. Because it can be expensive to search for the correct value of multiple hyperparameters, it is still reasonable to use the same weight decay at all layers just to reduce the size of search space.

7.1.1 L^2 Parameter Regularization

We have already seen, in section 5.2.2, one of the simplest and most common kinds of parameter norm penalty: the L^2 parameter norm penalty commonly known as **weight decay**. This regularization strategy drives the weights closer to the origin[1] by adding a regularization term $\Omega(\boldsymbol{\theta}) = \frac{1}{2}\|\boldsymbol{w}\|_2^2$ to the objective function. In other academic communities, L^2 regularization is also known as **ridge regression** or **Tikhonov regularization**.

We can gain some insight into the behavior of weight decay regularization by studying the gradient of the regularized objective function. To simplify the presentation, we assume no bias parameter, so $\boldsymbol{\theta}$ is just $\boldsymbol{w}$. Such a model has the following total objective function:

$$\tilde{J}(\boldsymbol{w}; \boldsymbol{X}, \boldsymbol{y}) = \frac{\alpha}{2}\boldsymbol{w}^\top \boldsymbol{w} + J(\boldsymbol{w}; \boldsymbol{X}, \boldsymbol{y}), \tag{7.2}$$

with the corresponding parameter gradient

$$\nabla_{\boldsymbol{w}} \tilde{J}(\boldsymbol{w}; \boldsymbol{X}, \boldsymbol{y}) = \alpha \boldsymbol{w} + \nabla_{\boldsymbol{w}} J(\boldsymbol{w}; \boldsymbol{X}, \boldsymbol{y}). \tag{7.3}$$

To take a single gradient step to update the weights, we perform this update:

$$\boldsymbol{w} \leftarrow \boldsymbol{w} - \epsilon \left(\alpha \boldsymbol{w} + \nabla_{\boldsymbol{w}} J(\boldsymbol{w}; \boldsymbol{X}, \boldsymbol{y})\right). \tag{7.4}$$

Written another way, the update is:

$$\boldsymbol{w} \leftarrow (1 - \epsilon\alpha)\boldsymbol{w} - \epsilon \nabla_{\boldsymbol{w}} J(\boldsymbol{w}; \boldsymbol{X}, \boldsymbol{y}). \tag{7.5}$$

We can see that the addition of the weight decay term has modified the learning rule to multiplicatively shrink the weight vector by a constant factor on each step, just before performing the usual gradient update. This describes what happens in a single step. But what happens over the entire course of training?

We will further simplify the analysis by making a quadratic approximation to the objective function in the neighborhood of the value of the weights that obtains minimal unregularized training cost, $\boldsymbol{w}^* = \arg\min_{\boldsymbol{w}} J(\boldsymbol{w})$. If the objective function is truly quadratic, as in the case of fitting a linear regression model with

[1] More generally, we could regularize the parameters to be near any specific point in space and, surprisingly, still get a regularization effect, but better results will be obtained for a value closer to the true one, with zero being a default value that makes sense when we do not know if the correct value should be positive or negative. Since it is far more common to regularize the model parameters towards zero, we will focus on this special case in our exposition.

mean squared error, then the approximation is perfect. The approximation $\hat{J}$ is given by

$$\hat{J}(\boldsymbol{\theta}) = J(\boldsymbol{w}^*) + \frac{1}{2}(\boldsymbol{w} - \boldsymbol{w}^*)^\top \boldsymbol{H}(\boldsymbol{w} - \boldsymbol{w}^*), \tag{7.6}$$

where $\boldsymbol{H}$ is the Hessian matrix of J with respect to $\boldsymbol{w}$ evaluated at $\boldsymbol{w}^*$. There is no first-order term in this quadratic approximation, because $\boldsymbol{w}^*$ is defined to be a minimum, where the gradient vanishes. Likewise, because $\boldsymbol{w}^*$ is the location of a minimum of J, we can conclude that $\boldsymbol{H}$ is positive semidefinite.

The minimum of $\hat{J}$ occurs where its gradient

$$\nabla_{\boldsymbol{w}} \hat{J}(\boldsymbol{w}) = \boldsymbol{H}(\boldsymbol{w} - \boldsymbol{w}^*) \tag{7.7}$$

is equal to $\boldsymbol{0}$.

To study the effect of weight decay, we modify equation 7.7 by adding the weight decay gradient. We can now solve for the minimum of the regularized version of $\hat{J}$. We use the variable $\tilde{\boldsymbol{w}}$ to represent the location of the minimum.

$$\alpha \tilde{\boldsymbol{w}} + \boldsymbol{H}(\tilde{\boldsymbol{w}} - \boldsymbol{w}^*) = 0 \tag{7.8}$$

$$(\boldsymbol{H} + \alpha \boldsymbol{I})\tilde{\boldsymbol{w}} = \boldsymbol{H}\boldsymbol{w}^* \tag{7.9}$$

$$\tilde{\boldsymbol{w}} = (\boldsymbol{H} + \alpha \boldsymbol{I})^{-1}\boldsymbol{H}\boldsymbol{w}^*. \tag{7.10}$$

As α approaches 0, the regularized solution $\tilde{\boldsymbol{w}}$ approaches $\boldsymbol{w}^*$. But what happens as α grows? Because $\boldsymbol{H}$ is real and symmetric, we can decompose it into a diagonal matrix $\boldsymbol{\Lambda}$ and an orthonormal basis of eigenvectors, $\boldsymbol{Q}$, such that $\boldsymbol{H} = \boldsymbol{Q}\boldsymbol{\Lambda}\boldsymbol{Q}^\top$. Applying the decomposition to equation 7.10, we obtain:

$$\tilde{\boldsymbol{w}} = (\boldsymbol{Q}\boldsymbol{\Lambda}\boldsymbol{Q}^\top + \alpha \boldsymbol{I})^{-1}\boldsymbol{Q}\boldsymbol{\Lambda}\boldsymbol{Q}^\top\boldsymbol{w}^* \tag{7.11}$$

$$= \left[\boldsymbol{Q}(\boldsymbol{\Lambda} + \alpha \boldsymbol{I})\boldsymbol{Q}^\top\right]^{-1}\boldsymbol{Q}\boldsymbol{\Lambda}\boldsymbol{Q}^\top\boldsymbol{w}^* \tag{7.12}$$

$$= \boldsymbol{Q}(\boldsymbol{\Lambda} + \alpha \boldsymbol{I})^{-1}\boldsymbol{\Lambda}\boldsymbol{Q}^\top\boldsymbol{w}^*. \tag{7.13}$$

We see that the effect of weight decay is to rescale $\boldsymbol{w}^*$ along the axes defined by the eigenvectors of $\boldsymbol{H}$. Specifically, the component of $\boldsymbol{w}^*$ that is aligned with the i-th eigenvector of $\boldsymbol{H}$ is rescaled by a factor of $\frac{\lambda_i}{\lambda_i + \alpha}$. (You may wish to review how this kind of scaling works, first explained in figure 2.3).

Along the directions where the eigenvalues of $\boldsymbol{H}$ are relatively large, for example, where $\lambda_i \gg \alpha$, the effect of regularization is relatively small. However, components with $\lambda_i \ll \alpha$ will be shrunk to have nearly zero magnitude. This effect is illustrated in figure 7.1.

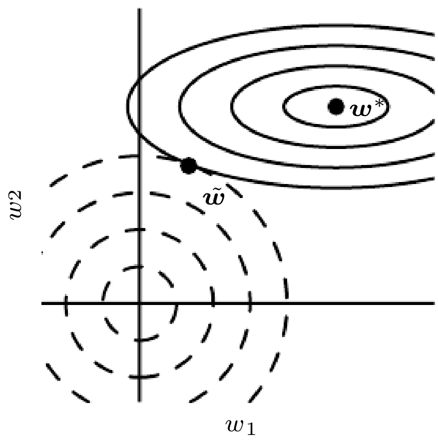

Figure 7.1: An illustration of the effect of L^2 (or weight decay) regularization on the value of the optimal $\boldsymbol{w}$. The solid ellipses represent contours of equal value of the unregularized objective. The dotted circles represent contours of equal value of the L^2 regularizer. At the point $\tilde{\boldsymbol{w}}$, these competing objectives reach an equilibrium. In the first dimension, the eigenvalue of the Hessian of J is small. The objective function does not increase much when moving horizontally away from $\boldsymbol{w}^*$. Because the objective function does not express a strong preference along this direction, the regularizer has a strong effect on this axis. The regularizer pulls w_1 close to zero. In the second dimension, the objective function is very sensitive to movements away from $\boldsymbol{w}^*$. The corresponding eigenvalue is large, indicating high curvature. As a result, weight decay affects the position of w_2 relatively little.

Only directions along which the parameters contribute significantly to reducing the objective function are preserved relatively intact. In directions that do not contribute to reducing the objective function, a small eigenvalue of the Hessian tells us that movement in this direction will not significantly increase the gradient. Components of the weight vector corresponding to such unimportant directions are decayed away through the use of the regularization throughout training.

So far we have discussed weight decay in terms of its effect on the optimization of an abstract, general, quadratic cost function. How do these effects relate to machine learning in particular? We can find out by studying linear regression, a model for which the true cost function is quadratic and therefore amenable to the same kind of analysis we have used so far. Applying the analysis again, we will be able to obtain a special case of the same results, but with the solution now phrased in terms of the training data. For linear regression, the cost function is the sum of squared errors:

$$(\boldsymbol{X}\boldsymbol{w} - \boldsymbol{y})^\top(\boldsymbol{X}\boldsymbol{w} - \boldsymbol{y}). \tag{7.14}$$

When we add L^2 regularization, the objective function changes to

$$(\boldsymbol{X}\boldsymbol{w} - \boldsymbol{y})^\top(\boldsymbol{X}\boldsymbol{w} - \boldsymbol{y}) + \frac{1}{2}\alpha\boldsymbol{w}^\top\boldsymbol{w}. \tag{7.15}$$

This changes the normal equations for the solution from

$$\boldsymbol{w} = (\boldsymbol{X}^\top\boldsymbol{X})^{-1}\boldsymbol{X}^\top\boldsymbol{y} \tag{7.16}$$

to

$$\boldsymbol{w} = (\boldsymbol{X}^\top\boldsymbol{X} + \alpha\boldsymbol{I})^{-1}\boldsymbol{X}^\top\boldsymbol{y}. \tag{7.17}$$

The matrix $\boldsymbol{X}^\top\boldsymbol{X}$ in equation 7.16 is proportional to the covariance matrix $\frac{1}{m}\boldsymbol{X}^\top\boldsymbol{X}$. Using L^2 regularization replaces this matrix with $\left(\boldsymbol{X}^\top\boldsymbol{X} + \alpha\boldsymbol{I}\right)^{-1}$ in equation 7.17. The new matrix is the same as the original one, but with the addition of α to the diagonal. The diagonal entries of this matrix correspond to the variance of each input feature. We can see that L^2 regularization causes the learning algorithm to "perceive" the input $\boldsymbol{X}$ as having higher variance, which makes it shrink the weights on features whose covariance with the output target is low compared to this added variance.

7.1.2 L^1 Regularization

While L^2 weight decay is the most common form of weight decay, there are other ways to penalize the size of the model parameters. Another option is to use L^1 regularization.

Formally, L^1 regularization on the model parameter $\boldsymbol{w}$ is defined as:

$$\Omega(\boldsymbol{\theta}) = ||\boldsymbol{w}||_1 = \sum_i |w_i|, \tag{7.18}$$

that is, as the sum of absolute values of the individual parameters.[2] We will now discuss the effect of L^1 regularization on the simple linear regression model, with no bias parameter, that we studied in our analysis of L^2 regularization. In particular, we are interested in delineating the differences between L^1 and L^2 forms

[2] As with L^2 regularization, we could regularize the parameters towards a value that is not zero, but instead towards some parameter value $\boldsymbol{w}^{(o)}$. In that case the L^1 regularization would introduce the term $\Omega(\boldsymbol{\theta}) = ||\boldsymbol{w} - \boldsymbol{w}^{(o)}||_1 = \sum_i |w_i - w_i^{(o)}|$.

of regularization. As with L^2 weight decay, L^1 weight decay controls the strength of the regularization by scaling the penalty Ω using a positive hyperparameter α. Thus, the regularized objective function $\tilde{J}(\boldsymbol{w}; \boldsymbol{X}, \boldsymbol{y})$ is given by

$$\tilde{J}(\boldsymbol{w}; \boldsymbol{X}, \boldsymbol{y}) = \alpha ||\boldsymbol{w}||_1 + J(\boldsymbol{w}; \boldsymbol{X}, \boldsymbol{y}), \tag{7.19}$$

with the corresponding gradient (actually, sub-gradient):

$$\nabla_{\boldsymbol{w}} \tilde{J}(\boldsymbol{w}; \boldsymbol{X}, \boldsymbol{y}) = \alpha \text{sign}(\boldsymbol{w}) + \nabla_{\boldsymbol{w}} J(\boldsymbol{X}, \boldsymbol{y}; \boldsymbol{w}) \tag{7.20}$$

where $\text{sign}(\boldsymbol{w})$ is simply the sign of $\boldsymbol{w}$ applied element-wise.

By inspecting equation 7.20, we can see immediately that the effect of L^1 regularization is quite different from that of L^2 regularization. Specifically, we can see that the regularization contribution to the gradient no longer scales linearly with each w_i; instead it is a constant factor with a sign equal to $\text{sign}(w_i)$. One consequence of this form of the gradient is that we will not necessarily see clean algebraic solutions to quadratic approximations of $J(\boldsymbol{X}, \boldsymbol{y}; \boldsymbol{w})$ as we did for L^2 regularization.

Our simple linear model has a quadratic cost function that we can represent via its Taylor series. Alternately, we could imagine that this is a truncated Taylor series approximating the cost function of a more sophisticated model. The gradient in this setting is given by

$$\nabla_{\boldsymbol{w}} \hat{J}(\boldsymbol{w}) = \boldsymbol{H}(\boldsymbol{w} - \boldsymbol{w}^*), \tag{7.21}$$

where, again, $\boldsymbol{H}$ is the Hessian matrix of J with respect to $\boldsymbol{w}$ evaluated at $\boldsymbol{w}^*$.

Because the L^1 penalty does not admit clean algebraic expressions in the case of a fully general Hessian, we will also make the further simplifying assumption that the Hessian is diagonal, $\boldsymbol{H} = \text{diag}([H_{1,1}, \ldots, H_{n,n}])$, where each $H_{i,i} > 0$. This assumption holds if the data for the linear regression problem has been preprocessed to remove all correlation between the input features, which may be accomplished using PCA.

Our quadratic approximation of the L^1 regularized objective function decomposes into a sum over the parameters:

$$\hat{J}(\boldsymbol{w}; \boldsymbol{X}, \boldsymbol{y}) = J(\boldsymbol{w}^*; \boldsymbol{X}, \boldsymbol{y}) + \sum_i \left[\frac{1}{2} H_{i,i}(\boldsymbol{w}_i - \boldsymbol{w}_i^*)^2 + \alpha |w_i| \right]. \tag{7.22}$$

The problem of minimizing this approximate cost function has an analytical solution (for each dimension i), with the following form:

$$w_i = \text{sign}(w_i^*) \max \left\{ |w_i^*| - \frac{\alpha}{H_{i,i}}, 0 \right\}. \tag{7.23}$$

Consider the situation where $w_i^* > 0$ for all i. There are two possible outcomes:

1. The case where $w_i^* \leq \frac{\alpha}{H_{i,i}}$. Here the optimal value of w_i under the regularized objective is simply $w_i = 0$. This occurs because the contribution of $J(\boldsymbol{w}; \boldsymbol{X}, \boldsymbol{y})$ to the regularized objective $\tilde{J}(\boldsymbol{w}; \boldsymbol{X}, \boldsymbol{y})$ is overwhelmed—in direction i—by the L^1 regularization which pushes the value of w_i to zero.

2. The case where $w_i^* > \frac{\alpha}{H_{i,i}}$. In this case, the regularization does not move the optimal value of w_i to zero but instead it just shifts it in that direction by a distance equal to $\frac{\alpha}{H_{i,i}}$.

A similar process happens when $w_i^* < 0$, but with the L^1 penalty making w_i less negative by $\frac{\alpha}{H_{i,i}}$, or 0.

In comparison to L^2 regularization, L^1 regularization results in a solution that is more **sparse**. Sparsity in this context refers to the fact that some parameters have an optimal value of zero. The sparsity of L^1 regularization is a qualitatively different behavior than arises with L^2 regularization. Equation 7.13 gave the solution $\tilde{w}$ for L^2 regularization. If we revisit that equation using the assumption of a diagonal and positive definite Hessian $\boldsymbol{H}$ that we introduced for our analysis of L^1 regularization, we find that $\tilde{w}_i = \frac{H_{i,i}}{H_{i,i}+\alpha} w_i^*$. If w_i^* was nonzero, then $\tilde{w}_i$ remains nonzero. This demonstrates that L^2 regularization does not cause the parameters to become sparse, while L^1 regularization may do so for large enough α.

The sparsity property induced by L^1 regularization has been used extensively as a **feature selection** mechanism. Feature selection simplifies a machine learning problem by choosing which subset of the available features should be used. In particular, the well known LASSO (Tibshirani, 1995) (least absolute shrinkage and selection operator) model integrates an L^1 penalty with a linear model and a least squares cost function. The L^1 penalty causes a subset of the weights to become zero, suggesting that the corresponding features may safely be discarded.

In section 5.6.1, we saw that many regularization strategies can be interpreted as MAP Bayesian inference, and that in particular, L^2 regularization is equivalent to MAP Bayesian inference with a Gaussian prior on the weights. For L^1 regularization, the penalty $\alpha\Omega(\boldsymbol{w}) = \alpha \sum_i |w_i|$ used to regularize a cost function is equivalent to the log-prior term that is maximized by MAP Bayesian inference when the prior is an isotropic Laplace distribution (equation 3.26) over $\boldsymbol{w} \in \mathbb{R}^n$:

$$\log p(\boldsymbol{w}) = \sum_i \log \text{Laplace}(w_i; 0, \frac{1}{\alpha}) = -\alpha ||\boldsymbol{w}||_1 + n \log \alpha - n \log 2. \tag{7.24}$$

From the point of view of learning via maximization with respect to $\boldsymbol{w}$, we can ignore the $\log \alpha - \log 2$ terms because they do not depend on $\boldsymbol{w}$.

7.2 Norm Penalties as Constrained Optimization

Consider the cost function regularized by a parameter norm penalty:

$$\tilde{J}(\boldsymbol{\theta}; \boldsymbol{X}, \boldsymbol{y}) = J(\boldsymbol{\theta}; \boldsymbol{X}, \boldsymbol{y}) + \alpha\Omega(\boldsymbol{\theta}). \tag{7.25}$$

Recall from section 4.4 that we can minimize a function subject to constraints by constructing a generalized Lagrange function, consisting of the original objective function plus a set of penalties. Each penalty is a product between a coefficient, called a Karush–Kuhn–Tucker (KKT) multiplier, and a function representing whether the constraint is satisfied. If we wanted to constrain $\Omega(\boldsymbol{\theta})$ to be less than some constant k, we could construct a generalized Lagrange function

$$\mathcal{L}(\boldsymbol{\theta}, \alpha; \boldsymbol{X}, \boldsymbol{y}) = J(\boldsymbol{\theta}; \boldsymbol{X}, \boldsymbol{y}) + \alpha(\Omega(\boldsymbol{\theta}) - k). \tag{7.26}$$

The solution to the constrained problem is given by

$$\boldsymbol{\theta}^* = \arg\min_{\boldsymbol{\theta}} \max_{\alpha, \alpha \geq 0} \mathcal{L}(\boldsymbol{\theta}, \alpha). \tag{7.27}$$

As described in section 4.4, solving this problem requires modifying both $\boldsymbol{\theta}$ and α. Section 4.5 provides a worked example of linear regression with an L^2 constraint. Many different procedures are possible—some may use gradient descent, while others may use analytical solutions for where the gradient is zero—but in all procedures α must increase whenever $\Omega(\boldsymbol{\theta}) > k$ and decrease whenever $\Omega(\boldsymbol{\theta}) < k$. All positive α encourage $\Omega(\boldsymbol{\theta})$ to shrink. The optimal value α^* will encourage $\Omega(\boldsymbol{\theta})$ to shrink, but not so strongly to make $\Omega(\boldsymbol{\theta})$ become less than k.

To gain some insight into the effect of the constraint, we can fix α^* and view the problem as just a function of $\boldsymbol{\theta}$:

$$\boldsymbol{\theta}^* = \arg\min_{\boldsymbol{\theta}} \mathcal{L}(\boldsymbol{\theta}, \alpha^*) = \arg\min_{\boldsymbol{\theta}} J(\boldsymbol{\theta}; \boldsymbol{X}, \boldsymbol{y}) + \alpha^*\Omega(\boldsymbol{\theta}). \tag{7.28}$$

This is exactly the same as the regularized training problem of minimizing $\tilde{J}$. We can thus think of a parameter norm penalty as imposing a constraint on the weights. If Ω is the L^2 norm, then the weights are constrained to lie in an L^2 ball. If Ω is the L^1 norm, then the weights are constrained to lie in a region of limited L^1 norm. Usually we do not know the size of the constraint region that we impose by using weight decay with coefficient α^* because the value of α^* does not directly tell us the value of k. In principle, one can solve for k, but the relationship between k and α^* depends on the form of J. While we do not know the exact size of the constraint region, we can control it roughly by increasing or decreasing α in order to grow or shrink the constraint region. Larger α will result in a smaller constraint region. Smaller α will result in a larger constraint region.

Sometimes we may wish to use explicit constraints rather than penalties. As described in section 4.4, we can modify algorithms such as stochastic gradient descent to take a step downhill on $J(\boldsymbol{\theta})$ and then project $\boldsymbol{\theta}$ back to the nearest point that satisfies $\Omega(\boldsymbol{\theta}) < k$. This can be useful if we have an idea of what value of k is appropriate and do not want to spend time searching for the value of α that corresponds to this k.

Another reason to use explicit constraints and reprojection rather than enforcing constraints with penalties is that penalties can cause non-convex optimization procedures to get stuck in local minima corresponding to small $\boldsymbol{\theta}$. When training neural networks, this usually manifests as neural networks that train with several "dead units." These are units that do not contribute much to the behavior of the function learned by the network because the weights going into or out of them are all very small. When training with a penalty on the norm of the weights, these configurations can be locally optimal, even if it is possible to significantly reduce J by making the weights larger. Explicit constraints implemented by re-projection can work much better in these cases because they do not encourage the weights to approach the origin. Explicit constraints implemented by re-projection only have an effect when the weights become large and attempt to leave the constraint region.

Finally, explicit constraints with reprojection can be useful because they impose some stability on the optimization procedure. When using high learning rates, it is possible to encounter a positive feedback loop in which large weights induce large gradients which then induce a large update to the weights. If these updates consistently increase the size of the weights, then $\boldsymbol{\theta}$ rapidly moves away from the origin until numerical overflow occurs. Explicit constraints with reprojection prevent this feedback loop from continuing to increase the magnitude of the weights without bound. Hinton *et al.* (2012c) recommend using constraints combined with a high learning rate to allow rapid exploration of parameter space while maintaining some stability.

In particular, Hinton *et al.* (2012c) recommend a strategy introduced by Srebro and Shraibman (2005): constraining the norm of each *column* of the weight matrix of a neural net layer, rather than constraining the Frobenius norm of the entire weight matrix. Constraining the norm of each column separately prevents any one hidden unit from having very large weights. If we converted this constraint into a penalty in a Lagrange function, it would be similar to L^2 weight decay but with a separate KKT multiplier for the weights of each hidden unit. Each of these KKT multipliers would be dynamically updated separately to make each hidden unit obey the constraint. In practice, column norm limitation is always implemented as an explicit constraint with reprojection.

7.3 Regularization and Under-Constrained Problems

In some cases, regularization is necessary for machine learning problems to be properly defined. Many linear models in machine learning, including linear regression and PCA, depend on inverting the matrix $\boldsymbol{X}^\top \boldsymbol{X}$. This is not possible whenever $\boldsymbol{X}^\top \boldsymbol{X}$ is singular. This matrix can be singular whenever the data generating distribution truly has no variance in some direction, or when no variance is *observed* in some direction because there are fewer examples (rows of $\boldsymbol{X}$) than input features (columns of $\boldsymbol{X}$). In this case, many forms of regularization correspond to inverting $\boldsymbol{X}^\top \boldsymbol{X} + \alpha \boldsymbol{I}$ instead. This regularized matrix is guaranteed to be invertible.

These linear problems have closed form solutions when the relevant matrix is invertible. It is also possible for a problem with no closed form solution to be underdetermined. An example is logistic regression applied to a problem where the classes are linearly separable. If a weight vector $\boldsymbol{w}$ is able to achieve perfect classification, then $2\boldsymbol{w}$ will also achieve perfect classification and higher likelihood. An iterative optimization procedure like stochastic gradient descent will continually increase the magnitude of $\boldsymbol{w}$ and, in theory, will never halt. In practice, a numerical implementation of gradient descent will eventually reach sufficiently large weights to cause numerical overflow, at which point its behavior will depend on how the programmer has decided to handle values that are not real numbers.

Most forms of regularization are able to guarantee the convergence of iterative methods applied to underdetermined problems. For example, weight decay will cause gradient descent to quit increasing the magnitude of the weights when the slope of the likelihood is equal to the weight decay coefficient.

The idea of using regularization to solve underdetermined problems extends beyond machine learning. The same idea is useful for several basic linear algebra problems.

As we saw in section 2.9, we can solve underdetermined linear equations using the Moore-Penrose pseudoinverse. Recall that one definition of the pseudoinverse $\boldsymbol{X}^+$ of a matrix $\boldsymbol{X}$ is

$$\boldsymbol{X}^+ = \lim_{\alpha \searrow 0} (\boldsymbol{X}^\top \boldsymbol{X} + \alpha \boldsymbol{I})^{-1} \boldsymbol{X}^\top. \tag{7.29}$$

We can now recognize equation 7.29 as performing linear regression with weight decay. Specifically, equation 7.29 is the limit of equation 7.17 as the regularization coefficient shrinks to zero. We can thus interpret the pseudoinverse as stabilizing underdetermined problems using regularization.

7.4 Dataset Augmentation

The best way to make a machine learning model generalize better is to train it on more data. Of course, in practice, the amount of data we have is limited. One way to get around this problem is to create fake data and add it to the training set. For some machine learning tasks, it is reasonably straightforward to create new fake data.

This approach is easiest for classification. A classifier needs to take a complicated, high dimensional input $\boldsymbol{x}$ and summarize it with a single category identity y. This means that the main task facing a classifier is to be invariant to a wide variety of transformations. We can generate new $(\boldsymbol{x}, y)$ pairs easily just by transforming the $\boldsymbol{x}$ inputs in our training set.

This approach is not as readily applicable to many other tasks. For example, it is difficult to generate new fake data for a density estimation task unless we have already solved the density estimation problem.

Dataset augmentation has been a particularly effective technique for a specific classification problem: object recognition. Images are high dimensional and include an enormous variety of factors of variation, many of which can be easily simulated. Operations like translating the training images a few pixels in each direction can often greatly improve generalization, even if the model has already been designed to be partially translation invariant by using the convolution and pooling techniques described in chapter 9. Many other operations such as rotating the image or scaling the image have also proven quite effective.

One must be careful not to apply transformations that would change the correct class. For example, optical character recognition tasks require recognizing the difference between 'b' and 'd' and the difference between '6' and '9', so horizontal flips and 180° rotations are not appropriate ways of augmenting datasets for these tasks.

There are also transformations that we would like our classifiers to be invariant to, but which are not easy to perform. For example, out-of-plane rotation can not be implemented as a simple geometric operation on the input pixels.

Dataset augmentation is effective for speech recognition tasks as well (Jaitly and Hinton, 2013).

Injecting noise in the input to a neural network (Sietsma and Dow, 1991) can also be seen as a form of data augmentation. For many classification and even some regression tasks, the task should still be possible to solve even if small random noise is added to the input. Neural networks prove not to be very robust to noise, however (Tang and Eliasmith, 2010). One way to improve the robustness of neural networks is simply to train them with random noise applied to their inputs. Input noise injection is part of some unsupervised learning algorithms such as the denoising autoencoder (Vincent *et al.*, 2008). Noise injection also works when the noise is applied to the hidden units, which can be seen as doing dataset augmentation at multiple levels of abstraction. Poole *et al.* (2014) recently showed that this approach can be highly effective provided that the magnitude of the noise is carefully tuned. Dropout, a powerful regularization strategy that will be described in section 7.12, can be seen as a process of constructing new inputs by *multiplying* by noise.

When comparing machine learning benchmark results, it is important to take the effect of dataset augmentation into account. Often, hand-designed dataset augmentation schemes can dramatically reduce the generalization error of a machine learning technique. To compare the performance of one machine learning algorithm to another, it is necessary to perform controlled experiments. When comparing machine learning algorithm A and machine learning algorithm B, it is necessary to make sure that both algorithms were evaluated using the same hand-designed dataset augmentation schemes. Suppose that algorithm A performs poorly with no dataset augmentation and algorithm B performs well when combined with numerous synthetic transformations of the input. In such a case it is likely the synthetic transformations caused the improved performance, rather than the use of machine learning algorithm B. Sometimes deciding whether an experiment has been properly controlled requires subjective judgment. For example, machine learning algorithms that inject noise into the input are performing a form of dataset augmentation. Usually, operations that are generally applicable (such as adding Gaussian noise to the input) are considered part of the machine learning algorithm, while operations that are specific to one application domain (such as randomly cropping an image) are considered to be separate pre-processing steps.

7.5 Noise Robustness

Section 7.4 has motivated the use of noise applied to the inputs as a dataset augmentation strategy. For some models, the addition of noise with infinitesimal variance at the input of the model is equivalent to imposing a penalty on the norm of the weights (Bishop, 1995a,b). In the general case, it is important to remember that noise injection can be much more powerful than simply shrinking the parameters, especially when the noise is added to the hidden units. Noise applied to the hidden units is such an important topic that it merit its own separate discussion; the dropout algorithm described in section 7.12 is the main development of that approach.

Another way that noise has been used in the service of regularizing models is by adding it to the weights. This technique has been used primarily in the context of recurrent neural networks (Jim *et al.*, 1996; Graves, 2011). This can be interpreted as a stochastic implementation of Bayesian inference over the weights. The Bayesian treatment of learning would consider the model weights to be uncertain and representable via a probability distribution that reflects this uncertainty. Adding noise to the weights is a practical, stochastic way to reflect this uncertainty.

Noise applied to the weights can also be interpreted as equivalent (under some assumptions) to a more traditional form of regularization, encouraging stability of the function to be learned. Consider the regression setting, where we wish to train a function $\hat{y}(\boldsymbol{x})$ that maps a set of features $\boldsymbol{x}$ to a scalar using the least-squares cost function between the model predictions $\hat{y}(\boldsymbol{x})$ and the true values y:

$$J = \mathbb{E}_{p(x,y)}\left[(\hat{y}(\boldsymbol{x}) - y)^2\right]. \tag{7.30}$$

The training set consists of m labeled examples $\{(\boldsymbol{x}^{(1)}, y^{(1)}), \ldots, (\boldsymbol{x}^{(m)}, y^{(m)})\}$.

We now assume that with each input presentation we also include a random perturbation $\epsilon_{\boldsymbol{W}} \sim \mathcal{N}(\boldsymbol{\epsilon}; \boldsymbol{0}, \eta \boldsymbol{I})$ of the network weights. Let us imagine that we have a standard l-layer MLP. We denote the perturbed model as $\hat{y}_{\boldsymbol{\epsilon_W}}(\boldsymbol{x})$. Despite the injection of noise, we are still interested in minimizing the squared error of the output of the network. The objective function thus becomes:

$$\tilde{J}_{\boldsymbol{W}} = \mathbb{E}_{p(\boldsymbol{x},y,\boldsymbol{\epsilon_W})}\left[(\hat{y}_{\boldsymbol{\epsilon_W}}(\boldsymbol{x}) - y)^2\right] \tag{7.31}$$

$$= \mathbb{E}_{p(\boldsymbol{x},y,\boldsymbol{\epsilon_W})}\left[\hat{y}^2_{\boldsymbol{\epsilon_W}}(\boldsymbol{x}) - 2y\hat{y}_{\boldsymbol{\epsilon_W}}(\boldsymbol{x}) + y^2\right]. \tag{7.32}$$

For small η, the minimization of J with added weight noise (with covariance $\eta \boldsymbol{I}$) is equivalent to minimization of J with an additional regularization term:

$\eta \mathbb{E}_{p(\boldsymbol{x},y)} \left[\|\nabla_{\boldsymbol{W}} \hat{y}(\boldsymbol{x})\|^2 \right]$. This form of regularization encourages the parameters to go to regions of parameter space where small perturbations of the weights have a relatively small influence on the output. In other words, it pushes the model into regions where the model is relatively insensitive to small variations in the weights, finding points that are not merely minima, but minima surrounded by flat regions (Hochreiter and Schmidhuber, 1995). In the simplified case of linear regression (where, for instance, $\hat{y}(\boldsymbol{x}) = \boldsymbol{w}^\top \boldsymbol{x} + b$), this regularization term collapses into $\eta \mathbb{E}_{p(\boldsymbol{x})} \left[\|\boldsymbol{x}\|^2 \right]$, which is not a function of parameters and therefore does not contribute to the gradient of $\tilde{J}_{\boldsymbol{W}}$ with respect to the model parameters.

7.5.1 Injecting Noise at the Output Targets

Most datasets have some amount of mistakes in the y labels. It can be harmful to maximize $\log p(y \mid \boldsymbol{x})$ when y is a mistake. One way to prevent this is to explicitly model the noise on the labels. For example, we can assume that for some small constant ϵ, the training set label y is correct with probability $1 - \epsilon$, and otherwise any of the other possible labels might be correct. This assumption is easy to incorporate into the cost function analytically, rather than by explicitly drawing noise samples. For example, **label smoothing** regularizes a model based on a softmax with k output values by replacing the hard 0 and 1 classification targets with targets of $\frac{\epsilon}{k-1}$ and $1 - \epsilon$, respectively. The standard cross-entropy loss may then be used with these soft targets. Maximum likelihood learning with a softmax classifier and hard targets may actually never converge—the softmax can never predict a probability of exactly 0 or exactly 1, so it will continue to learn larger and larger weights, making more extreme predictions forever. It is possible to prevent this scenario using other regularization strategies like weight decay. Label smoothing has the advantage of preventing the pursuit of hard probabilities without discouraging correct classification. This strategy has been used since the 1980s and continues to be featured prominently in modern neural networks (Szegedy *et al.*, 2015).

7.6 Semi-Supervised Learning

In the paradigm of semi-supervised learning, both unlabeled examples from $P(\mathbf{x})$ and labeled examples from $P(\mathbf{x}, \mathbf{y})$ are used to estimate $P(\mathbf{y} \mid \mathbf{x})$ or predict $\mathbf{y}$ from $\mathbf{x}$.

In the context of deep learning, semi-supervised learning usually refers to learning a representation $\boldsymbol{h} = f(\boldsymbol{x})$. The goal is to learn a representation so that examples from the same class have similar representations. Unsupervised learning can provide useful cues for how to group examples in representation space. Examples that cluster tightly in the input space should be mapped to similar representations. A linear classifier in the new space may achieve better generalization in many cases (Belkin and Niyogi, 2002; Chapelle *et al.*, 2003). A long-standing variant of this approach is the application of principal components analysis as a pre-processing step before applying a classifier (on the projected data).

Instead of having separate unsupervised and supervised components in the model, one can construct models in which a generative model of either $P(\mathbf{x})$ or $P(\mathbf{x}, \mathbf{y})$ shares parameters with a discriminative model of $P(\mathbf{y} \mid \mathbf{x})$. One can then trade-off the supervised criterion $-\log P(\mathbf{y} \mid \mathbf{x})$ with the unsupervised or generative one (such as $-\log P(\mathbf{x})$ or $-\log P(\mathbf{x}, \mathbf{y})$). The generative criterion then expresses a particular form of prior belief about the solution to the supervised learning problem (Lasserre *et al.*, 2006), namely that the structure of $P(\mathbf{x})$ is connected to the structure of $P(\mathbf{y} \mid \mathbf{x})$ in a way that is captured by the shared parametrization. By controlling how much of the generative criterion is included in the total criterion, one can find a better trade-off than with a purely generative or a purely discriminative training criterion (Lasserre *et al.*, 2006; Larochelle and Bengio, 2008).

Salakhutdinov and Hinton (2008) describe a method for learning the kernel function of a kernel machine used for regression, in which the usage of unlabeled examples for modeling $P(\mathbf{x})$ improves $P(\mathbf{y} \mid \mathbf{x})$ quite significantly.

See Chapelle *et al.* (2006) for more information about semi-supervised learning.

7.7 Multi-Task Learning

Multi-task learning (Caruana, 1993) is a way to improve generalization by pooling the examples (which can be seen as soft constraints imposed on the parameters) arising out of several tasks. In the same way that additional training examples put more pressure on the parameters of the model towards values that generalize well, when part of a model is shared across tasks, that part of the model is more constrained towards good values (assuming the sharing is justified), often yielding better generalization.

Figure 7.2 illustrates a very common form of multi-task learning, in which different supervised tasks (predicting $\mathbf{y}^{(i)}$ given $\mathbf{x}$) share the same input $\mathbf{x}$, as well as some intermediate-level representation $\boldsymbol{h}^{(\text{shared})}$ capturing a common pool of factors. The model can generally be divided into two kinds of parts and associated parameters:

1. Task-specific parameters (which only benefit from the examples of their task to achieve good generalization). These are the upper layers of the neural network in figure 7.2.

2. Generic parameters, shared across all the tasks (which benefit from the pooled data of all the tasks). These are the lower layers of the neural network in figure 7.2.

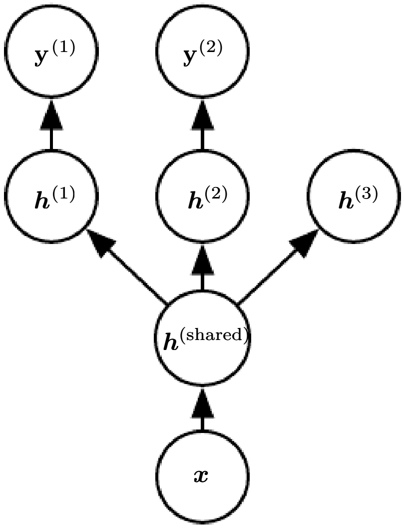

Figure 7.2: Multi-task learning can be cast in several ways in deep learning frameworks and this figure illustrates the common situation where the tasks share a common input but involve different target random variables. The lower layers of a deep network (whether it is supervised and feedforward or includes a generative component with downward arrows) can be shared across such tasks, while task-specific parameters (associated respectively with the weights into and from $\boldsymbol{h}^{(1)}$ and $\boldsymbol{h}^{(2)}$) can be learned on top of those yielding a shared representation $\boldsymbol{h}^{(\text{shared})}$. The underlying assumption is that there exists a common pool of factors that explain the variations in the input $\mathbf{x}$, while each task is associated with a subset of these factors. In this example, it is additionally assumed that top-level hidden units $\boldsymbol{h}^{(1)}$ and $\boldsymbol{h}^{(2)}$ are specialized to each task (respectively predicting $\mathbf{y}^{(1)}$ and $\mathbf{y}^{(2)}$) while some intermediate-level representation $\boldsymbol{h}^{(\text{shared})}$ is shared across all tasks. In the unsupervised learning context, it makes sense for some of the top-level factors to be associated with none of the output tasks ($\boldsymbol{h}^{(3)}$): these are the factors that explain some of the input variations but are not relevant for predicting $\mathbf{y}^{(1)}$ or $\mathbf{y}^{(2)}$.

Improved generalization and generalization error bounds (Baxter, 1995) can be achieved because of the shared parameters, for which statistical strength can be

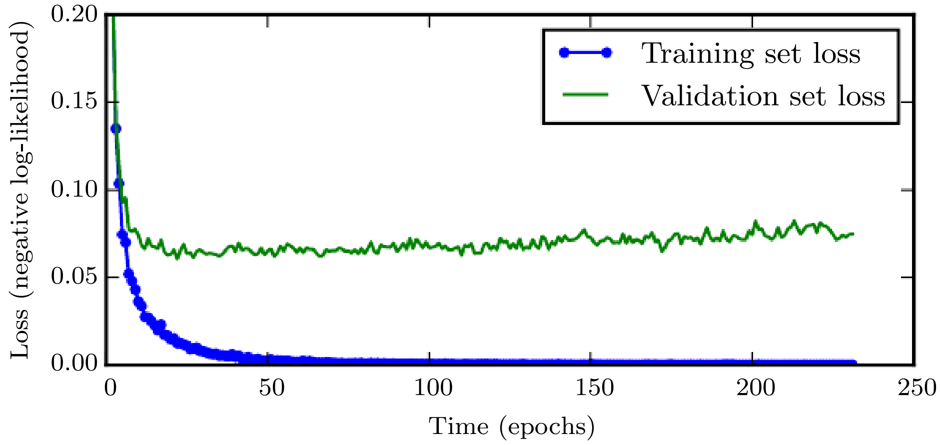

Figure 7.3: Learning curves showing how the negative log-likelihood loss changes over time (indicated as number of training iterations over the dataset, or **epochs**). In this example, we train a maxout network on MNIST. Observe that the training objective decreases consistently over time, but the validation set average loss eventually begins to increase again, forming an asymmetric U-shaped curve.

greatly improved (in proportion with the increased number of examples for the shared parameters, compared to the scenario of single-task models). Of course this will happen only if some assumptions about the statistical relationship between the different tasks are valid, meaning that there is something shared across some of the tasks.

From the point of view of deep learning, the underlying prior belief is the following: *among the factors that explain the variations observed in the data associated with the different tasks, some are shared across two or more tasks.*

7.8 Early Stopping

When training large models with sufficient representational capacity to overfit the task, we often observe that training error decreases steadily over time, but validation set error begins to rise again. See figure 7.3 for an example of this behavior. This behavior occurs very reliably.

This means we can obtain a model with better validation set error (and thus, hopefully better test set error) by returning to the parameter setting at the point in time with the lowest validation set error. Every time the error on the validation set improves, we store a copy of the model parameters. When the training algorithm terminates, we return these parameters, rather than the latest parameters. The algorithm terminates when no parameters have improved over the best recorded validation error for some pre-specified number of iterations. This procedure is specified more formally in algorithm 7.1.

Algorithm 7.1 The early stopping meta-algorithm for determining the best amount of time to train. This meta-algorithm is a general strategy that works well with a variety of training algorithms and ways of quantifying error on the validation set.

Let n be the number of steps between evaluations.
Let p be the "patience," the number of times to observe worsening validation set error before giving up.
Let $\boldsymbol{\theta}_o$ be the initial parameters.
$\boldsymbol{\theta} \leftarrow \boldsymbol{\theta}_o$
$i \leftarrow 0$
$j \leftarrow 0$
$v \leftarrow \infty$
$\boldsymbol{\theta}^* \leftarrow \boldsymbol{\theta}$
$i^* \leftarrow i$
while $j < p$ **do**
  Update $\boldsymbol{\theta}$ by running the training algorithm for n steps.
  $i \leftarrow i + n$
  $v' \leftarrow \text{ValidationSetError}(\boldsymbol{\theta})$
  if $v' < v$ **then**
    $j \leftarrow 0$
    $\boldsymbol{\theta}^* \leftarrow \boldsymbol{\theta}$
    $i^* \leftarrow i$
    $v \leftarrow v'$
  else
    $j \leftarrow j + 1$
  end if
end while
Best parameters are $\boldsymbol{\theta}^*$, best number of training steps is i^*

This strategy is known as **early stopping**. It is probably the most commonly used form of regularization in deep learning. Its popularity is due both to its effectiveness and its simplicity.

One way to think of early stopping is as a very efficient hyperparameter selection algorithm. In this view, the number of training steps is just another hyperparameter. We can see in figure 7.3 that this hyperparameter has a U-shaped validation set performance curve. Most hyperparameters that control model capacity have such a U-shaped validation set performance curve, as illustrated in figure 5.3. In the case of early stopping, we are controlling the effective capacity of the model by determining how many steps it can take to fit the training set. Most hyperparameters must be chosen using an expensive guess and check process, where we set a hyperparameter at the start of training, then run training for several steps to see its effect. The "training time" hyperparameter is unique in that by definition a single run of training tries out many values of the hyperparameter. The only significant cost to choosing this hyperparameter automatically via early stopping is running the validation set evaluation periodically during training. Ideally, this is done in parallel to the training process on a separate machine, separate CPU, or separate GPU from the main training process. If such resources are not available, then the cost of these periodic evaluations may be reduced by using a validation set that is small compared to the training set or by evaluating the validation set error less frequently and obtaining a lower resolution estimate of the optimal training time.

An additional cost to early stopping is the need to maintain a copy of the best parameters. This cost is generally negligible, because it is acceptable to store these parameters in a slower and larger form of memory (for example, training in GPU memory, but storing the optimal parameters in host memory or on a disk drive). Since the best parameters are written to infrequently and never read during training, these occasional slow writes have little effect on the total training time.

Early stopping is a very unobtrusive form of regularization, in that it requires almost no change in the underlying training procedure, the objective function, or the set of allowable parameter values. This means that it is easy to use early stopping without damaging the learning dynamics. This is in contrast to weight decay, where one must be careful not to use too much weight decay and trap the network in a bad local minimum corresponding to a solution with pathologically small weights.

Early stopping may be used either alone or in conjunction with other regularization strategies. Even when using regularization strategies that modify the objective function to encourage better generalization, it is rare for the best generalization to occur at a local minimum of the training objective.

Early stopping requires a validation set, which means some training data is not fed to the model. To best exploit this extra data, one can perform extra training after the initial training with early stopping has completed. In the second, extra training step, all of the training data is included. There are two basic strategies one can use for this second training procedure.

One strategy (algorithm 7.2) is to initialize the model again and retrain on all of the data. In this second training pass, we train for the same number of steps as the early stopping procedure determined was optimal in the first pass. There are some subtleties associated with this procedure. For example, there is not a good way of knowing whether to retrain for the same number of parameter updates or the same number of passes through the dataset. On the second round of training, each pass through the dataset will require more parameter updates because the training set is bigger.

Algorithm 7.2 A meta-algorithm for using early stopping to determine how long to train, then retraining on all the data.

Let $\boldsymbol{X}^{(\text{train})}$ and $\boldsymbol{y}^{(\text{train})}$ be the training set.
Split $\boldsymbol{X}^{(\text{train})}$ and $\boldsymbol{y}^{(\text{train})}$ into $(\boldsymbol{X}^{(\text{subtrain})}, \boldsymbol{X}^{(\text{valid})})$ and $(\boldsymbol{y}^{(\text{subtrain})}, \boldsymbol{y}^{(\text{valid})})$ respectively.
Run early stopping (algorithm 7.1) starting from random $\boldsymbol{\theta}$ using $\boldsymbol{X}^{(\text{subtrain})}$ and $\boldsymbol{y}^{(\text{subtrain})}$ for training data and $\boldsymbol{X}^{(\text{valid})}$ and $\boldsymbol{y}^{(\text{valid})}$ for validation data. This returns i^*, the optimal number of steps.
Set $\boldsymbol{\theta}$ to random values again.
Train on $\boldsymbol{X}^{(\text{train})}$ and $\boldsymbol{y}^{(\text{train})}$ for i^* steps.

Another strategy for using all of the data is to keep the parameters obtained from the first round of training and then *continue* training but now using all of the data. At this stage, we now no longer have a guide for when to stop in terms of a number of steps. Instead, we can monitor the average loss function on the validation set, and continue training until it falls below the value of the training set objective at which the early stopping procedure halted. This strategy avoids the high cost of retraining the model from scratch, but is not as well-behaved. For example, there is not any guarantee that the objective on the validation set will ever reach the target value, so this strategy is not even guaranteed to terminate. This procedure is presented more formally in algorithm 7.3.

Early stopping is also useful because it reduces the computational cost of the training procedure. Besides the obvious reduction in cost due to limiting the number of training iterations, it also has the benefit of providing regularization without requiring the addition of penalty terms to the cost function or the computation of the gradients of such additional terms.

How early stopping acts as a regularizer: So far we have stated that early stopping *is* a regularization strategy, but we have supported this claim only by showing learning curves where the validation set error has a U-shaped curve. What

Algorithm 7.3 Meta-algorithm using early stopping to determine at what objective value we start to overfit, then continue training until that value is reached.

Let $\boldsymbol{X}^{(\text{train})}$ and $\boldsymbol{y}^{(\text{train})}$ be the training set.
Split $\boldsymbol{X}^{(\text{train})}$ and $\boldsymbol{y}^{(\text{train})}$ into $(\boldsymbol{X}^{(\text{subtrain})}, \boldsymbol{X}^{(\text{valid})})$ and $(\boldsymbol{y}^{(\text{subtrain})}, \boldsymbol{y}^{(\text{valid})})$ respectively.
Run early stopping (algorithm 7.1) starting from random $\boldsymbol{\theta}$ using $\boldsymbol{X}^{(\text{subtrain})}$ and $\boldsymbol{y}^{(\text{subtrain})}$ for training data and $\boldsymbol{X}^{(\text{valid})}$ and $\boldsymbol{y}^{(\text{valid})}$ for validation data. This updates $\boldsymbol{\theta}$.
$\epsilon \leftarrow J(\boldsymbol{\theta}, \boldsymbol{X}^{(\text{subtrain})}, \boldsymbol{y}^{(\text{subtrain})})$
while $J(\boldsymbol{\theta}, \boldsymbol{X}^{(\text{valid})}, \boldsymbol{y}^{(\text{valid})}) > \epsilon$ **do**
  Train on $\boldsymbol{X}^{(\text{train})}$ and $\boldsymbol{y}^{(\text{train})}$ for n steps.
end while

---

is the actual mechanism by which early stopping regularizes the model? Bishop (1995a) and Sjöberg and Ljung (1995) argued that early stopping has the effect of restricting the optimization procedure to a relatively small volume of parameter space in the neighborhood of the initial parameter value $\boldsymbol{\theta}_o$, as illustrated in figure 7.4. More specifically, imagine taking τ optimization steps (corresponding to τ training iterations) and with learning rate ϵ. We can view the product $\epsilon\tau$ as a measure of effective capacity. Assuming the gradient is bounded, restricting both the number of iterations and the learning rate limits the volume of parameter space reachable from $\boldsymbol{\theta}_o$. In this sense, $\epsilon\tau$ behaves as if it were the reciprocal of the coefficient used for weight decay.

Indeed, we can show how—in the case of a simple linear model with a quadratic error function and simple gradient descent—early stopping is equivalent to L^2 regularization.

In order to compare with classical L^2 regularization, we examine a simple setting where the only parameters are linear weights ($\boldsymbol{\theta} = \boldsymbol{w}$). We can model the cost function J with a quadratic approximation in the neighborhood of the empirically optimal value of the weights $\boldsymbol{w}^*$:

$$\hat{J}(\boldsymbol{\theta}) = J(\boldsymbol{w}^*) + \frac{1}{2}(\boldsymbol{w} - \boldsymbol{w}^*)^\top \boldsymbol{H}(\boldsymbol{w} - \boldsymbol{w}^*), \tag{7.33}$$

where $\boldsymbol{H}$ is the Hessian matrix of J with respect to $\boldsymbol{w}$ evaluated at $\boldsymbol{w}^*$. Given the assumption that $\boldsymbol{w}^*$ is a minimum of $J(\boldsymbol{w})$, we know that $\boldsymbol{H}$ is positive semidefinite. Under a local Taylor series approximation, the gradient is given by:

$$\nabla_{\boldsymbol{w}} \hat{J}(\boldsymbol{w}) = \boldsymbol{H}(\boldsymbol{w} - \boldsymbol{w}^*). \tag{7.34}$$

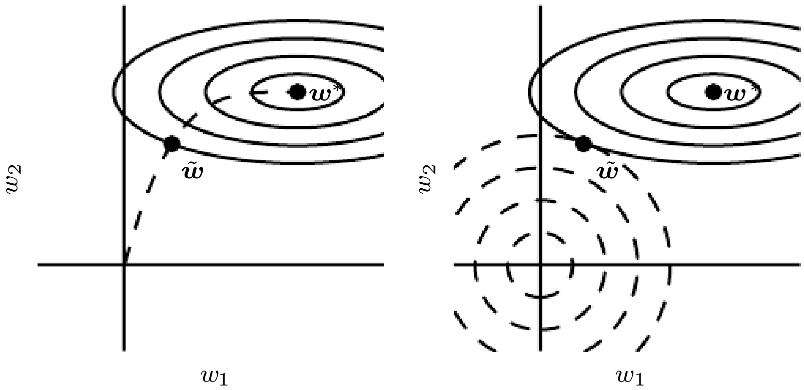

Figure 7.4: An illustration of the effect of early stopping. *(Left)*The solid contour lines indicate the contours of the negative log-likelihood. The dashed line indicates the trajectory taken by SGD beginning from the origin. Rather than stopping at the point $\boldsymbol{w}^*$ that minimizes the cost, early stopping results in the trajectory stopping at an earlier point $\tilde{\boldsymbol{w}}$. *(Right)*An illustration of the effect of L^2 regularization for comparison. The dashed circles indicate the contours of the L^2 penalty, which causes the minimum of the total cost to lie nearer the origin than the minimum of the unregularized cost.

We are going to study the trajectory followed by the parameter vector during training. For simplicity, let us set the initial parameter vector to the origin,[3] that is $\boldsymbol{w}^{(0)} = \boldsymbol{0}$. Let us study the approximate behavior of gradient descent on J by analyzing gradient descent on $\hat{J}$:

$$\boldsymbol{w}^{(\tau)} = \boldsymbol{w}^{(\tau-1)} - \epsilon \nabla_{\boldsymbol{w}} \hat{J}(\boldsymbol{w}^{(\tau-1)}) \tag{7.35}$$

$$= \boldsymbol{w}^{(\tau-1)} - \epsilon \boldsymbol{H}(\boldsymbol{w}^{(\tau-1)} - \boldsymbol{w}^*) \tag{7.36}$$

$$\boldsymbol{w}^{(\tau)} - \boldsymbol{w}^* = (\boldsymbol{I} - \epsilon \boldsymbol{H})(\boldsymbol{w}^{(\tau-1)} - \boldsymbol{w}^*). \tag{7.37}$$

Let us now rewrite this expression in the space of the eigenvectors of $\boldsymbol{H}$, exploiting the eigendecomposition of $\boldsymbol{H}$: $\boldsymbol{H} = \boldsymbol{Q}\boldsymbol{\Lambda}\boldsymbol{Q}^\top$, where $\boldsymbol{\Lambda}$ is a diagonal matrix and $\boldsymbol{Q}$ is an orthonormal basis of eigenvectors.

$$\boldsymbol{w}^{(\tau)} - \boldsymbol{w}^* = (\boldsymbol{I} - \epsilon \boldsymbol{Q}\boldsymbol{\Lambda}\boldsymbol{Q}^\top)(\boldsymbol{w}^{(\tau-1)} - \boldsymbol{w}^*) \tag{7.38}$$

$$\boldsymbol{Q}^\top(\boldsymbol{w}^{(\tau)} - \boldsymbol{w}^*) = (\boldsymbol{I} - \epsilon \boldsymbol{\Lambda})\boldsymbol{Q}^\top(\boldsymbol{w}^{(\tau-1)} - \boldsymbol{w}^*) \tag{7.39}$$

[3]For neural networks, to obtain symmetry breaking between hidden units, we cannot initialize all the parameters to $\boldsymbol{0}$, as discussed in section 6.2. However, the argument holds for any other initial value $\boldsymbol{w}^{(0)}$.

Assuming that $\boldsymbol{w}^{(0)} = 0$ and that ϵ is chosen to be small enough to guarantee $|1 - \epsilon\lambda_i| < 1$, the parameter trajectory during training after τ parameter updates is as follows:

$$\boldsymbol{Q}^\top \boldsymbol{w}^{(\tau)} = [\boldsymbol{I} - (\boldsymbol{I} - \epsilon\boldsymbol{\Lambda})^\tau]\boldsymbol{Q}^\top \boldsymbol{w}^*. \tag{7.40}$$

Now, the expression for $\boldsymbol{Q}^\top \tilde{\boldsymbol{w}}$ in equation 7.13 for L^2 regularization can be rearranged as:

$$\boldsymbol{Q}^\top \tilde{\boldsymbol{w}} = (\boldsymbol{\Lambda} + \alpha\boldsymbol{I})^{-1}\boldsymbol{\Lambda}\boldsymbol{Q}^\top \boldsymbol{w}^* \tag{7.41}$$

$$\boldsymbol{Q}^\top \tilde{\boldsymbol{w}} = [\boldsymbol{I} - (\boldsymbol{\Lambda} + \alpha\boldsymbol{I})^{-1}\alpha]\boldsymbol{Q}^\top \boldsymbol{w}^* \tag{7.42}$$

Comparing equation 7.40 and equation 7.42, we see that if the hyperparameters ϵ, α, and τ are chosen such that

$$(\boldsymbol{I} - \epsilon\boldsymbol{\Lambda})^\tau = (\boldsymbol{\Lambda} + \alpha\boldsymbol{I})^{-1}\alpha, \tag{7.43}$$

then L^2 regularization and early stopping can be seen to be equivalent (at least under the quadratic approximation of the objective function). Going even further, by taking logarithms and using the series expansion for $\log(1 + x)$, we can conclude that if all λ_i are small (that is, $\epsilon\lambda_i \ll 1$ and $\lambda_i/\alpha \ll 1$) then

$$\tau \approx \frac{1}{\epsilon\alpha}, \tag{7.44}$$

$$\alpha \approx \frac{1}{\tau\epsilon}. \tag{7.45}$$

That is, under these assumptions, the number of training iterations τ plays a role inversely proportional to the L^2 regularization parameter, and the inverse of $\tau\epsilon$ plays the role of the weight decay coefficient.

Parameter values corresponding to directions of significant curvature (of the objective function) are regularized less than directions of less curvature. Of course, in the context of early stopping, this really means that parameters that correspond to directions of significant curvature tend to learn early relative to parameters corresponding to directions of less curvature.

The derivations in this section have shown that a trajectory of length τ ends at a point that corresponds to a minimum of the L^2-regularized objective. Early stopping is of course more than the mere restriction of the trajectory length; instead, early stopping typically involves monitoring the validation set error in order to stop the trajectory at a particularly good point in space. Early stopping therefore has the advantage over weight decay that early stopping automatically determines the correct amount of regularization while weight decay requires many training experiments with different values of its hyperparameter.

7.9 Parameter Tying and Parameter Sharing

Thus far, in this chapter, when we have discussed adding constraints or penalties to the parameters, we have always done so with respect to a fixed region or point. For example, L^2 regularization (or weight decay) penalizes model parameters for deviating from the fixed value of zero. However, sometimes we may need other ways to express our prior knowledge about suitable values of the model parameters. Sometimes we might not know precisely what values the parameters should take but we know, from knowledge of the domain and model architecture, that there should be some dependencies between the model parameters.

A common type of dependency that we often want to express is that certain parameters should be close to one another. Consider the following scenario: we have two models performing the same classification task (with the same set of classes) but with somewhat different input distributions. Formally, we have model A with parameters $\boldsymbol{w}^{(A)}$ and model B with parameters $\boldsymbol{w}^{(B)}$. The two models map the input to two different, but related outputs: $\hat{y}^{(A)} = f(\boldsymbol{w}^{(A)}, \boldsymbol{x})$ and $\hat{y}^{(B)} = g(\boldsymbol{w}^{(B)}, \boldsymbol{x})$.

Let us imagine that the tasks are similar enough (perhaps with similar input and output distributions) that we believe the model parameters should be close to each other: $\forall i$, $w_i^{(A)}$ should be close to $w_i^{(B)}$. We can leverage this information through regularization. Specifically, we can use a parameter norm penalty of the form: $\Omega(\boldsymbol{w}^{(A)}, \boldsymbol{w}^{(B)}) = \|\boldsymbol{w}^{(A)} - \boldsymbol{w}^{(B)}\|_2^2$. Here we used an L^2 penalty, but other choices are also possible.

This kind of approach was proposed by Lasserre *et al.* (2006), who regularized the parameters of one model, trained as a classifier in a supervised paradigm, to be close to the parameters of another model, trained in an unsupervised paradigm (to capture the distribution of the observed input data). The architectures were constructed such that many of the parameters in the classifier model could be paired to corresponding parameters in the unsupervised model.

While a parameter norm penalty is one way to regularize parameters to be close to one another, the more popular way is to use constraints: *to force sets of parameters to be equal*. This method of regularization is often referred to as **parameter sharing**, because we interpret the various models or model components as sharing a unique set of parameters. A significant advantage of parameter sharing over regularizing the parameters to be close (via a norm penalty) is that only a subset of the parameters (the unique set) need to be stored in memory. In certain models—such as the convolutional neural network—this can lead to significant reduction in the memory footprint of the model.

Convolutional Neural Networks By far the most popular and extensive use of parameter sharing occurs in **convolutional neural networks** (CNNs) applied to computer vision.

Natural images have many statistical properties that are invariant to translation. For example, a photo of a cat remains a photo of a cat if it is translated one pixel to the right. CNNs take this property into account by sharing parameters across multiple image locations. The same feature (a hidden unit with the same weights) is computed over different locations in the input. This means that we can find a cat with the same cat detector whether the cat appears at column i or column $i+1$ in the image.

Parameter sharing has allowed CNNs to dramatically lower the number of unique model parameters and to significantly increase network sizes without requiring a corresponding increase in training data. It remains one of the best examples of how to effectively incorporate domain knowledge into the network architecture.

CNNs will be discussed in more detail in chapter 9.

7.10 Sparse Representations

Weight decay acts by placing a penalty directly on the model parameters. Another strategy is to place a penalty on the activations of the units in a neural network, encouraging their activations to be sparse. This indirectly imposes a complicated penalty on the model parameters.

We have already discussed (in section 7.1.2) how L^1 penalization induces a sparse parametrization—meaning that many of the parameters become zero (or close to zero). Representational sparsity, on the other hand, describes a representation where many of the elements of the representation are zero (or close to zero). A simplified view of this distinction can be illustrated in the context of linear regression:

$$\underbrace{\begin{bmatrix} 18 \\ 5 \\ 15 \\ -9 \\ -3 \end{bmatrix}}_{\boldsymbol{y} \in \mathbb{R}^m} = \underbrace{\begin{bmatrix} 4 & 0 & 0 & -2 & 0 & 0 \\ 0 & 0 & -1 & 0 & 3 & 0 \\ 0 & 5 & 0 & 0 & 0 & 0 \\ 1 & 0 & 0 & -1 & 0 & -4 \\ 1 & 0 & 0 & 0 & -5 & 0 \end{bmatrix}}_{\boldsymbol{A} \in \mathbb{R}^{m \times n}} \underbrace{\begin{bmatrix} 2 \\ 3 \\ -2 \\ -5 \\ 1 \\ 4 \end{bmatrix}}_{\boldsymbol{x} \in \mathbb{R}^n} \tag{7.46}$$

$$\underset{\boldsymbol{y} \in \mathbb{R}^m}{\begin{bmatrix} -14 \\ 1 \\ 19 \\ 2 \\ 23 \end{bmatrix}} = \underset{\boldsymbol{B} \in \mathbb{R}^{m \times n}}{\begin{bmatrix} 3 & -1 & 2 & -5 & 4 & 1 \\ 4 & 2 & -3 & -1 & 1 & 3 \\ -1 & 5 & 4 & 2 & -3 & -2 \\ 3 & 1 & 2 & -3 & 0 & -3 \\ -5 & 4 & -2 & 2 & -5 & -1 \end{bmatrix}} \underset{\boldsymbol{h} \in \mathbb{R}^n}{\begin{bmatrix} 0 \\ 2 \\ 0 \\ 0 \\ -3 \\ 0 \end{bmatrix}} \tag{7.47}$$

In the first expression, we have an example of a sparsely parametrized linear regression model. In the second, we have linear regression with a sparse representation $\boldsymbol{h}$ of the data $\boldsymbol{x}$. That is, $\boldsymbol{h}$ is a function of $\boldsymbol{x}$ that, in some sense, represents the information present in $\boldsymbol{x}$, but does so with a sparse vector.

Representational regularization is accomplished by the same sorts of mechanisms that we have used in parameter regularization.

Norm penalty regularization of representations is performed by adding to the loss function J a norm penalty on the *representation*. This penalty is denoted $\Omega(\boldsymbol{h})$. As before, we denote the regularized loss function by $\tilde{J}$:

$$\tilde{J}(\boldsymbol{\theta}; \boldsymbol{X}, \boldsymbol{y}) = J(\boldsymbol{\theta}; \boldsymbol{X}, \boldsymbol{y}) + \alpha\Omega(\boldsymbol{h}) \tag{7.48}$$

where $\alpha \in [0, \infty)$ weights the relative contribution of the norm penalty term, with larger values of α corresponding to more regularization.

Just as an L^1 penalty on the parameters induces parameter sparsity, an L^1 penalty on the elements of the representation induces representational sparsity: $\Omega(\boldsymbol{h}) = ||\boldsymbol{h}||_1 = \sum_i |h_i|$. Of course, the L^1 penalty is only one choice of penalty that can result in a sparse representation. Others include the penalty derived from a Student-t prior on the representation (Olshausen and Field, 1996; Bergstra, 2011) and KL divergence penalties (Larochelle and Bengio, 2008) that are especially useful for representations with elements constrained to lie on the unit interval. Lee *et al.* (2008) and Goodfellow *et al.* (2009) both provide examples of strategies based on regularizing the average activation across several examples, $\frac{1}{m}\sum_i \boldsymbol{h}^{(i)}$, to be near some target value, such as a vector with .01 for each entry.

Other approaches obtain representational sparsity with a hard constraint on the activation values. For example, **orthogonal matching pursuit** (Pati *et al.*, 1993) encodes an input $\boldsymbol{x}$ with the representation $\boldsymbol{h}$ that solves the constrained optimization problem

$$\underset{\boldsymbol{h}, \|\boldsymbol{h}\|_0 < k}{\arg\min} \|\boldsymbol{x} - \boldsymbol{W}\boldsymbol{h}\|^2, \tag{7.49}$$

where $\|\boldsymbol{h}\|_0$ is the number of non-zero entries of $\boldsymbol{h}$. This problem can be solved efficiently when $\boldsymbol{W}$ is constrained to be orthogonal. This method is often called

OMP-k with the value of k specified to indicate the number of non-zero features allowed. Coates and Ng (2011) demonstrated that OMP-1 can be a very effective feature extractor for deep architectures.

Essentially any model that has hidden units can be made sparse. Throughout this book, we will see many examples of sparsity regularization used in a variety of contexts.

7.11 Bagging and Other Ensemble Methods

Bagging (short for **bootstrap aggregating**) is a technique for reducing generalization error by combining several models (Breiman, 1994). The idea is to train several different models separately, then have all of the models vote on the output for test examples. This is an example of a general strategy in machine learning called **model averaging**. Techniques employing this strategy are known as **ensemble methods**.

The reason that model averaging works is that different models will usually not make all the same errors on the test set.

Consider for example a set of k regression models. Suppose that each model makes an error ϵ_i on each example, with the errors drawn from a zero-mean multivariate normal distribution with variances $\mathbb{E}[\epsilon_i^2] = v$ and covariances $\mathbb{E}[\epsilon_i \epsilon_j] = c$. Then the error made by the average prediction of all the ensemble models is $\frac{1}{k}\sum_i \epsilon_i$. The expected squared error of the ensemble predictor is

$$\mathbb{E}\left[\left(\frac{1}{k}\sum_i \epsilon_i\right)^2\right] = \frac{1}{k^2}\mathbb{E}\left[\sum_i \left(\epsilon_i^2 + \sum_{j \neq i} \epsilon_i \epsilon_j\right)\right] \tag{7.50}$$

$$= \frac{1}{k}v + \frac{k-1}{k}c. \tag{7.51}$$

In the case where the errors are perfectly correlated and $c = v$, the mean squared error reduces to v, so the model averaging does not help at all. In the case where the errors are perfectly uncorrelated and $c = 0$, the expected squared error of the ensemble is only $\frac{1}{k}v$. This means that the expected squared error of the ensemble decreases linearly with the ensemble size. In other words, on average, the ensemble will perform at least as well as any of its members, and if the members make independent errors, the ensemble will perform significantly better than its members.

Different ensemble methods construct the ensemble of models in different ways. For example, each member of the ensemble could be formed by training a completely

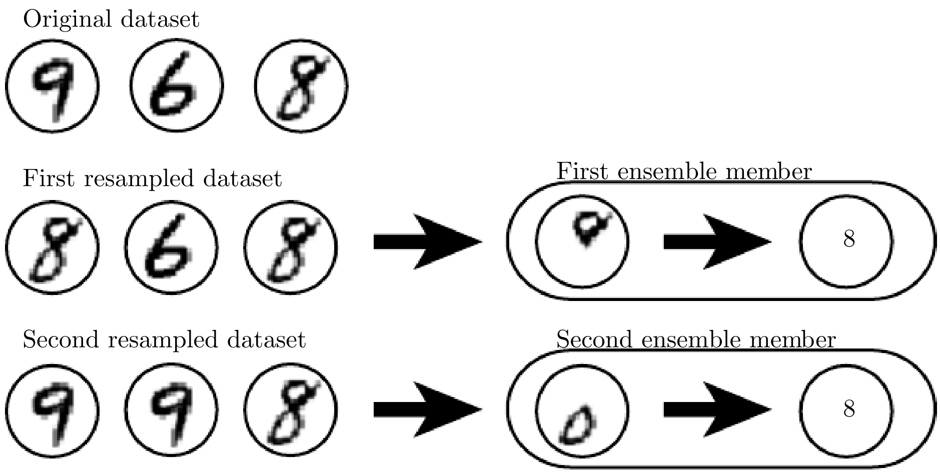

Figure 7.5: A cartoon depiction of how bagging works. Suppose we train an 8 detector on the dataset depicted above, containing an 8, a 6 and a 9. Suppose we make two different resampled datasets. The bagging training procedure is to construct each of these datasets by sampling with replacement. The first dataset omits the 9 and repeats the 8. On this dataset, the detector learns that a loop on top of the digit corresponds to an 8. On the second dataset, we repeat the 9 and omit the 6. In this case, the detector learns that a loop on the bottom of the digit corresponds to an 8. Each of these individual classification rules is brittle, but if we average their output then the detector is robust, achieving maximal confidence only when both loops of the 8 are present.

different kind of model using a different algorithm or objective function. Bagging is a method that allows the same kind of model, training algorithm and objective function to be reused several times.

Specifically, bagging involves constructing k different datasets. Each dataset has the same number of examples as the original dataset, but each dataset is constructed by sampling with replacement from the original dataset. This means that, with high probability, each dataset is missing some of the examples from the original dataset and also contains several duplicate examples (on average around $2/3$ of the examples from the original dataset are found in the resulting training set, if it has the same size as the original). Model i is then trained on dataset i. The differences between which examples are included in each dataset result in differences between the trained models. See figure 7.5 for an example.

Neural networks reach a wide enough variety of solution points that they can often benefit from model averaging even if all of the models are trained on the same dataset. Differences in random initialization, random selection of minibatches, differences in hyperparameters, or different outcomes of non-deterministic implementations of neural networks are often enough to cause different members of the ensemble to make partially independent errors.

Model averaging is an extremely powerful and reliable method for reducing generalization error. Its use is usually discouraged when benchmarking algorithms for scientific papers, because any machine learning algorithm can benefit substantially from model averaging at the price of increased computation and memory. For this reason, benchmark comparisons are usually made using a single model.

Machine learning contests are usually won by methods using model averaging over dozens of models. A recent prominent example is the Netflix Grand Prize (Koren, 2009).

Not all techniques for constructing ensembles are designed to make the ensemble more regularized than the individual models. For example, a technique called **boosting** (Freund and Schapire, 1996b,a) constructs an ensemble with higher capacity than the individual models. Boosting has been applied to build ensembles of neural networks (Schwenk and Bengio, 1998) by incrementally adding neural networks to the ensemble. Boosting has also been applied interpreting an individual neural network as an ensemble (Bengio *et al.*, 2006a), incrementally adding hidden units to the neural network.

7.12 Dropout

Dropout (Srivastava *et al.*, 2014) provides a computationally inexpensive but powerful method of regularizing a broad family of models. To a first approximation, dropout can be thought of as a method of making bagging practical for ensembles of very many large neural networks. Bagging involves training multiple models, and evaluating multiple models on each test example. This seems impractical when each model is a large neural network, since training and evaluating such networks is costly in terms of runtime and memory. It is common to use ensembles of five to ten neural networks—Szegedy *et al.* (2014a) used six to win the ILSVRC—but more than this rapidly becomes unwieldy. Dropout provides an inexpensive approximation to training and evaluating a bagged ensemble of exponentially many neural networks.

Specifically, dropout trains the ensemble consisting of all sub-networks that can be formed by removing non-output units from an underlying base network, as illustrated in figure 7.6. In most modern neural networks, based on a series of affine transformations and nonlinearities, we can effectively remove a unit from a network by multiplying its output value by zero. This procedure requires some slight modification for models such as radial basis function networks, which take the difference between the unit's state and some reference value. Here, we present the dropout algorithm in terms of multiplication by zero for simplicity, but it can be trivially modified to work with other operations that remove a unit from the network.

Recall that to learn with bagging, we define k different models, construct k different datasets by sampling from the training set with replacement, and then train model i on dataset i. Dropout aims to approximate this process, but with an exponentially large number of neural networks. Specifically, to train with dropout, we use a minibatch-based learning algorithm that makes small steps, such as stochastic gradient descent. Each time we load an example into a minibatch, we randomly sample a different binary mask to apply to all of the input and hidden units in the network. The mask for each unit is sampled independently from all of the others. The probability of sampling a mask value of one (causing a unit to be included) is a hyperparameter fixed before training begins. It is not a function of the current value of the model parameters or the input example. Typically, an input unit is included with probability 0.8 and a hidden unit is included with probability 0.5. We then run forward propagation, back-propagation, and the learning update as usual. Figure 7.7 illustrates how to run forward propagation with dropout.

More formally, suppose that a mask vector $\boldsymbol{\mu}$ specifies which units to include, and $J(\boldsymbol{\theta}, \boldsymbol{\mu})$ defines the cost of the model defined by parameters $\boldsymbol{\theta}$ and mask $\boldsymbol{\mu}$. Then dropout training consists in minimizing $\mathbb{E}_{\boldsymbol{\mu}} J(\boldsymbol{\theta}, \boldsymbol{\mu})$. The expectation contains exponentially many terms but we can obtain an unbiased estimate of its gradient by sampling values of $\boldsymbol{\mu}$.

Dropout training is not quite the same as bagging training. In the case of bagging, the models are all independent. In the case of dropout, the models share parameters, with each model inheriting a different subset of parameters from the parent neural network. This parameter sharing makes it possible to represent an exponential number of models with a tractable amount of memory. In the case of bagging, each model is trained to convergence on its respective training set. In the case of dropout, typically most models are not explicitly trained at all—usually, the model is large enough that it would be infeasible to sample all possible sub-networks within the lifetime of the universe. Instead, a tiny fraction of the possible sub-networks are each trained for a single step, and the parameter sharing causes the remaining sub-networks to arrive at good settings of the parameters. These are the only differences. Beyond these, dropout follows the bagging algorithm. For example, the training set encountered by each sub-network is indeed a subset of the original training set sampled with replacement.

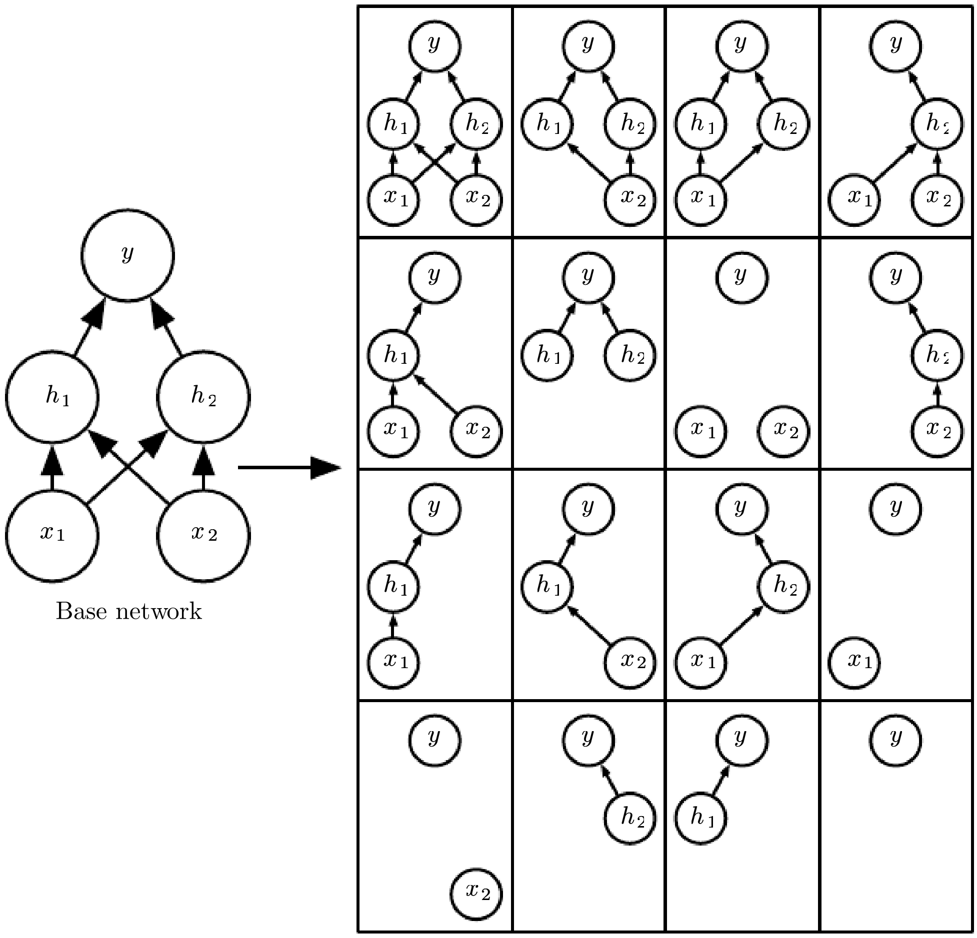

Figure 7.6: Dropout trains an ensemble consisting of all sub-networks that can be constructed by removing non-output units from an underlying base network. Here, we begin with a base network with two visible units and two hidden units. There are sixteen possible subsets of these four units. We show all sixteen subnetworks that may be formed by dropping out different subsets of units from the original network. In this small example, a large proportion of the resulting networks have no input units or no path connecting the input to the output. This problem becomes insignificant for networks with wider layers, where the probability of dropping all possible paths from inputs to outputs becomes smaller.

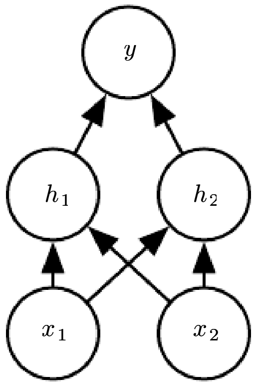

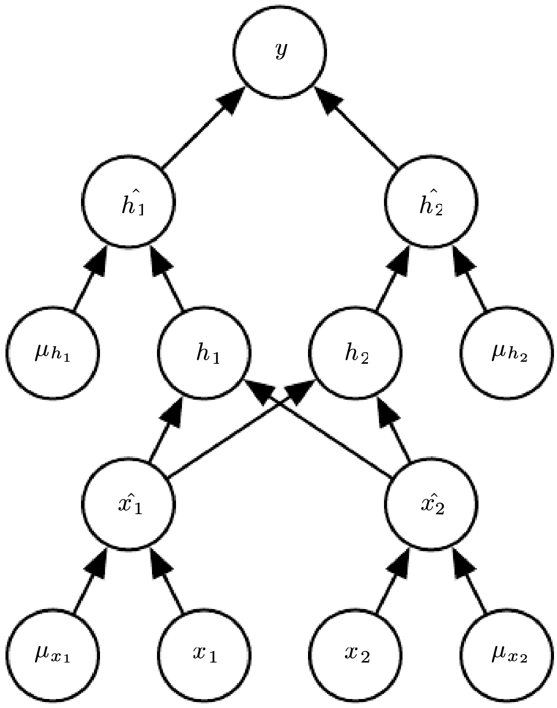

Figure 7.7: An example of forward propagation through a feedforward network using dropout. *(Top)*In this example, we use a feedforward network with two input units, one hidden layer with two hidden units, and one output unit. *(Bottom)*To perform forward propagation with dropout, we randomly sample a vector $\boldsymbol{\mu}$ with one entry for each input or hidden unit in the network. The entries of $\boldsymbol{\mu}$ are binary and are sampled independently from each other. The probability of each entry being 1 is a hyperparameter, usually 0.5 for the hidden layers and 0.8 for the input. Each unit in the network is multiplied by the corresponding mask, and then forward propagation continues through the rest of the network as usual. This is equivalent to randomly selecting one of the sub-networks from figure 7.6 and running forward propagation through it.

To make a prediction, a bagged ensemble must accumulate votes from all of its members. We refer to this process as **inference** in this context. So far, our description of bagging and dropout has not required that the model be explicitly probabilistic. Now, we assume that the model's role is to output a probability distribution. In the case of bagging, each model i produces a probability distribution $p^{(i)}(y \mid \boldsymbol{x})$. The prediction of the ensemble is given by the arithmetic mean of all of these distributions,

$$\frac{1}{k}\sum_{i=1}^{k} p^{(i)}(y \mid \boldsymbol{x}). \tag{7.52}$$

In the case of dropout, each sub-model defined by mask vector $\boldsymbol{\mu}$ defines a probability distribution $p(y \mid \boldsymbol{x}, \boldsymbol{\mu})$. The arithmetic mean over all masks is given by

$$\sum_{\boldsymbol{\mu}} p(\boldsymbol{\mu}) p(y \mid \boldsymbol{x}, \boldsymbol{\mu}) \tag{7.53}$$

where $p(\boldsymbol{\mu})$ is the probability distribution that was used to sample $\boldsymbol{\mu}$ at training time.

Because this sum includes an exponential number of terms, it is intractable to evaluate except in cases where the structure of the model permits some form of simplification. So far, deep neural nets are not known to permit any tractable simplification. Instead, we can approximate the inference with sampling, by averaging together the output from many masks. Even 10-20 masks are often sufficient to obtain good performance.

However, there is an even better approach, that allows us to obtain a good approximation to the predictions of the entire ensemble, at the cost of only one forward propagation. To do so, we change to using the geometric mean rather than the arithmetic mean of the ensemble members' predicted distributions. Warde-Farley *et al.* (2014) present arguments and empirical evidence that the geometric mean performs comparably to the arithmetic mean in this context.

The geometric mean of multiple probability distributions is not guaranteed to be a probability distribution. To guarantee that the result is a probability distribution, we impose the requirement that none of the sub-models assigns probability 0 to any event, and we renormalize the resulting distribution. The unnormalized probability distribution defined directly by the geometric mean is given by

$$\tilde{p}_{\text{ensemble}}(y \mid \boldsymbol{x}) = \sqrt[2^d]{\prod_{\boldsymbol{\mu}} p(y \mid \boldsymbol{x}, \boldsymbol{\mu})} \tag{7.54}$$

where d is the number of units that may be dropped. Here we use a uniform distribution over $\boldsymbol{\mu}$ to simplify the presentation, but non-uniform distributions are also possible. To make predictions we must re-normalize the ensemble:

$$p_{\text{ensemble}}(y \mid \boldsymbol{x}) = \frac{\tilde{p}_{\text{ensemble}}(y \mid \boldsymbol{x})}{\sum_{y'} \tilde{p}_{\text{ensemble}}(y' \mid \boldsymbol{x})}. \tag{7.55}$$

A key insight (Hinton *et al.*, 2012c) involved in dropout is that we can approximate p_{ensemble} by evaluating $p(y \mid \boldsymbol{x})$ in one model: the model with all units, but with the weights going out of unit i multiplied by the probability of including unit i. The motivation for this modification is to capture the right expected value of the output from that unit. We call this approach the **weight scaling inference rule**. There is not yet any theoretical argument for the accuracy of this approximate inference rule in deep nonlinear networks, but empirically it performs very well.

Because we usually use an inclusion probability of $\frac{1}{2}$, the weight scaling rule usually amounts to dividing the weights by 2 at the end of training, and then using the model as usual. Another way to achieve the same result is to multiply the states of the units by 2 during training. Either way, the goal is to make sure that the expected total input to a unit at test time is roughly the same as the expected total input to that unit at train time, even though half the units at train time are missing on average.

For many classes of models that do not have nonlinear hidden units, the weight scaling inference rule is exact. For a simple example, consider a softmax regression classifier with n input variables represented by the vector $\mathbf{v}$:

$$P(\mathrm{y} = y \mid \mathbf{v}) = \text{softmax}\left(\boldsymbol{W}^\top \mathbf{v} + \boldsymbol{b}\right)_y. \tag{7.56}$$

We can index into the family of sub-models by element-wise multiplication of the input with a binary vector d:

$$P(\mathrm{y} = y \mid \mathbf{v}; \boldsymbol{d}) = \text{softmax}\left(\boldsymbol{W}^\top (\boldsymbol{d} \odot \mathbf{v}) + \boldsymbol{b}\right)_y. \tag{7.57}$$

The ensemble predictor is defined by re-normalizing the geometric mean over all ensemble members' predictions:

$$P_{\text{ensemble}}(\mathrm{y} = y \mid \mathbf{v}) = \frac{\tilde{P}_{\text{ensemble}}(\mathrm{y} = y \mid \mathbf{v})}{\sum_{y'} \tilde{P}_{\text{ensemble}}(\mathrm{y} = y' \mid \mathbf{v})} \tag{7.58}$$

where

$$\tilde{P}_{\text{ensemble}}(\mathrm{y} = y \mid \mathbf{v}) = \sqrt[2^n]{\prod_{\boldsymbol{d} \in \{0,1\}^n} P(\mathrm{y} = y \mid \mathbf{v}; \boldsymbol{d})}. \tag{7.59}$$

To see that the weight scaling rule is exact, we can simplify $\tilde{P}_{\text{ensemble}}$:

$$\tilde{P}_{\text{ensemble}}(\mathrm{y} = y \mid \mathbf{v}) = \sqrt[2^n]{\prod_{\boldsymbol{d} \in \{0,1\}^n} P(\mathrm{y} = y \mid \mathbf{v}; \boldsymbol{d})} \tag{7.60}$$

$$= \sqrt[2^n]{\prod_{\boldsymbol{d} \in \{0,1\}^n} \operatorname{softmax}\left(\boldsymbol{W}^\top (\boldsymbol{d} \odot \mathbf{v}) + \boldsymbol{b}\right)_y} \tag{7.61}$$

$$= \sqrt[2^n]{\prod_{\boldsymbol{d} \in \{0,1\}^n} \frac{\exp\left(\boldsymbol{W}_{y,:}^\top (\boldsymbol{d} \odot \mathbf{v}) + b_y\right)}{\sum_{y'} \exp\left(\boldsymbol{W}_{y',:}^\top (\boldsymbol{d} \odot \mathbf{v}) + b_{y'}\right)}} \tag{7.62}$$

$$= \frac{\sqrt[2^n]{\prod_{\boldsymbol{d} \in \{0,1\}^n} \exp\left(\boldsymbol{W}_{y,:}^\top (\boldsymbol{d} \odot \mathbf{v}) + b_y\right)}}{\sqrt[2^n]{\prod_{\boldsymbol{d} \in \{0,1\}^n} \sum_{y'} \exp\left(\boldsymbol{W}_{y',:}^\top (\boldsymbol{d} \odot \mathbf{v}) + b_{y'}\right)}} \tag{7.63}$$

Because $\tilde{P}$ will be normalized, we can safely ignore multiplication by factors that are constant with respect to y:

$$\tilde{P}_{\text{ensemble}}(\mathrm{y} = y \mid \mathbf{v}) \propto \sqrt[2^n]{\prod_{\boldsymbol{d} \in \{0,1\}^n} \exp\left(\boldsymbol{W}_{y,:}^\top (\boldsymbol{d} \odot \mathbf{v}) + b_y\right)} \tag{7.64}$$

$$= \exp\left(\frac{1}{2^n} \sum_{\boldsymbol{d} \in \{0,1\}^n} \boldsymbol{W}_{y,:}^\top (\boldsymbol{d} \odot \mathbf{v}) + b_y\right) \tag{7.65}$$

$$= \exp\left(\frac{1}{2} \boldsymbol{W}_{y,:}^\top \mathbf{v} + b_y\right). \tag{7.66}$$

Substituting this back into equation 7.58 we obtain a softmax classifier with weights $\frac{1}{2}\boldsymbol{W}$.

The weight scaling rule is also exact in other settings, including regression networks with conditionally normal outputs, and deep networks that have hidden layers without nonlinearities. However, the weight scaling rule is only an approximation for deep models that have nonlinearities. Though the approximation has not been theoretically characterized, it often works well, empirically. Goodfellow *et al.* (2013a) found experimentally that the weight scaling approximation can work better (in terms of classification accuracy) than Monte Carlo approximations to the ensemble predictor. This held true even when the Monte Carlo approximation was allowed to sample up to 1,000 sub-networks. Gal and Ghahramani (2015) found that some models obtain better classification accuracy using twenty samples and the Monte Carlo approximation. It appears that the optimal choice of inference approximation is problem-dependent.

Srivastava *et al.* (2014) showed that dropout is more effective than other standard computationally inexpensive regularizers, such as weight decay, filter norm constraints and sparse activity regularization. Dropout may also be combined with other forms of regularization to yield a further improvement.

One advantage of dropout is that it is very computationally cheap. Using dropout during training requires only $O(n)$ computation per example per update, to generate n random binary numbers and multiply them by the state. Depending on the implementation, it may also require $O(n)$ memory to store these binary numbers until the back-propagation stage. Running inference in the trained model has the same cost per-example as if dropout were not used, though we must pay the cost of dividing the weights by 2 once before beginning to run inference on examples.

Another significant advantage of dropout is that it does not significantly limit the type of model or training procedure that can be used. It works well with nearly any model that uses a distributed representation and can be trained with stochastic gradient descent. This includes feedforward neural networks, probabilistic models such as restricted Boltzmann machines (Srivastava *et al.*, 2014), and recurrent neural networks (Bayer and Osendorfer, 2014; Pascanu *et al.*, 2014a). Many other regularization strategies of comparable power impose more severe restrictions on the architecture of the model.

Though the cost per-step of applying dropout to a specific model is negligible, the cost of using dropout in a complete system can be significant. Because dropout is a regularization technique, it reduces the effective capacity of a model. To offset this effect, we must increase the size of the model. Typically the optimal validation set error is much lower when using dropout, but this comes at the cost of a much larger model and many more iterations of the training algorithm. For very large datasets, regularization confers little reduction in generalization error. In these cases, the computational cost of using dropout and larger models may outweigh the benefit of regularization.

When extremely few labeled training examples are available, dropout is less effective. Bayesian neural networks (Neal, 1996) outperform dropout on the Alternative Splicing Dataset (Xiong *et al.*, 2011) where fewer than 5,000 examples are available (Srivastava *et al.*, 2014). When additional unlabeled data is available, unsupervised feature learning can gain an advantage over dropout.

Wager *et al.* (2013) showed that, when applied to linear regression, dropout is equivalent to L^2 weight decay, with a different weight decay coefficient for each input feature. The magnitude of each feature's weight decay coefficient is determined by its variance. Similar results hold for other linear models. For deep models, dropout is not equivalent to weight decay.

The stochasticity used while training with dropout is not necessary for the approach's success. It is just a means of approximating the sum over all sub-models. Wang and Manning (2013) derived analytical approximations to this marginalization. Their approximation, known as **fast dropout** resulted in faster convergence time due to the reduced stochasticity in the computation of the gradient. This method can also be applied at test time, as a more principled (but also more computationally expensive) approximation to the average over all sub-networks than the weight scaling approximation. Fast dropout has been used to nearly match the performance of standard dropout on small neural network problems, but has not yet yielded a significant improvement or been applied to a large problem.

Just as stochasticity is not necessary to achieve the regularizing effect of dropout, it is also not sufficient. To demonstrate this, Warde-Farley *et al.* (2014) designed control experiments using a method called **dropout boosting** that they designed to use exactly the same mask noise as traditional dropout but lack its regularizing effect. Dropout boosting trains the entire ensemble to jointly maximize the log-likelihood on the training set. In the same sense that traditional dropout is analogous to bagging, this approach is analogous to boosting. As intended, experiments with dropout boosting show almost no regularization effect compared to training the entire network as a single model. This demonstrates that the interpretation of dropout as bagging has value beyond the interpretation of dropout as robustness to noise. The regularization effect of the bagged ensemble is only achieved when the stochastically sampled ensemble members are trained to perform well independently of each other.

Dropout has inspired other stochastic approaches to training exponentially large ensembles of models that share weights. DropConnect is a special case of dropout where each product between a single scalar weight and a single hidden unit state is considered a unit that can be dropped (Wan *et al.*, 2013). Stochastic pooling is a form of randomized pooling (see section 9.3) for building ensembles of convolutional networks with each convolutional network attending to different spatial locations of each feature map. So far, dropout remains the most widely used implicit ensemble method.

One of the key insights of dropout is that training a network with stochastic behavior and making predictions by averaging over multiple stochastic decisions implements a form of bagging with parameter sharing. Earlier, we described dropout as bagging an ensemble of models formed by including or excluding units. However, there is no need for this model averaging strategy to be based on inclusion and exclusion. In principle, any kind of random modification is admissible. In practice, we must choose modification families that neural networks are able to learn to resist. Ideally, we should also use model families that allow a fast approximate inference rule. We can think of any form of modification parametrized by a vector $\boldsymbol{\mu}$ as training an ensemble consisting of $p(y \mid \boldsymbol{x}, \boldsymbol{\mu})$ for all possible values of $\boldsymbol{\mu}$. There is no requirement that $\boldsymbol{\mu}$ have a finite number of values. For example, $\boldsymbol{\mu}$ can be real-valued. Srivastava *et al.* (2014) showed that multiplying the weights by $\boldsymbol{\mu} \sim \mathcal{N}(\mathbf{1}, I)$ can outperform dropout based on binary masks. Because $\mathbb{E}[\boldsymbol{\mu}] = \mathbf{1}$ the standard network automatically implements approximate inference in the ensemble, without needing any weight scaling.

So far we have described dropout purely as a means of performing efficient, approximate bagging. However, there is another view of dropout that goes further than this. Dropout trains not just a bagged ensemble of models, but an ensemble of models that share hidden units. This means each hidden unit must be able to perform well regardless of which other hidden units are in the model. Hidden units must be prepared to be swapped and interchanged between models. Hinton *et al.* (2012c) were inspired by an idea from biology: sexual reproduction, which involves swapping genes between two different organisms, creates evolutionary pressure for genes to become not just good, but to become readily swapped between different organisms. Such genes and such features are very robust to changes in their environment because they are not able to incorrectly adapt to unusual features of any one organism or model. Dropout thus regularizes each hidden unit to be not merely a good feature but a feature that is good in many contexts. Warde-Farley *et al.* (2014) compared dropout training to training of large ensembles and concluded that dropout offers additional improvements to generalization error beyond those obtained by ensembles of independent models.

It is important to understand that a large portion of the power of dropout arises from the fact that the masking noise is applied to the hidden units. This can be seen as a form of highly intelligent, adaptive destruction of the information content of the input rather than destruction of the raw values of the input. For example, if the model learns a hidden unit h_i that detects a face by finding the nose, then dropping h_i corresponds to erasing the information that there is a nose in the image. The model must learn another h_i, either that redundantly encodes the presence of a nose, or that detects the face by another feature, such as the mouth. Traditional noise injection techniques that add unstructured noise at the input are not able to randomly erase the information about a nose from an image of a face unless the magnitude of the noise is so great that nearly all of the information in the image is removed. Destroying extracted features rather than original values allows the destruction process to make use of all of the knowledge about the input distribution that the model has acquired so far.

Another important aspect of dropout is that the noise is multiplicative. If the noise were additive with fixed scale, then a rectified linear hidden unit h_i with added noise ϵ could simply learn to have h_i become very large in order to make the added noise ϵ insignificant by comparison. Multiplicative noise does not allow such a pathological solution to the noise robustness problem.

Another deep learning algorithm, batch normalization, reparametrizes the model in a way that introduces both additive and multiplicative noise on the hidden units at training time. The primary purpose of batch normalization is to improve optimization, but the noise can have a regularizing effect, and sometimes makes dropout unnecessary. Batch normalization is described further in section 8.7.1.

7.13 Adversarial Training

In many cases, neural networks have begun to reach human performance when evaluated on an i.i.d. test set. It is natural therefore to wonder whether these models have obtained a true human-level understanding of these tasks. In order to probe the level of understanding a network has of the underlying task, we can search for examples that the model misclassifies. Szegedy *et al.* (2014b) found that even neural networks that perform at human level accuracy have a nearly 100% error rate on examples that are intentionally constructed by using an optimization procedure to search for an input $\boldsymbol{x}'$ near a data point $\boldsymbol{x}$ such that the model output is very different at $\boldsymbol{x}'$. In many cases, $\boldsymbol{x}'$ can be so similar to $\boldsymbol{x}$ that a human observer cannot tell the difference between the original example and the **adversarial example**, but the network can make highly different predictions. See figure 7.8 for an example.

Adversarial examples have many implications, for example, in computer security, that are beyond the scope of this chapter. However, they are interesting in the context of regularization because one can reduce the error rate on the original i.i.d. test set via **adversarial training**—training on adversarially perturbed examples from the training set (Szegedy *et al.*, 2014b; Goodfellow *et al.*, 2014b).

Goodfellow *et al.* (2014b) showed that one of the primary causes of these adversarial examples is excessive linearity. Neural networks are built out of primarily linear building blocks. In some experiments the overall function they implement proves to be highly linear as a result. These linear functions are easy

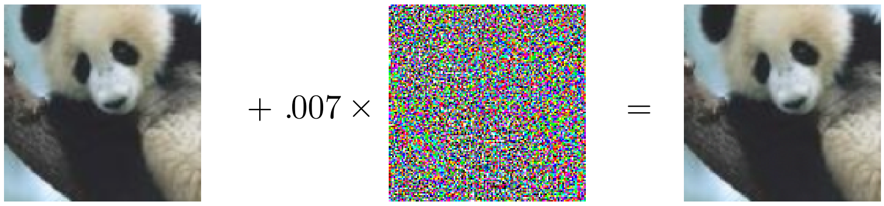

$\boldsymbol{x}$	$\text{sign}(\nabla_{\boldsymbol{x}} J(\boldsymbol{\theta}, \boldsymbol{x}, y))$	$\boldsymbol{x} + \epsilon\,\text{sign}(\nabla_{\boldsymbol{x}} J(\boldsymbol{\theta}, \boldsymbol{x}, y))$
$y =$"panda" w/ 57.7% confidence	"nematode" w/ 8.2% confidence	"gibbon" w/ 99.3 % confidence

Figure 7.8: A demonstration of adversarial example generation applied to GoogLeNet (Szegedy *et al.*, 2014a) on ImageNet. By adding an imperceptibly small vector whose elements are equal to the sign of the elements of the gradient of the cost function with respect to the input, we can change GoogLeNet's classification of the image. Reproduced with permission from Goodfellow *et al.* (2014b).

to optimize. Unfortunately, the value of a linear function can change very rapidly if it has numerous inputs. If we change each input by ϵ, then a linear function with weights $\boldsymbol{w}$ can change by as much as $\epsilon||\boldsymbol{w}||_1$, which can be a very large amount if $\boldsymbol{w}$ is high-dimensional. Adversarial training discourages this highly sensitive locally linear behavior by encouraging the network to be locally constant in the neighborhood of the training data. This can be seen as a way of explicitly introducing a local constancy prior into supervised neural nets.

Adversarial training helps to illustrate the power of using a large function family in combination with aggressive regularization. Purely linear models, like logistic regression, are not able to resist adversarial examples because they are forced to be linear. Neural networks are able to represent functions that can range from nearly linear to nearly locally constant and thus have the flexibility to capture linear trends in the training data while still learning to resist local perturbation.

Adversarial examples also provide a means of accomplishing semi-supervised learning. At a point $\boldsymbol{x}$ that is not associated with a label in the dataset, the model itself assigns some label $\hat{y}$. The model's label $\hat{y}$ may not be the true label, but if the model is high quality, then $\hat{y}$ has a high probability of providing the true label. We can seek an adversarial example $\boldsymbol{x}'$ that causes the classifier to output a label y' with $y' \neq \hat{y}$. Adversarial examples generated using not the true label but a label provided by a trained model are called **virtual adversarial examples** (Miyato *et al.*, 2015). The classifier may then be trained to assign the same label to $\boldsymbol{x}$ and $\boldsymbol{x}'$. This encourages the classifier to learn a function that is robust to small changes anywhere along the manifold where the unlabeled data lies. The assumption motivating this approach is that different classes usually lie on disconnected manifolds, and a small perturbation should not be able to jump from one class manifold to another class manifold.

7.14 Tangent Distance, Tangent Prop, and Manifold Tangent Classifier

Many machine learning algorithms aim to overcome the curse of dimensionality by assuming that the data lies near a low-dimensional manifold, as described in section 5.11.3.

One of the early attempts to take advantage of the manifold hypothesis is the **tangent distance** algorithm (Simard *et al.*, 1993, 1998). It is a non-parametric nearest-neighbor algorithm in which the metric used is not the generic Euclidean distance but one that is derived from knowledge of the manifolds near which probability concentrates. It is assumed that we are trying to classify examples and that examples on the same manifold share the same category. Since the classifier should be invariant to the local factors of variation that correspond to movement on the manifold, it would make sense to use as nearest-neighbor distance between points $\boldsymbol{x}_1$ and $\boldsymbol{x}_2$ the distance between the manifolds M_1 and M_2 to which they respectively belong. Although that may be computationally difficult (it would require solving an optimization problem, to find the nearest pair of points on M_1 and M_2), a cheap alternative that makes sense locally is to approximate M_i by its tangent plane at $\boldsymbol{x}_i$ and measure the distance between the two tangents, or between a tangent plane and a point. That can be achieved by solving a low-dimensional linear system (in the dimension of the manifolds). Of course, this algorithm requires one to specify the tangent vectors.

In a related spirit, the **tangent prop** algorithm (Simard *et al.*, 1992) (figure 7.9) trains a neural net classifier with an extra penalty to make each output $f(\boldsymbol{x})$ of the neural net locally invariant to known factors of variation. These factors of variation correspond to movement along the manifold near which examples of the same class concentrate. Local invariance is achieved by requiring $\nabla_{\boldsymbol{x}} f(\boldsymbol{x})$ to be orthogonal to the known manifold tangent vectors $\boldsymbol{v}^{(i)}$ at $\boldsymbol{x}$, or equivalently that the directional derivative of f at $\boldsymbol{x}$ in the directions $\boldsymbol{v}^{(i)}$ be small by adding a regularization penalty Ω:

$$\Omega(f) = \sum_i \left((\nabla_{\boldsymbol{x}} f(\boldsymbol{x}))^\top \boldsymbol{v}^{(i)} \right)^2. \tag{7.67}$$

This regularizer can of course be scaled by an appropriate hyperparameter, and, for most neural networks, we would need to sum over many outputs rather than the lone output $f(\boldsymbol{x})$ described here for simplicity. As with the tangent distance algorithm, the tangent vectors are derived a priori, usually from the formal knowledge of the effect of transformations such as translation, rotation, and scaling in images. Tangent prop has been used not just for supervised learning (Simard *et al.*, 1992) but also in the context of reinforcement learning (Thrun, 1995).

Tangent propagation is closely related to dataset augmentation. In both cases, the user of the algorithm encodes his or her prior knowledge of the task by specifying a set of transformations that should not alter the output of the network. The difference is that in the case of dataset augmentation, the network is explicitly trained to correctly classify distinct inputs that were created by applying more than an infinitesimal amount of these transformations. Tangent propagation does not require explicitly visiting a new input point. Instead, it analytically regularizes the model to resist perturbation in the directions corresponding to the specified transformation. While this analytical approach is intellectually elegant, it has two major drawbacks. First, it only regularizes the model to resist infinitesimal perturbation. Explicit dataset augmentation confers resistance to larger perturbations. Second, the infinitesimal approach poses difficulties for models based on rectified linear units. These models can only shrink their derivatives by turning units off or shrinking their weights. They are not able to shrink their derivatives by saturating at a high value with large weights, as sigmoid or tanh units can. Dataset augmentation works well with rectified linear units because different subsets of rectified units can activate for different transformed versions of each original input.

Tangent propagation is also related to **double backprop** (Drucker and LeCun, 1992) and adversarial training (Szegedy *et al.*, 2014b; Goodfellow *et al.*, 2014b). Double backprop regularizes the Jacobian to be small, while adversarial training finds inputs near the original inputs and trains the model to produce the same output on these as on the original inputs. Tangent propagation and dataset augmentation using manually specified transformations both require that the model should be invariant to certain specified directions of change in the input. Double backprop and adversarial training both require that the model should be invariant to *all* directions of change in the input so long as the change is small. Just as dataset augmentation is the non-infinitesimal version of tangent propagation, adversarial training is the non-infinitesimal version of double backprop.

The manifold tangent classifier (Rifai *et al.*, 2011c), eliminates the need to know the tangent vectors a priori. As we will see in chapter 14, autoencoders can

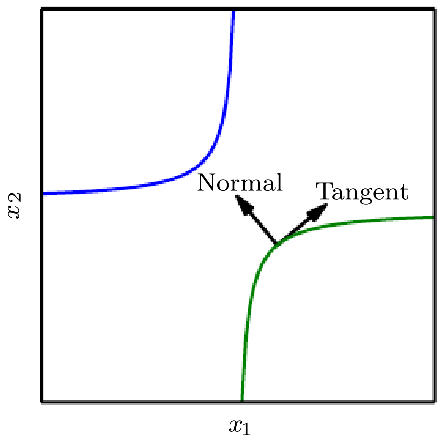

Figure 7.9: Illustration of the main idea of the tangent prop algorithm (Simard *et al.*, 1992) and manifold tangent classifier (Rifai *et al.*, 2011c), which both regularize the classifier output function $f(\boldsymbol{x})$. Each curve represents the manifold for a different class, illustrated here as a one-dimensional manifold embedded in a two-dimensional space. On one curve, we have chosen a single point and drawn a vector that is tangent to the class manifold (parallel to and touching the manifold) and a vector that is normal to the class manifold (orthogonal to the manifold). In multiple dimensions there may be many tangent directions and many normal directions. We expect the classification function to change rapidly as it moves in the direction normal to the manifold, and not to change as it moves along the class manifold. Both tangent propagation and the manifold tangent classifier regularize $f(\boldsymbol{x})$ to not change very much as $\boldsymbol{x}$ moves along the manifold. Tangent propagation requires the user to manually specify functions that compute the tangent directions (such as specifying that small translations of images remain in the same class manifold) while the manifold tangent classifier estimates the manifold tangent directions by training an autoencoder to fit the training data. The use of autoencoders to estimate manifolds will be described in chapter 14.

estimate the manifold tangent vectors. The manifold tangent classifier makes use of this technique to avoid needing user-specified tangent vectors. As illustrated in figure 14.10, these estimated tangent vectors go beyond the classical invariants that arise out of the geometry of images (such as translation, rotation and scaling) and include factors that must be learned because they are object-specific (such as moving body parts). The algorithm proposed with the manifold tangent classifier is therefore simple: (1) use an autoencoder to learn the manifold structure by unsupervised learning, and (2) use these tangents to regularize a neural net classifier as in tangent prop (equation 7.67).

This chapter has described most of the general strategies used to regularize neural networks. Regularization is a central theme of machine learning and as such will be revisited periodically by most of the remaining chapters. Another central theme of machine learning is optimization, described next.

Chapter 8

Optimization for Training Deep Models

Deep learning algorithms involve optimization in many contexts. For example, performing inference in models such as PCA involves solving an optimization problem. We often use analytical optimization to write proofs or design algorithms. Of all of the many optimization problems involved in deep learning, the most difficult is neural network training. It is quite common to invest days to months of time on hundreds of machines in order to solve even a single instance of the neural network training problem. Because this problem is so important and so expensive, a specialized set of optimization techniques have been developed for solving it. This chapter presents these optimization techniques for neural network training.

If you are unfamiliar with the basic principles of gradient-based optimization, we suggest reviewing chapter 4. That chapter includes a brief overview of numerical optimization in general.

This chapter focuses on one particular case of optimization: finding the parameters $\boldsymbol{\theta}$ of a neural network that significantly reduce a cost function $J(\boldsymbol{\theta})$, which typically includes a performance measure evaluated on the entire training set as well as additional regularization terms.

We begin with a description of how optimization used as a training algorithm for a machine learning task differs from pure optimization. Next, we present several of the concrete challenges that make optimization of neural networks difficult. We then define several practical algorithms, including both optimization algorithms themselves and strategies for initializing the parameters. More advanced algorithms adapt their learning rates during training or leverage information contained in the second derivatives of the cost function. Finally, we conclude with a review of several optimization strategies that are formed by combining simple optimization algorithms into higher-level procedures.

8.1 How Learning Differs from Pure Optimization

Optimization algorithms used for training of deep models differ from traditional optimization algorithms in several ways. Machine learning usually acts indirectly. In most machine learning scenarios, we care about some performance measure P, that is defined with respect to the test set and may also be intractable. We therefore optimize P only indirectly. We reduce a different cost function $J(\boldsymbol{\theta})$ in the hope that doing so will improve P. This is in contrast to pure optimization, where minimizing J is a goal in and of itself. Optimization algorithms for training deep models also typically include some specialization on the specific structure of machine learning objective functions.

Typically, the cost function can be written as an average over the training set, such as

$$J(\boldsymbol{\theta}) = \mathbb{E}_{(\boldsymbol{x},\mathrm{y})\sim \hat{p}_{\text{data}}} L(f(\boldsymbol{x};\boldsymbol{\theta}), y), \tag{8.1}$$

where L is the per-example loss function, $f(\boldsymbol{x};\boldsymbol{\theta})$ is the predicted output when the input is $\boldsymbol{x}$, $\hat{p}_{\text{data}}$ is the empirical distribution. In the supervised learning case, y is the target output. Throughout this chapter, we develop the unregularized supervised case, where the arguments to L are $f(\boldsymbol{x};\boldsymbol{\theta})$ and y. However, it is trivial to extend this development, for example, to include $\boldsymbol{\theta}$ or $\boldsymbol{x}$ as arguments, or to exclude y as arguments, in order to develop various forms of regularization or unsupervised learning.

Equation 8.1 defines an objective function with respect to the training set. We would usually prefer to minimize the corresponding objective function where the expectation is taken across *the data generating distribution* p_{data} rather than just over the finite training set:

$$J^*(\boldsymbol{\theta}) = \mathbb{E}_{(\boldsymbol{x},\mathrm{y})\sim p_{\text{data}}} L(f(\boldsymbol{x};\boldsymbol{\theta}), y). \tag{8.2}$$

8.1.1 Empirical Risk Minimization

The goal of a machine learning algorithm is to reduce the expected generalization error given by equation 8.2. This quantity is known as the **risk**. We emphasize here that the expectation is taken over the true underlying distribution p_{data}. If we knew the true distribution $p_{\text{data}}(\boldsymbol{x}, y)$, risk minimization would be an optimization task solvable by an optimization algorithm. However, when we do not know $p_{\text{data}}(\boldsymbol{x}, y)$ but only have a training set of samples, we have a machine learning problem.

The simplest way to convert a machine learning problem back into an optimization problem is to minimize the expected loss on the training set. This means replacing the true distribution $p(\boldsymbol{x}, y)$ with the empirical distribution $\hat{p}(\boldsymbol{x}, y)$ defined by the training set. We now minimize the **empirical risk**

$$\mathbb{E}_{\boldsymbol{x},\mathrm{y}\sim\hat{p}_{\text{data}}(\boldsymbol{x},y)}[L(f(\boldsymbol{x};\boldsymbol{\theta}), y)] = \frac{1}{m}\sum_{i=1}^{m} L(f(\boldsymbol{x}^{(i)};\boldsymbol{\theta}), y^{(i)}) \tag{8.3}$$

where m is the number of training examples.

The training process based on minimizing this average training error is known as **empirical risk minimization**. In this setting, machine learning is still very similar to straightforward optimization. Rather than optimizing the risk directly, we optimize the empirical risk, and hope that the risk decreases significantly as well. A variety of theoretical results establish conditions under which the true risk can be expected to decrease by various amounts.

However, empirical risk minimization is prone to overfitting. Models with high capacity can simply memorize the training set. In many cases, empirical risk minimization is not really feasible. The most effective modern optimization algorithms are based on gradient descent, but many useful loss functions, such as 0-1 loss, have no useful derivatives (the derivative is either zero or undefined everywhere). These two problems mean that, in the context of deep learning, we rarely use empirical risk minimization. Instead, we must use a slightly different approach, in which the quantity that we actually optimize is even more different from the quantity that we truly want to optimize.

8.1.2 Surrogate Loss Functions and Early Stopping

Sometimes, the loss function we actually care about (say classification error) is not one that can be optimized efficiently. For example, exactly minimizing expected 0-1 loss is typically intractable (exponential in the input dimension), even for a linear classifier (Marcotte and Savard, 1992). In such situations, one typically optimizes a **surrogate loss function** instead, which acts as a proxy but has advantages. For example, the negative log-likelihood of the correct class is typically used as a surrogate for the 0-1 loss. The negative log-likelihood allows the model to estimate the conditional probability of the classes, given the input, and if the model can do that well, then it can pick the classes that yield the least classification error in expectation.

In some cases, a surrogate loss function actually results in being able to learn more. For example, the test set 0-1 loss often continues to decrease for a long time after the training set 0-1 loss has reached zero, when training using the log-likelihood surrogate. This is because even when the expected 0-1 loss is zero, one can improve the robustness of the classifier by further pushing the classes apart from each other, obtaining a more confident and reliable classifier, thus extracting more information from the training data than would have been possible by simply minimizing the average 0-1 loss on the training set.

A very important difference between optimization in general and optimization as we use it for training algorithms is that training algorithms do not usually halt at a local minimum. Instead, a machine learning algorithm usually minimizes a surrogate loss function but halts when a convergence criterion based on early stopping (section 7.8) is satisfied. Typically the early stopping criterion is based on the true underlying loss function, such as 0-1 loss measured on a validation set, and is designed to cause the algorithm to halt whenever overfitting begins to occur. Training often halts while the surrogate loss function still has large derivatives, which is very different from the pure optimization setting, where an optimization algorithm is considered to have converged when the gradient becomes very small.

8.1.3 Batch and Minibatch Algorithms

One aspect of machine learning algorithms that separates them from general optimization algorithms is that the objective function usually decomposes as a sum over the training examples. Optimization algorithms for machine learning typically compute each update to the parameters based on an expected value of the cost function estimated using only a subset of the terms of the full cost function.

For example, maximum likelihood estimation problems, when viewed in log space, decompose into a sum over each example:

$$\boldsymbol{\theta}_{\text{ML}} = \arg\max_{\boldsymbol{\theta}} \sum_{i=1}^{m} \log p_{\text{model}}(\boldsymbol{x}^{(i)}, y^{(i)}; \boldsymbol{\theta}). \tag{8.4}$$

Maximizing this sum is equivalent to maximizing the expectation over the empirical distribution defined by the training set:

$$J(\boldsymbol{\theta}) = \mathbb{E}_{\mathbf{x},\mathrm{y}\sim\hat{p}_{\text{data}}} \log p_{\text{model}}(\boldsymbol{x}, y; \boldsymbol{\theta}). \tag{8.5}$$

Most of the properties of the objective function J used by most of our optimization algorithms are also expectations over the training set. For example, the most commonly used property is the gradient:

$$\nabla_{\boldsymbol{\theta}} J(\boldsymbol{\theta}) = \mathbb{E}_{\mathbf{x},\mathrm{y}\sim\hat{p}_{\mathrm{data}}} \nabla_{\boldsymbol{\theta}} \log p_{\mathrm{model}}(\boldsymbol{x}, y; \boldsymbol{\theta}). \tag{8.6}$$

Computing this expectation exactly is very expensive because it requires evaluating the model on every example in the entire dataset. In practice, we can compute these expectations by randomly sampling a small number of examples from the dataset, then taking the average over only those examples.

Recall that the standard error of the mean (equation 5.46) estimated from n samples is given by $\sigma/\sqrt{n}$, where σ is the true standard deviation of the value of the samples. The denominator of $\sqrt{n}$ shows that there are less than linear returns to using more examples to estimate the gradient. Compare two hypothetical estimates of the gradient, one based on 100 examples and another based on 10,000 examples. The latter requires 100 times more computation than the former, but reduces the standard error of the mean only by a factor of 10. Most optimization algorithms converge much faster (in terms of total computation, not in terms of number of updates) if they are allowed to rapidly compute approximate estimates of the gradient rather than slowly computing the exact gradient.

Another consideration motivating statistical estimation of the gradient from a small number of samples is redundancy in the training set. In the worst case, all m samples in the training set could be identical copies of each other. A sampling-based estimate of the gradient could compute the correct gradient with a single sample, using m times less computation than the naive approach. In practice, we are unlikely to truly encounter this worst-case situation, but we may find large numbers of examples that all make very similar contributions to the gradient.

Optimization algorithms that use the entire training set are called **batch** or **deterministic** gradient methods, because they process all of the training examples simultaneously in a large batch. This terminology can be somewhat confusing because the word "batch" is also often used to describe the minibatch used by minibatch stochastic gradient descent. Typically the term "batch gradient descent" implies the use of the full training set, while the use of the term "batch" to describe a group of examples does not. For example, it is very common to use the term "batch size" to describe the size of a minibatch.

Optimization algorithms that use only a single example at a time are sometimes called **stochastic** or sometimes **online** methods. The term online is usually reserved for the case where the examples are drawn from a stream of continually created examples rather than from a fixed-size training set over which several passes are made.

Most algorithms used for deep learning fall somewhere in between, using more than one but less than all of the training examples. These were traditionally called **minibatch** or **minibatch stochastic** methods and it is now common to simply call them **stochastic** methods.

The canonical example of a stochastic method is stochastic gradient descent, presented in detail in section 8.3.1.

Minibatch sizes are generally driven by the following factors:

- Larger batches provide a more accurate estimate of the gradient, but with less than linear returns.

- Multicore architectures are usually underutilized by extremely small batches. This motivates using some absolute minimum batch size, below which there is no reduction in the time to process a minibatch.

- If all examples in the batch are to be processed in parallel (as is typically the case), then the amount of memory scales with the batch size. For many hardware setups this is the limiting factor in batch size.

- Some kinds of hardware achieve better runtime with specific sizes of arrays. Especially when using GPUs, it is common for power of 2 batch sizes to offer better runtime. Typical power of 2 batch sizes range from 32 to 256, with 16 sometimes being attempted for large models.

- Small batches can offer a regularizing effect (Wilson and Martinez, 2003), perhaps due to the noise they add to the learning process. Generalization error is often best for a batch size of 1. Training with such a small batch size might require a small learning rate to maintain stability due to the high variance in the estimate of the gradient. The total runtime can be very high due to the need to make more steps, both because of the reduced learning rate and because it takes more steps to observe the entire training set.

Different kinds of algorithms use different kinds of information from the minibatch in different ways. Some algorithms are more sensitive to sampling error than others, either because they use information that is difficult to estimate accurately with few samples, or because they use information in ways that amplify sampling errors more. Methods that compute updates based only on the gradient $\boldsymbol{g}$ are usually relatively robust and can handle smaller batch sizes like 100. Second-order methods, which use also the Hessian matrix $\boldsymbol{H}$ and compute updates such as $\boldsymbol{H}^{-1}\boldsymbol{g}$, typically require much larger batch sizes like 10,000. These large batch sizes are required to minimize fluctuations in the estimates of $\boldsymbol{H}^{-1}\boldsymbol{g}$. Suppose that $\boldsymbol{H}$ is estimated perfectly but has a poor condition number. Multiplication by

$\boldsymbol{H}$ or its inverse amplifies pre-existing errors, in this case, estimation errors in $\boldsymbol{g}$. Very small changes in the estimate of $\boldsymbol{g}$ can thus cause large changes in the update $\boldsymbol{H}^{-1}\boldsymbol{g}$, even if $\boldsymbol{H}$ were estimated perfectly. Of course, $\boldsymbol{H}$ will be estimated only approximately, so the update $\boldsymbol{H}^{-1}\boldsymbol{g}$ will contain even more error than we would predict from applying a poorly conditioned operation to the estimate of $\boldsymbol{g}$.

It is also crucial that the minibatches be selected randomly. Computing an unbiased estimate of the expected gradient from a set of samples requires that those samples be independent. We also wish for two subsequent gradient estimates to be independent from each other, so two subsequent minibatches of examples should also be independent from each other. Many datasets are most naturally arranged in a way where successive examples are highly correlated. For example, we might have a dataset of medical data with a long list of blood sample test results. This list might be arranged so that first we have five blood samples taken at different times from the first patient, then we have three blood samples taken from the second patient, then the blood samples from the third patient, and so on. If we were to draw examples in order from this list, then each of our minibatches would be extremely biased, because it would represent primarily one patient out of the many patients in the dataset. In cases such as these where the order of the dataset holds some significance, it is necessary to shuffle the examples before selecting minibatches. For very large datasets, for example datasets containing billions of examples in a data center, it can be impractical to sample examples truly uniformly at random every time we want to construct a minibatch. Fortunately, in practice it is usually sufficient to shuffle the order of the dataset once and then store it in shuffled fashion. This will impose a fixed set of possible minibatches of consecutive examples that all models trained thereafter will use, and each individual model will be forced to reuse this ordering every time it passes through the training data. However, this deviation from true random selection does not seem to have a significant detrimental effect. Failing to ever shuffle the examples in any way can seriously reduce the effectiveness of the algorithm.

Many optimization problems in machine learning decompose over examples well enough that we can compute entire separate updates over different examples in parallel. In other words, we can compute the update that minimizes $J(\boldsymbol{X})$ for one minibatch of examples $\boldsymbol{X}$ at the same time that we compute the update for several other minibatches. Such asynchronous parallel distributed approaches are discussed further in section 12.1.3.

An interesting motivation for minibatch stochastic gradient descent is that it follows the gradient of the true *generalization error* (equation 8.2) so long as no examples are repeated. Most implementations of minibatch stochastic gradient descent shuffle the dataset once and then pass through it multiple times. On the first pass, each minibatch is used to compute an unbiased estimate of the true generalization error. On the second pass, the estimate becomes biased because it is formed by re-sampling values that have already been used, rather than obtaining new fair samples from the data generating distribution.

The fact that stochastic gradient descent minimizes generalization error is easiest to see in the online learning case, where examples or minibatches are drawn from a **stream** of data. In other words, instead of receiving a fixed-size training set, the learner is similar to a living being who sees a new example at each instant, with every example $(\boldsymbol{x}, y)$ coming from the data generating distribution $p_{\text{data}}(\boldsymbol{x}, y)$. In this scenario, examples are never repeated; every experience is a fair sample from p_{data}.

The equivalence is easiest to derive when both $\boldsymbol{x}$ and y are discrete. In this case, the generalization error (equation 8.2) can be written as a sum

$$J^*(\boldsymbol{\theta}) = \sum_{\boldsymbol{x}} \sum_{y} p_{\text{data}}(\boldsymbol{x}, y) L(f(\boldsymbol{x}; \boldsymbol{\theta}), y), \tag{8.7}$$

with the exact gradient

$$\boldsymbol{g} = \nabla_{\boldsymbol{\theta}} J^*(\boldsymbol{\theta}) = \sum_{\boldsymbol{x}} \sum_{y} p_{\text{data}}(\boldsymbol{x}, y) \nabla_{\boldsymbol{\theta}} L(f(\boldsymbol{x}; \boldsymbol{\theta}), y). \tag{8.8}$$

We have already seen the same fact demonstrated for the log-likelihood in equation 8.5 and equation 8.6; we observe now that this holds for other functions L besides the likelihood. A similar result can be derived when $\boldsymbol{x}$ and y are continuous, under mild assumptions regarding p_{data} and L.

Hence, we can obtain an unbiased estimator of the exact gradient of the generalization error by sampling a minibatch of examples $\{\boldsymbol{x}^{(1)}, \ldots \boldsymbol{x}^{(m)}\}$ with corresponding targets $y^{(i)}$ from the data generating distribution p_{data}, and computing the gradient of the loss with respect to the parameters for that minibatch:

$$\hat{\boldsymbol{g}} = \frac{1}{m} \nabla_{\boldsymbol{\theta}} \sum_{i} L(f(\boldsymbol{x}^{(i)}; \boldsymbol{\theta}), y^{(i)}). \tag{8.9}$$

Updating $\boldsymbol{\theta}$ in the direction of $\hat{\boldsymbol{g}}$ performs SGD on the generalization error.

Of course, this interpretation only applies when examples are not reused. Nonetheless, it is usually best to make several passes through the training set, unless the training set is extremely large. When multiple such epochs are used, only the first epoch follows the unbiased gradient of the generalization error, but of course, the additional epochs usually provide enough benefit due to decreased training error to offset the harm they cause by increasing the gap between training error and test error.

With some datasets growing rapidly in size, faster than computing power, it is becoming more common for machine learning applications to use each training example only once or even to make an incomplete pass through the training set. When using an extremely large training set, overfitting is not an issue, so underfitting and computational efficiency become the predominant concerns. See also Bottou and Bousquet (2008) for a discussion of the effect of computational bottlenecks on generalization error, as the number of training examples grows.

8.2 Challenges in Neural Network Optimization

Optimization in general is an extremely difficult task. Traditionally, machine learning has avoided the difficulty of general optimization by carefully designing the objective function and constraints to ensure that the optimization problem is convex. When training neural networks, we must confront the general non-convex case. Even convex optimization is not without its complications. In this section, we summarize several of the most prominent challenges involved in optimization for training deep models.

8.2.1 Ill-Conditioning

Some challenges arise even when optimizing convex functions. Of these, the most prominent is ill-conditioning of the Hessian matrix $\boldsymbol{H}$. This is a very general problem in most numerical optimization, convex or otherwise, and is described in more detail in section 4.3.1.

The ill-conditioning problem is generally believed to be present in neural network training problems. Ill-conditioning can manifest by causing SGD to get "stuck" in the sense that even very small steps increase the cost function.

Recall from equation 4.9 that a second-order Taylor series expansion of the cost function predicts that a gradient descent step of $-\epsilon \boldsymbol{g}$ will add

$$\frac{1}{2}\epsilon^2 \boldsymbol{g}^\top \boldsymbol{H} \boldsymbol{g} - \epsilon \boldsymbol{g}^\top \boldsymbol{g} \tag{8.10}$$

to the cost. Ill-conditioning of the gradient becomes a problem when $\frac{1}{2}\epsilon^2 \boldsymbol{g}^\top \boldsymbol{H} \boldsymbol{g}$ exceeds $\epsilon \boldsymbol{g}^\top \boldsymbol{g}$. To determine whether ill-conditioning is detrimental to a neural network training task, one can monitor the squared gradient norm $\boldsymbol{g}^\top \boldsymbol{g}$ and

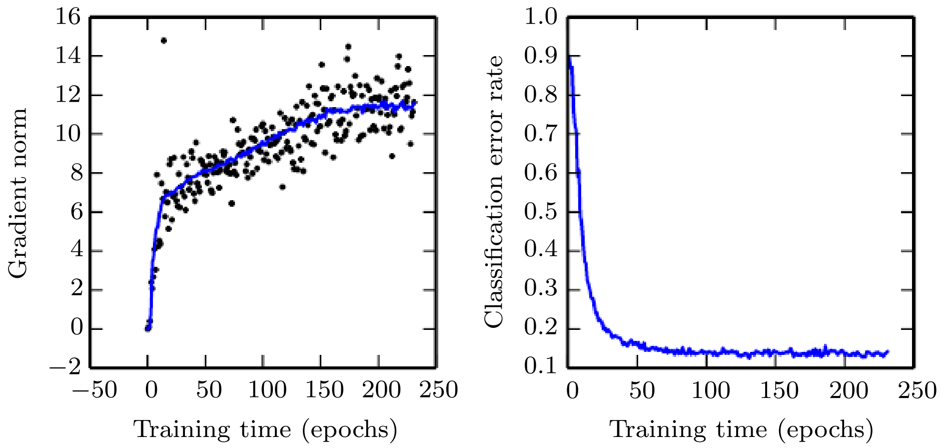

Figure 8.1: Gradient descent often does not arrive at a critical point of any kind. In this example, the gradient norm increases throughout training of a convolutional network used for object detection. *(Left)*A scatterplot showing how the norms of individual gradient evaluations are distributed over time. To improve legibility, only one gradient norm is plotted per epoch. The running average of all gradient norms is plotted as a solid curve. The gradient norm clearly increases over time, rather than decreasing as we would expect if the training process converged to a critical point. *(Right)*Despite the increasing gradient, the training process is reasonably successful. The validation set classification error decreases to a low level.

the $\boldsymbol{g}^\top \boldsymbol{H}\boldsymbol{g}$ term. In many cases, the gradient norm does not shrink significantly throughout learning, but the $\boldsymbol{g}^\top \boldsymbol{H}\boldsymbol{g}$ term grows by more than an order of magnitude. The result is that learning becomes very slow despite the presence of a strong gradient because the learning rate must be shrunk to compensate for even stronger curvature. Figure 8.1 shows an example of the gradient increasing significantly during the successful training of a neural network.

Though ill-conditioning is present in other settings besides neural network training, some of the techniques used to combat it in other contexts are less applicable to neural networks. For example, Newton's method is an excellent tool for minimizing convex functions with poorly conditioned Hessian matrices, but in the subsequent sections we will argue that Newton's method requires significant modification before it can be applied to neural networks.

8.2.2 Local Minima

One of the most prominent features of a convex optimization problem is that it can be reduced to the problem of finding a local minimum. Any local minimum is guaranteed to be a global minimum. Some convex functions have a flat region at the bottom rather than a single global minimum point, but any point within such a flat region is an acceptable solution. When optimizing a convex function, we know that we have reached a good solution if we find a critical point of any kind.

With non-convex functions, such as neural nets, it is possible to have many local minima. Indeed, nearly any deep model is essentially guaranteed to have an extremely large number of local minima. However, as we will see, this is not necessarily a major problem.

Neural networks and any models with multiple equivalently parametrized latent variables all have multiple local minima because of the **model identifiability** problem. A model is said to be identifiable if a sufficiently large training set can rule out all but one setting of the model's parameters. Models with latent variables are often not identifiable because we can obtain equivalent models by exchanging latent variables with each other. For example, we could take a neural network and modify layer 1 by swapping the incoming weight vector for unit i with the incoming weight vector for unit j, then doing the same for the outgoing weight vectors. If we have m layers with n units each, then there are $n!^m$ ways of arranging the hidden units. This kind of non-identifiability is known as **weight space symmetry**.

In addition to weight space symmetry, many kinds of neural networks have additional causes of non-identifiability. For example, in any rectified linear or maxout network, we can scale all of the incoming weights and biases of a unit by α if we also scale all of its outgoing weights by $\frac{1}{\alpha}$. This means that—if the cost function does not include terms such as weight decay that depend directly on the weights rather than the models' outputs—every local minimum of a rectified linear or maxout network lies on an $(m \times n)$-dimensional hyperbola of equivalent local minima.

These model identifiability issues mean that there can be an extremely large or even uncountably infinite amount of local minima in a neural network cost function. However, all of these local minima arising from non-identifiability are equivalent to each other in cost function value. As a result, these local minima are not a problematic form of non-convexity.

Local minima can be problematic if they have high cost in comparison to the global minimum. One can construct small neural networks, even without hidden units, that have local minima with higher cost than the global minimum (Sontag and Sussman, 1989; Brady *et al.*, 1989; Gori and Tesi, 1992). If local minima with high cost are common, this could pose a serious problem for gradient-based optimization algorithms.

It remains an open question whether there are many local minima of high cost for networks of practical interest and whether optimization algorithms encounter them. For many years, most practitioners believed that local minima were a common problem plaguing neural network optimization. Today, that does not appear to be the case. The problem remains an active area of research, but experts now suspect that, for sufficiently large neural networks, most local minima have a low cost function value, and that it is not important to find a true global minimum rather than to find a point in parameter space that has low but not minimal cost (Saxe *et al.*, 2013; Dauphin *et al.*, 2014; Goodfellow *et al.*, 2015; Choromanska *et al.*, 2014).

Many practitioners attribute nearly all difficulty with neural network optimization to local minima. We encourage practitioners to carefully test for specific problems. A test that can rule out local minima as the problem is to plot the norm of the gradient over time. If the norm of the gradient does not shrink to insignificant size, the problem is neither local minima nor any other kind of critical point. This kind of negative test can rule out local minima. In high dimensional spaces, it can be very difficult to positively establish that local minima are the problem. Many structures other than local minima also have small gradients.

8.2.3 Plateaus, Saddle Points and Other Flat Regions

For many high-dimensional non-convex functions, local minima (and maxima) are in fact rare compared to another kind of point with zero gradient: a saddle point. Some points around a saddle point have greater cost than the saddle point, while others have a lower cost. At a saddle point, the Hessian matrix has both positive and negative eigenvalues. Points lying along eigenvectors associated with positive eigenvalues have greater cost than the saddle point, while points lying along negative eigenvalues have lower value. We can think of a saddle point as being a local minimum along one cross-section of the cost function and a local maximum along another cross-section. See figure 4.5 for an illustration.

Many classes of random functions exhibit the following behavior: in low-dimensional spaces, local minima are common. In higher dimensional spaces, local minima are rare and saddle points are more common. For a function $f : \mathbb{R}^n \rightarrow \mathbb{R}$ of this type, the expected ratio of the number of saddle points to local minima grows exponentially with n. To understand the intuition behind this behavior, observe that the Hessian matrix at a local minimum has only positive eigenvalues. The Hessian matrix at a saddle point has a mixture of positive and negative eigenvalues. Imagine that the sign of each eigenvalue is generated by flipping a coin. In a single dimension, it is easy to obtain a local minimum by tossing a coin and getting heads once. In n-dimensional space, it is exponentially unlikely that all n coin tosses will